ENVIRONMENTAL PROGRESS

May 1983
Volume 2, No. 2

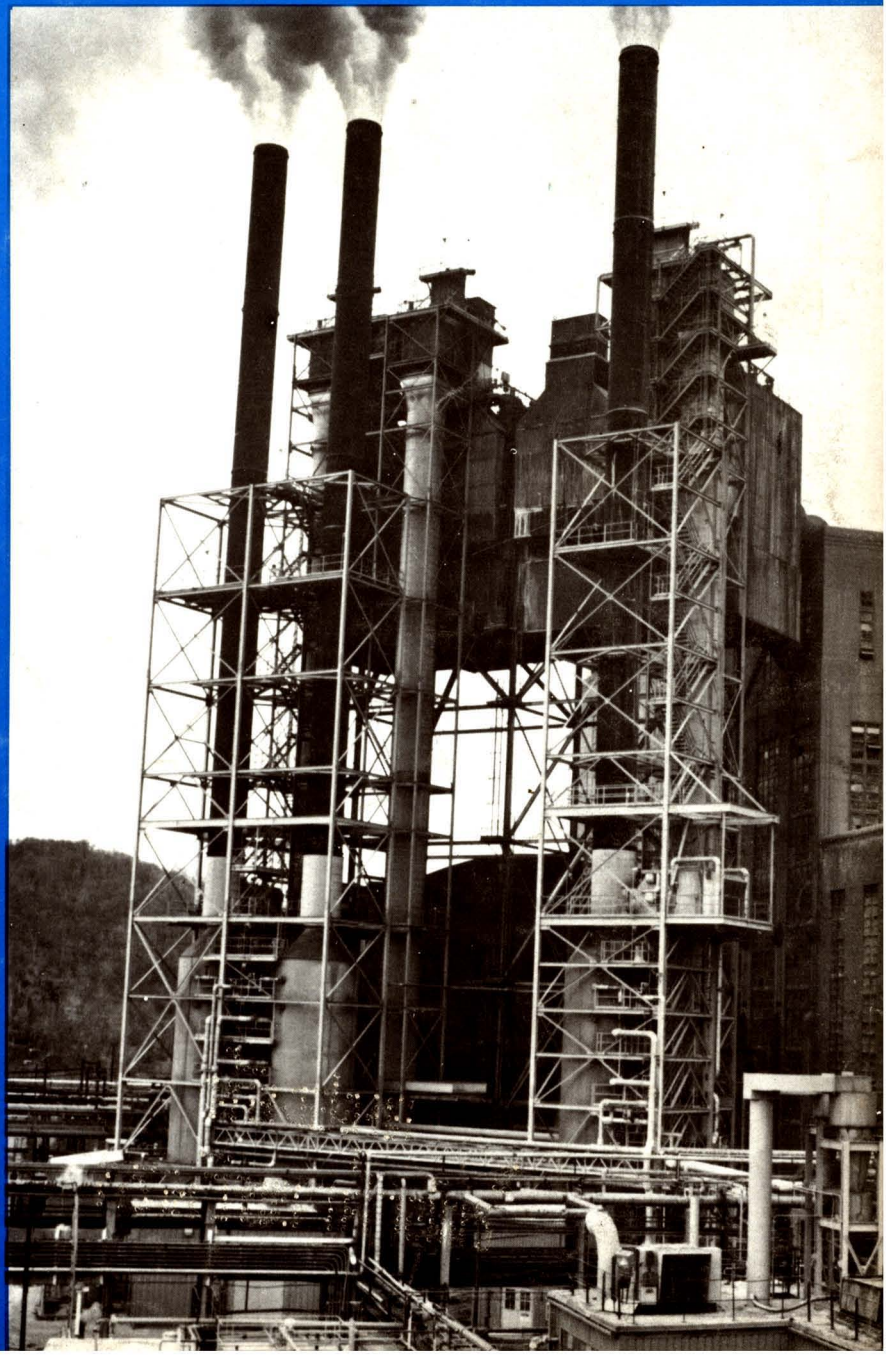

CONTENTS

SEVENTY FIVE YEARS OF PROGRESS

ENVIRONMENTAL®
PROGRESS

May 1983 Vol. 2, No. 2

Environmental Progress is a publication of the American Institute of Chemical Engineers. It will deal with multi-faceted aspects of the pollution problem. It will provide thorough coverage of abatement, control, and containment of effluents and emissions within compliance standards. Papers will cover all aspects including water, air, liquid and solid wastes. Progress and technological advances vital to the environmental engineer will be reported.

AIChE EXECUTIVE DIRECTOR
J. C. Forman

PUBLICATIONS DIRECTOR
Larry Resen
(212) 705-7335

EDITOR
Gary F. Bennett
(419) 537-2520

PRODUCTION EDITOR
Maura Mullen
(212) 705-7327

TECHNICAL EDITOR
Waldo B. Hoffman
(207) 729-3701

EDITORIAL REVIEW BOARD
D. Bhattacharyya
S. L. Daniels
T. H. Goodgame
P. Lederman
R. Mahalingham
C. J. Touhill
Andrew Benedek
J. A. Scher
R. Siegel

Publication Office, 215 Canal Street, Manchester, N.H. Published quarterly by the American Institute of Chemical Engineers, 345 East 47 St., New York, N.Y. 10017. (ISSN 0278-4491). Manuscripts should be submitted to the Manuscript Center, American Institute of Chemical Engineers, 345 East 47 St., New York, N.Y. 10017. Statements and opinions in *Environmental Progress* are those of the contributors, and the American Institute of Chemical Engineers assumes no responsibility for them. Subscription price per year: AIChE members $20; others $40. Single copies $15. U.S. postage is prepaid. Outside the U.S. please add $5 per subscription. Payment must be made in U.S. dollars. Application to mail at second-class postage rates is pending at New York, N.Y. and additional mailing offices. Copyright 1983 by the American Institute of Chemical Engineers.

Postmaster: Please send change of addresses to Environmental Progress, AIChE, 345 East 47 Street, New York, N.Y. 10017.

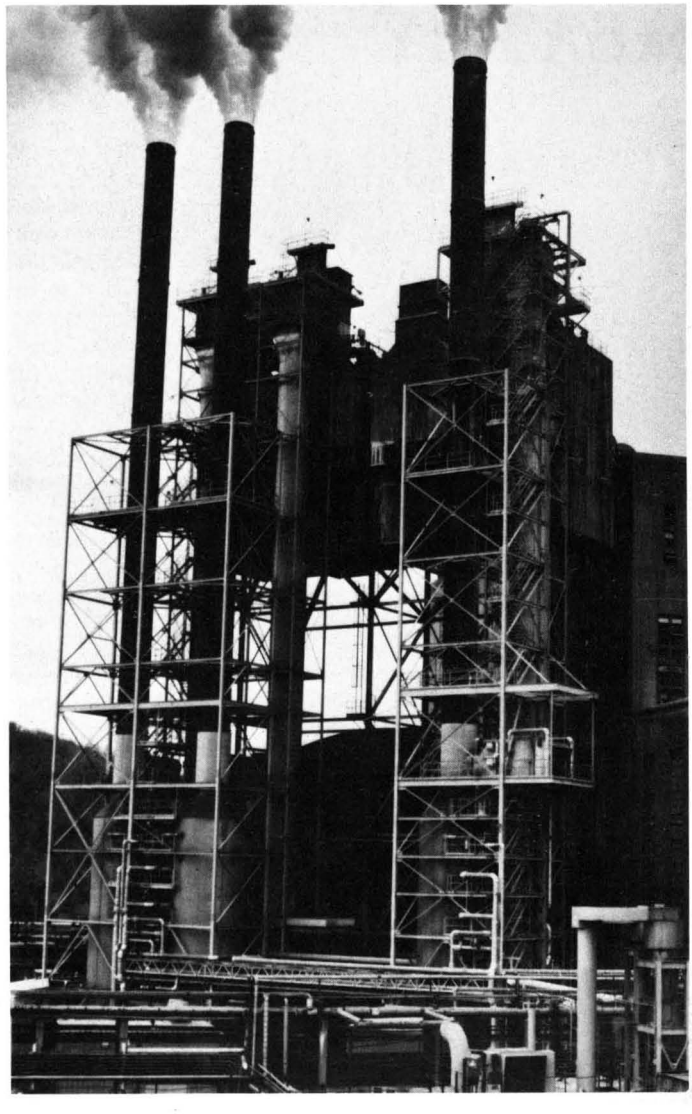

Dual Alkali flue gas desulfurization unit at ARCO Chemical Co. plant, Monaca, Penn. Photo courtesy FMC Corp.

Reproducing Copies

Authorization to photocopy items for internal or personal use, or the internal or personal use of specific clients, is granted by AIChE for libraries and other users registered with the Copyright Clearance Center (CCC) Transactional Reporting Service, provided that the $2.00 fee is paid directly to CCC, 21 Congress St., Salem, MA 01970. This consent does not extend to copying for general distribution, for advertising or promotional purposes, for inclusion in a publication, or for resale.

Environmental Progress fee code: 0278-4491/83 $2.00

ห้องสมุดกรมวิทยาศาสตร์บริการ
28 ก.ย. 2526

APATHY

RICHARD D. SIEGEL

I have been involved in the activities of the Environmental Division of the Institute for many years, dating back to Larry Cecil's challenge to those of us attending the Division dinner meeting in Houston in late February 1971 to "Get Involved." During the 12 years that have passed since Larry's challenge, I have had the opportunity to work with many of you in developing technical symposia, identifying work issues for your Pollution Solution (Critical Issues) Groups, and, most recently, in preparing materials and testimony for the Air Task Force.

For those of you who, over these years, have given of yourselves to work with us, I extend my heartfelt thanks. It is you who have made our efforts successful and professionally meaningful. But what of the others of you from whom we never hear? Why don't you choose to participate? Are you involved in other professional associations instead of AIChE? If so, as chemical engineers, why aren't you involved in the Institute's environmental programs? Or perhaps you are not involved at all. If this is the case, why not?

Frankly my friends, I grow tired of hearing people complain about the environment—that the environmental laws and regulations are too stringent and complex, or that they are not stringent enough. If you are truly concerned, give voice to your frustrations through our Task Forces! Those of us involved in these groups are not omniscient. We cannot possibly hope to understand how the various environmental rules, regulations and procedures affects you unless you communicate or, better, work with us.

At this time the Congress is debating reauthorization and amendment of the Clean Air Act (CAA). No consensus has yet to emerge either with respect to potential change in existing programs, or with the need for new mandates such as in the area of acid precipitation control. With a new Congress convened in January, *now* is the opportunity for you to help us inform the new Congress and its staff on matters of concern to AIChE. During 1983, we intend to develop a number of information documents articulating CAA revision needs as we see them. We need help in identifying topics and in preparing necessary documents. Similar activities are planned by the Water and Hazardous Waste Task Forces.

As we say in the Environmental Division's brochure, *What have you done today as a professional chemical engineer to aid your fellow citizens? If you really care join us.* If you don't, the loss is yours.

Richard D. Siegel holds a PhD in Chemical Engineering. He is Chairman of the Air Technical Section and Co-Chairman of the Air Task Force.

Environmental Shorts. . .

World's Largest Landfill Methane Recovery Facility

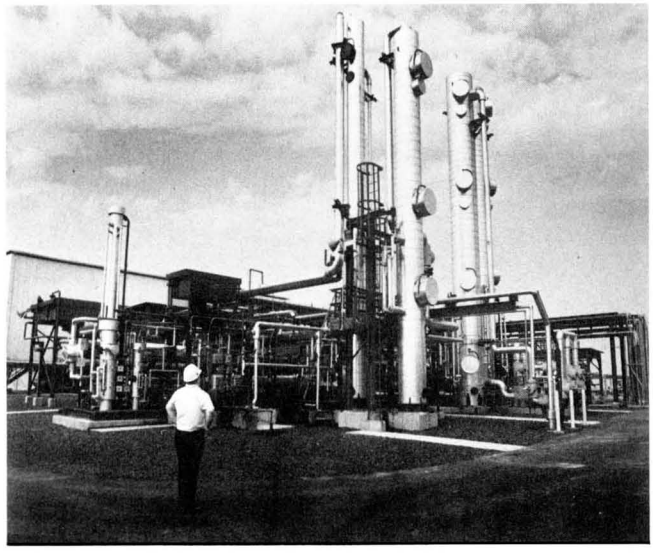

C-E Lummus, a unit of Combustion Engineering, Inc., engineered and constructed the world's largest landfill methane recovery facility which began operations recently at the Fresh Kills landfill on Staten Island, New York. The plant, a joint venture between Getty Synthetic Fuels, Inc., and Methane Development Corporation, a Brooklyn Union Gas subsidiary, is the first large-scale facility of its kind on the East Coast.

C-E Lummus' Bloomfield, NJ, Division initiated engineering studies for the project in 1979, completed engineering and procurement activities in 1981, and construction in 1982.

New York City has leased the gas rights from 400 acres of the 2,200-acre landfill to the joint venture. The 400-acre site is expected to yield up to 1.3 billion cubic feet of product gas annually and will heat 10,000 homes this winter. The $20 million plant is capable of processing up to ten million cubic feet per day of raw landfill gas. This is another step in reducing dependence on unstable and expensive foreign oil.

The gas is withdrawn from the landfill through more than 100 wells drilled to depths of 60 to 75 feet, then transported under vacuum to the plant via an underground collection system. The plant will operate 24 hours a day. It has automatic and safety systems to shut down operations in the event of a malfunction.

The raw gas is processed to remove moisture, carbon dioxide and trace elements. The resulting product gas, which is virtually pure methane with a heating value equivalent to natural gas, is then delivered to Brooklyn Union's West Shore facility where it is mixed with natural gas and distributed to Brooklyn Union customers.

Synthesis Gas Made From Coal Used to Manufacture Ammonia

TVA has begun using synthesis gas made from coal to manufacture ammonia for nitrogen fertilizer production at its National Fertilizer Development Center, Muscle Shoals, AL.

This is the first prototype demonstration of modern coal gasification technology in an integrated U.S. production operation. Gas made from coal is being fed to TVA's adjoining small ammonia plant.

TVA began the ammonia from coal project at the urging of the fertilizer industry in the late 1970s. At that time, prospective shortages of natural gas threatened fertilizer and food production. Nearly all of the country's ammonia, the building block for most nitrogen fertilizers, is made from natural gas.

The amount initially was limited to 5% of the plant's total gas use, then increased to 10%. Synthesis gas use is being increased as its sulfur content is reduced toward the required level of about one part in 10 million.

The coal gasification experiment is designed to use 200 tons of coal per day to supply 60% of the gas required to make 225 tons of ammonia per day.

The Texaco gasifier, heart of the coal conversion complex, continues to operate very well. It is producing synthesis gas at the desired production rate, temperature, pressure, and composition. Downstream operations to remove solid particles from the gas, react carbon monoxide and steam to produce hydrogen, and remove sulfur from the synthesis gas are performing well.

However, after the purification equipment gets the sulfur content of the gas to near zero, the gas is picking up traces of sulfur, either from a tiny leak or from residual sulfur in the system. This problem is considered relatively minor.

ห้องสมุดกรมวิทยาศาสตร์บริการ

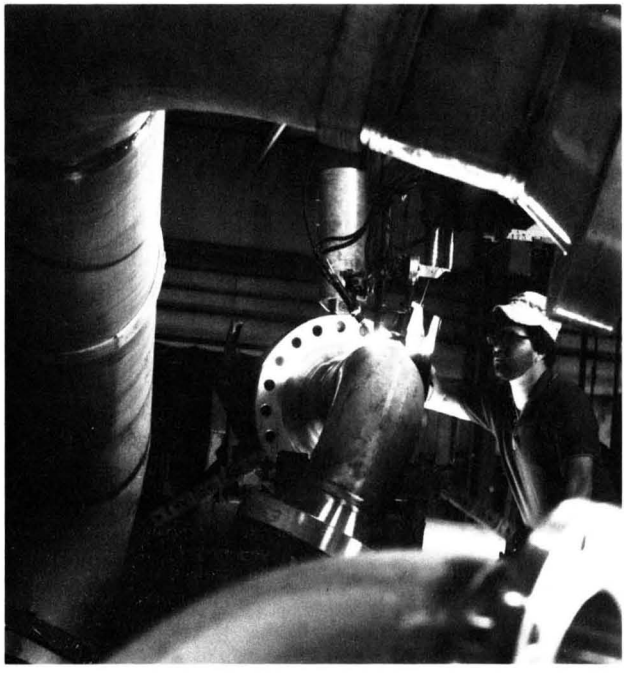

Chemicals From Coal Plant Piping

Watching his work through a protective shield, a welder at Dravo Corp.'s pipe fabrication plant in Marietta, OH, uses an automatic welding machine to join two pieces of 10-in.-dia. stainless steel piping destined for Tennessee Eastman Co.'s new chemicals from coal facilities in Kingsport, TN. The new Tennessee Eastman facilities will gasify about 900 tons of coal per day to produce acetic anhydride, an industrial chemical used in the manufacture of photographic film base, fibers, plastics, and other products. Dravo's Pipe Fabrication Division has provided a variety of shop fabrication, procurement, and engineering services to the Houston-based Refinery and Chemical Division of Bechtel Corporation in connection with the project.

Growing Petroleum Coke Supplies Could Present Problems

Continuing decreases in residual fuel oil demand combined with heavier crude inputs is resulting in growing investments in delayed coking capacity. The result, as presented in a current Chem Systems study, will be significant increases in world production of petroleum coke.

In the "Global Outlook for Petroleum Coke", Chem Systems points out that the increase in coke production exceeds the demand in premium use markets, such as aluminum anodes. Hence, there must be an increase in the use of petroleum coke as a fuel. Current marketing mechanisms may not be adequate to dispose of this increased output. The problem can be resolved however, through a concerted effort on behalf of coke producers and resellers/brokers oriented towards development of new markets in which fuel coke is in direct competition with coal. These efforts will require a thorough understanding of the potential consumers' concerns for price, contracts and quality. Details on availability of the study "Global Outlook for Petroleum Coke" can be obtained from Chem Systems Inc., 14925 Memorial Drive, Suite 210, Houston, Texas 77079: Telephone, (713)493-4115.

WORLD GREEN COKE PRODUCTION
(Million Short Tons)

	1980	1985	1990	2000	Growth Rate 1980-2000
United States	14.9	18.0	19.5	21.5	1.9
Western Europe	1.9	2.3	3.5	4.2	4.0
Japan	0.4	0.4	1.5	2.0	8.4
Other World	4.7	5.0	5.7	6.6	1.7
Total	21.9	25.7	30.2	34.3	2.3
Calcined Anode Uses	12.4	13.9	15.5	17.7	1.8
Fuel and Other Uses	9.5	11.8	14.7	16.6	2.8

The above brochure was prepared by the Synthetic Fuels Task Force of the American Institute of Chemical Engineers. AIChE is the national technical society representing chemical engineers with a wide range of professional affiliations in academia, government, industry and private research and consulting firms. *The Synthetic Fuel Program* is the first in a series of publications discussing various aspects of U.S. alternate energy needs. Further information on this and other topics may be obtained by contacting Public Relations Department, American Institute of Chemical Engineers, 345 East 47th Street, New York, N.Y. 10017.

Measuring Volatile Chemical Emission Rates from Large Waste Disposal Facilities

A novel method for measuring emission rates from large surface impoundments.

Seong T. Hwang, U.S. Environmental Protection Agency, Washington, D.C. 20460
and
L. J. Thibodeaux, University of Arkansas, Fayetteville, AK 72701.

Quantification of volatile atmospheric emissions from large-area sources has been the subject of various investigators [1], [3], [5], [6], and [7]. Interest in this area has intensified recently as a result of concern with regard to toxic air emissions associated with disposal of hazardous wastes, and potential health effects upon inhalation or contact. The Resource Conservation and Recovery Act of 1976 (RCRA) mandates protection of public health and the environment from exposure to hazardous constituents discharged into the environment. Protection of public health and the environment cannot be achieved without considering adverse effects due to the released hazardous pollutants on all environmental media including air. Assessment of the impact of toxic emissions on population will require accurate information on the extent of such emissions into the air. This can be achieved by direct measurements, or by estimation using mathematical models. The present paper is concerned with reviewing the available methods of measuring emission rates of volatile compounds from non-point source hazardous waste facilities. Although the methods reviewed are mostly applied for measuring emissions from surface impoundments and pesticide volatilization rates, the applications can be extended to landfills and land-treatment facilities. In addition, a new method developed, based on the theory of a turbulent atmosphere, will be proposed. The proposed method has the advantage of requiring substantially fewer concentration measurements than the currently available methods.

AVAILABLE MEASUREMENT TECHNIQUES

The methods currently considered most promising for measuring toxic emissions from area sources include the "Concentration Profile Technique" [1] and the "Plume Mapping Method" [3]. Other methods, though not actively considered for technical reasons, include the "Sample Head Technique" [17], "Exposure Profile Method" [14], "Tracer Technique" [15], "Line Source Technique" [16], and those based on Reynolds stresses [2, p. 110] and remote optical sensing [4] and "Emission Flux Chamber" method [18].

The "Concentration Profile Technique" [1], [8] utilizes the principles of micrometeorology and atmospheric transport to determine the emission rate of volatile chemicals from a large liquid surface by the following equation:

$$J_i = -\left(\frac{D_i}{D_{H_2O}}\right)^{2/3} S_r S_c k^2/\phi_m^2 Sc_{H_2O}^{(l)} \qquad (1)$$

where J_i is the emission rate of component i, gr/cm², sec.; Di is the diffusivity of component i in the air; D_{H_2O} is the diffusivity of water vapor in the air; S_r is the slope of a line from a graphical plot of velocity (v, cm/sec) versus logarithmic height above the liquid surface (ln$z$, with z in cm); S_c is the slope of a line from a graphical plot of concentration of species i (c_i, gr/cm³) versus the logarithmic height; k is the von Karman constant (= 0.4); ϕm is the Businger wind-shear parameter (called the adiabatic velocity-profile correction factor); $Sc_{H_2O}^{(l)}$ is the turbulent Schmidt number for water vapor, where water vapor is used as a reference compound because of the availability of many field experimental data. The stability correction factor $(\phi_m^2 Sc_{H_2O}^{(l)})^{-1}$ is correlated by

$$(\phi_m^2 Sc_{H_2O}^{(l)})^{-1} = (1 \pm 50Ri)^{\pm 1/2} \qquad (2)$$

where R_i is the Richardson Number, represented by [11]

$$Ri = \frac{g}{T_{av.}} \frac{(T_2 - T_1)(z_2 - z_1)}{(v_2 - v_1)^2} \qquad (3)$$

In Equation (3), T_2 and T_1, are the temperature of the air at heights z_2 and z_1, respectively; v_2 and v_1 are the average wind speed at heights z_2 and z_1, respectively; $T_{av.}$ is the arithmetic average of T_2 and T_1, °K; and g is the acceleration due to gravity (980.7 cm/sec²). The range of Ri tested for applicability of Equation (2) includes $|Ri| \leq 4$ for unstable conditions (Ri negative) and $|Ri| \leq 1$ for stable conditions (Ri positive). In equation (2), -50 and $+1/2$ apply for unstable conditions and $+50$ and $-1/2$ apply for stable conditions. The stability correction factor is unity for neutral conditions.

In order to obtain S_r and S_c, the concentrations and velocities are simultaneously measured at several different heights (6 logarithmic heights are normally used).

The "Plume Mapping Method" involves back-calculation of the emission rate based on a Gaussian-Dispersion Model. The governing equation is

$$q = \sum_1^n \pi \chi K \sigma_y \sigma_z C N \bar{v} \qquad (4)$$

where q is the emission rate of non-methane hydrocarbons, gr/sec; χ is the peak concentration of hydrocarbons in a Gaussian-fit curve, ppm; σ_y and σ_z are the lateral and vertical extent of the Gaussian plume, m; $K = 665 \times 10^{-6}$ gr/ppm for methane; C is the correction factor for methane equivalent and instrument response; N is the non-methane fraction of the total hydrocarbons; and $\bar{v}$ is the mean wind velocity, m/sec.

The measurements are performed to determine χ, σ_y, σ_z, and $\bar{v}$, and involve determination of the concentration distribution at various horizontal and vertical downwind locations and constructions of plumes. From these measurements, the width and vertical extent of the plume can be determined for use in Equation (4). This technique has been used for total hydrocarbon emissions with limited success, but has not been tried for determination of the emission rate of component chemicals.

Sutton [5], in a study of diffusion in the lower atmosphere, for mathematical convenience used power-law expressions for variations of the velocity and the turbulent diffusivity with height. While solution (10) with the power-law expressions demonstrates the importance of fetch (evaporation distance) on the emission rate, no practical use has been made of it because of its limitation requiring the curve-fitting of experimental velocity and diffusivity data with power laws.

THEORETICAL BACKGROUND

No theory completely explains the dispersion of pollutants in the atmosphere. Dispersion may be molecular transport in a highly stable atmosphere. In an unstable atmosphere and a turbulent shear flow, diffusion takes place by eddy transport, which is characterized by a Reynolds number greater than 10^3. The Reynolds number is defined by

$$Re = zv/\nu \tag{5}$$

where z is the characteristic length chosen as the height above the liquid surface; v is the mean velocity at z; and ν is the kinematic viscosity. For example, the wind velocity which will start to cause turbulence at a height of 1 m corresponds to 1.5 cm/sec ($\nu = 0.15$ cm²/sec used), which indicates that the atmosphere is normally turbulent.

If the lapse rate (rate of temperature decrease with height) is adiabatic, the wind varies according to a power law. In turbulent conditions below 9 m from the surface, however, logarithmic profiles are observed [1], [9]. For neutral and non-neutral conditions and with turbulent flow, the velocity profile can be expressed, following Prandtl, as [1], [2].

$$\frac{dv}{dz} = \frac{v_*}{kz}\phi_m \tag{6}$$

where the Businger correction factor, ϕ_m, corrects for wind-shear observations occurring under thermally unstable boundary-layer conditions. Upon integration, Equation (6) is commonly expressed by

$$v = \frac{v_*\phi_m}{k}\ln\frac{z}{z_o} \tag{7}$$

where z_o is called the "roughness length."

The rate of vertical mass transfer of component i, J_i, under turbulent atmospheric conditions, can be represented by

$$J_i = -(D_{zi} + D_{zi}^{(t)})\frac{dc_i}{dz} \tag{8}$$

where D_{zi} and $D_{zi}^{(t)}$ are the molecular and eddy diffusivity in the vertical direction, respectively, cm²/sec, and c_i is the concentration of component i, gr/cm³. Under turbulent conditions, eddy transport dominates over molecular diffusion. Hence, Equation (8) can be written as

$$J_i = -D_{zi}^{(t)}\frac{dc_i}{dz} \tag{9}$$

The shear stress can be expressed by the momentum-transport equation,

$$\tau_o = \rho\nu^{(t)}\frac{dv}{dz} \tag{10}$$

where τ_o is the shear stress exerted by the air on the surface, gr cm^{-1} sec^{-2}; ρ is the density of air, gr/cm³; $\nu^{(t)}$ is the eddy viscosity, cm²/sec.

Dividing Equation (9) by Equation (10), one gets

$$J_i = -\frac{\tau_o}{\rho}\left(\frac{D_{zi}^{(t)}}{\nu^{(t)}}\right)\frac{dc_i/dz}{dv/dz} \tag{11}$$

From the definition of the surface-friction velocity, $v_* = \sqrt{\tau_o/\rho}$, we get

$$\frac{\tau_o}{\rho} = v_*^2 \tag{12}$$

Combining Equation (6) and Equation (12), and using the relationship given by Equation (6), results in

$$\frac{\tau_o}{\rho} = \frac{kv_*z}{\phi_m}\frac{dv}{dz} \tag{13}$$

Substitution of Equation (13) into Equation (11) will give

$$J_i = -\frac{kv_*z}{\phi_m}\frac{D_{zi}^{(t)}}{\nu^{(t)}}\frac{dc_i}{dz} \tag{14}$$

Because of extensive data on the water-vapor Schmidt number defined by $Sc_{H_2O}^{(t)} = \nu^{(t)}/D_{H_2O}^{(t)}$, it is recommended to apply a correction of the turbulent diffusivity of water vapor for compound i by use of the molecular diffusivity ratio [1]. Then, Equation (14) becomes

$$J_i = -\frac{kv_*z}{\phi_m}\left(\frac{D_i}{D_{H_2O}}\right)^{2/3}\frac{1}{Sc_{H_2O}^{(t)}}\frac{dc_i}{dz} \tag{15}$$

where D_i or D_{H_2O} are the molecular diffusivity of component i and water vapor, respectively. Comparison of Equation (9) and Equation (15) indicates that the turbulent diffusivity of component i in the vertical direction can be represented by

$$D_{zi}^{(t)} = \frac{kv_*z}{\phi_m}\left(\frac{D_i}{D_{H_2O}}\right)^{2/3}\frac{1}{Sc_{H_2O}^{(t)}} \tag{16}$$

DERIVATION OF PROPOSED MODEL

The dispersion of pollutants in the atmosphere under turbulent conditions occurs due to convective transport by wind, molecular diffusion, eddy diffusion resulting from flow turbulence, and turbulence created by temperature difference or unstable lapse rate. In three dimensions, the dispersion of pollutants in the atmosphere with wind at a velocity of v, cm/sec, above an area source as shown in Figure 1, can be expressed by

$$v\frac{\partial c}{\partial x} = \frac{\partial}{\partial x}\left[(D_x + D_x^{(t)})\frac{\partial c}{\partial x}\right] + \frac{\partial}{\partial y}\left[(D_y + D_y^{(t)})\frac{\partial c}{\partial y}\right] + \frac{\partial}{\partial z}\left[(D_z + D_z^{(t)})\frac{\partial c}{\partial z}\right] \tag{17}$$

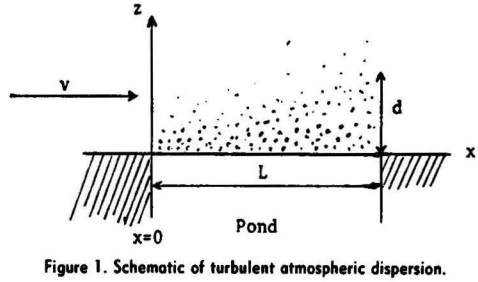

Figure 1. Schematic of turbulent atmospheric dispersion.

As indicated previously, under turbulent conditions, molecular diffusion is negligible compared with turbulent diffusion [2]. Hence, the atmospheric dispersion can be adequately expressed by

$$v\frac{\partial c}{\partial x} = \frac{\partial}{\partial x}\left(D_x^{(t)}\frac{\partial c}{\partial x}\right) + \frac{\partial}{\partial y}\left(D_y^{(t)}\frac{\partial c}{\partial y}\right) + \frac{\partial}{\partial z}\left(D_z^{(t)}\frac{\partial c}{\partial z}\right) \quad (18)$$

We simplify Equation (18) under the condition that the dimensionless $Lv/D \gg 1$, where D is a representative value of the diffusivity, and L is the length of the area-type emission source under consideration.

In the region below the thickness d, the concentration of component i, c_i, is the order of the concentration on the emitting surface, c_{oi}. Equation (18) can be written in terms of the dimensionless variables $\bar{X} = x/L$, $\bar{Y} = y/L$, $\bar{Z} = z/d$, and $Q = c_i/c_{oi}$.

$$\left(\frac{d}{L}\right)\left(\frac{Lv}{D}\right)\frac{dQ}{d\bar{X}} = \left(\frac{d}{L}\right)^2\frac{\partial}{\partial\bar{X}}\left(\frac{D_x^{(t)}}{D}\frac{\partial Q}{\partial\bar{X}}\right) + \left(\frac{d}{L}\right)^2\frac{\partial}{\partial\bar{Y}}\left(\frac{D_y^{(t)}}{D}\frac{\partial Q}{\partial\bar{Y}}\right) + \frac{\partial}{\partial\bar{Z}}\left(\frac{D_z^{(t)}}{D}\frac{\partial Q}{\partial\bar{Z}}\right) \quad (19)$$

The variables Q, $\bar{X}$, $\bar{Y}$, and $\bar{Z}$ vary from 0 to 1. If the region $x \leqq L$ and $y \leqq L$ is excluded from consideration, the first and second derivatives of Q with respect to $\bar{X}$, $\bar{Y}$, and $\bar{Z}$ are all of the order of unity. Since $D_x^{(t)}/D$, $D_y^{(t)}/D$, and $D_z^{(t)}/D$ are also of the order of unity, the relative magnitude of the four terms in Equation (19) depends on the values of d/L and Lv/D.

All four terms in Equation (19) may be of comparable magnitude. In order to obtain a solution for Equation (19), the first and last terms must be of the same order of magnitude, or

$$\left(\frac{d}{L}\right)^2\left(\frac{Lv}{D}\right) = o(1) \quad (20)$$

where $o(1)$ means the order of magnitude of 1. Equation (20) can be rearranged as

$$\frac{d}{L} = o\left(\frac{1}{\sqrt{Lv/D}}\right) \quad (21)$$

For very large values of Lv/D, or $Lv/D \gg 1$, d becomes small compared with the value of L. In such a case, the second and third terms in Equation (19), being of the order of magnitude of $(d/L)^2$, can be neglected. This can be exemplified as follows: For a lagoon with a length of 100 cm, and with a wind velocity of 180 cm/sec (4 mph) and a diffusivity in air of 0.1 cm²/s, $Lv/D = 180{,}000 \gg 1$. Hence, under normal turbulent conditions for a relatively large-area source, the assumption of $Lv/D \gg 1$ could be satisfied, and $(d/L)^2$ becomes small in Equation (19). Thus, Equation (19) can be approximated as

$$v\frac{\partial c_i}{\partial x} = \frac{\partial}{\partial z}\left(D_{zi}^{(t)}\frac{\partial c_i}{\partial x}\right) \quad (22)$$

The logarithmic velocity profile and the turbulent diffusion coefficient given by Equations (7) and (16), respectively, are substituted into Equation (22) to yield

$$\frac{1}{M}\ln\frac{z}{z_o}\frac{\partial c_i}{\partial x} \approx \frac{\partial}{\partial z}\left(z\frac{\partial c_i}{\partial z}\right) \quad (23)$$

where $M = k^2(D_i/D_{H_2O}^{(t)})^{2/3}/\phi_m^2 Sc_{H_2O}^{(t)}$

For a steady-state line source located at $x = 0$ of the turbulent shear flow shown in Figure 1, Equation (23) must be solved with the condition

$$\int_0^\infty c_i v dz = \dot{m}_i \text{ at all } x \geq 0 \quad (24)$$

where $\dot{m}_i$ is the emission rate of the line source per unit length, or gr/cm · sec. Combining Equations (7) and (24) will give

$$\int_0^\infty c_i \ln\frac{z}{z_o}dz = \frac{\dot{m}_i k}{v_*\phi_m} \quad (25)$$

If we let $Mx = X$, it can be shown that X and $c_i z$ are dimensionally consistent with z and $\dot{m}_i k/v_*\phi_m$ respectively. Hence, if we use the dimensionless variables $\xi = z/X$, and $f(\xi) = (c_i v_*\phi_m/\dot{m}_i k)\,X$, Equation (23) can be expressed in terms of the dimensionless parameters (see Appendix A for details).

$$\left(\frac{d^2f}{d\xi^2} + \ln\frac{z}{z_o}\frac{df}{d\xi}\right) + \frac{1}{\xi}\left(\frac{df}{d\xi} + \ln\frac{z}{z_o}f\right) = 0 \quad (26)$$

The solution of Equation (26) is (see Appendix A for details)

$$c_i = \frac{\dot{m}_i k}{0.8 v_*\phi_m X}\, e^{-\ln\frac{z}{z_o}\cdot\frac{z}{X}} \quad (27)$$

So far, the treatment has pertained to an analysis of the dispersion of pollutants emitted from a line source. For an area source on the xy plane shown in Figure 2, the concentration at a receptor R due to emission from the area source at the rate of J_i, gr/cm² sec will consist of a summation of the concentrations resulting from all line sources with an emission rate $J_i dx'$. The incremental concentration at R due to a line source $J_i dx'$ displaced by x' can be expressed by Equation (28),

$$dc_i = \frac{kJ_i dx'}{0.8 v_*\phi_m M(x - x')}\, e^{-\frac{z}{M(x-x')}\ln\frac{z}{z_o}} \quad (28)$$

Equation (28) can be integrated along the length (L) of the area source, or

$$c_i = \frac{kJ_i}{0.8 v_*\phi_m M}\int_0^L \frac{1}{x - x'}\, e^{-\frac{z}{M(x-x')}\ln\frac{z}{z_o}} dx' \quad (29)$$

By letting $P = x - x'$, Equation (29) reduces to

$$c_i = \frac{J_i k}{0.8 v_*\phi_m M}\int_{x-L}^{x} \frac{1}{P}\, e^{-\frac{B}{P}} dP \quad (30)$$

where $B = \frac{z}{M}\ln\frac{z}{zo}$

By letting $P = B/S$ in Equation (30), the equation becomes

$$c_i = \frac{J_i \phi_m^2 Sc_{H_2O}^{(t)}}{0.8 v_*\phi_m k(D_i/D_{H_2O})^{2/3}}\int_{B/x}^{B/(x-L)} \frac{1}{S}\, e^{-S} dS \quad (31)$$

It can be noted that the integral in Equation (31) is the exponential integral E_1, the value of which can be found in Reference 13. Equation (31) becomes

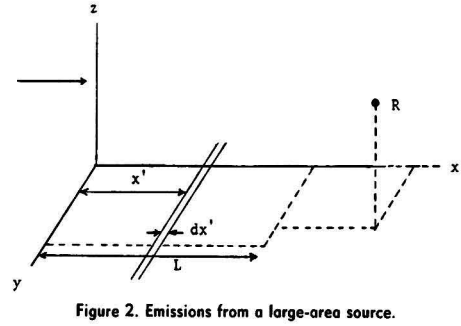

Figure 2. Emissions from a large-area source.

$$J_i = \frac{0.8 v_* \phi_m k (D_i/D_{H_2O})^{2/3}}{\phi_m^2 Sc_{H_2O}^{(\omega)} \left[E_1\left(\frac{B}{x}\right) - E_1\left(\frac{B}{x-L}\right)\right]} c_i \qquad (32)$$

where

$$B = \frac{z \phi_m^2 Sc_{H_2O}^{(\omega)}}{k^2 (D_i/D_{H_2O})^{2/3}} \ln \frac{z}{z_o} \qquad (34)$$

In practice, the upwind and downwind measurements would be required for c_i to represent the net concentration difference. If the downwind concentration measurement is made at the edge of the area source ($x = L$), then, the term $E_1(B/x - L)$ in Equation (32) becomes zero. Based on Equation (7), the slope of a plot of velocity versus the logarithmic height, S_r, is equal to

$$S_r = \frac{v_* \phi_m}{k} \qquad (35)$$

Combining Equations (32) and (35) will give

$$J_i = \frac{0.8 S_r k^2 (D_i/D_{H_2O})^{2/3}}{\phi_m^2 Sc_{H_2O}^{(\omega)} \left[E_1\left(\frac{B}{x}\right) - E_1\left(\frac{B}{x-L}\right)\right]} c_i \qquad (36)$$

In Equation (36), x represents the distance of a sampling location from the original boundary ($x = 0$) of the area source, and $x - L$ represents the distance from the edge of the area source to the sampling location.

COMPARISON OF EXPERIMENTAL RESULTS

The data given in Reference 1 are used to compare the results of the "Concentration Profile Technique," and of the method presented in this paper. To facilitate the use of the proposed method, an example calculation is furnished below. Some of the data given in Table 1 are calculated from the data in Reference 1. Reference 1 also gives $(\phi_m^2 Sc_{H_2O}^{(\omega)})^{-1} = 1.3$ and $(D_{MeOH}/D_{H_2O})^{2/3} = 0.711$.

One can calculate B from Equation (34).

$$B = \frac{43}{0.4^2(0.711)(1.3)} (3.46) = 1006 \text{ cm}$$

Hence

$$E_1\left(\frac{B}{x}\right) = E_1\left(\frac{1006}{3279}\right) = 0.9$$

The numerical value of the exponential integral, E_1, is tabulated in Table 2 for the reader's convenience. Since the sampling was performed inside the aerated lagoon, $x - L = 0$. Hence $E_1(B/x - L) = 0$. Substitution of the available values into Equation (36) yields

$$J_i = \frac{0.8\left(130 \frac{\text{cm}}{\text{sec}}\right)(0.4)^2(0.711)(1.3)}{0.9} \left(330 - 73 \frac{\mu g}{L}\right) \frac{1}{1000}$$

$$= 4.4 \frac{\mu g}{\text{cm}^2 \cdot \text{sec}} \qquad \text{for methanol emission.}$$

The emission rate reported in Reference 1 is 3.2 μg(micrograms)/cm^2. sec.

It should be noted that in the present example the distance from the original edge to the sampling point, x, is an estimated value. Also, the assumption in the derivation of the proposed method involves the exclusion of sampling points inside the area source. The distance was not exactly measured during the profile measurements for the "Concentration Profile Technique." Because of the unavailability of experimental data from other sources, adequate comparison of the proposed method with the available methods cannot be given at this time. In the use of this method, the original assumption incorporated in the derivation must be kept in mind, so that the criteria assumed are met and the experimental data obtained accordingly.

TABLE 1. EXPERIMENTAL DATA [1]

S_r, $\frac{\text{cm}}{\text{sec}}$	130
$\ln \frac{z}{z_o}$ at z = 43 cm	3.46
x cm	3280
Background conc. for MeOH, $\frac{\mu g}{L}$	73
c_i for MeOH at z = 43 cm	330
$\frac{\mu g}{L}$	

TABLE 2. TABLE OF EXPONENTIAL INTEGRAL, $E_1(x)$

x	$E_1(x)$
0.1	1.8
0.2	1.25
0.3	1
0.4	0.75
0.6	0.4
0.8	0.3
1.0	0.2

SUMMARY

The methods for quantifying emission rates from surface impoundments are reviewed. In addition, a new method is proposed which requires measurements of background and downwind concentrations, along with accurate information on the height of the sampling point relative to the surface impoundment. For both "the concentration profile technique" and the proposed method, velocity and temperature profiles are needed. However, the amount of data needed on the downwind concentrations in the proposed method is minimal compared with other methods currently available. The methods presented should as well be applicable to other area emission sources such as landfills and land-treatment facilities.

APPENDIX A

$$\ln \frac{z}{z_o} \frac{\partial c_i}{\partial X} = \frac{\partial}{\partial z}\left[z \frac{\partial c_i}{\partial z}\right] \qquad (A\text{-}1)$$

with

$$\xi = z/X \qquad (A\text{-}2)$$

$$f(\xi) = \frac{c_i v_* \phi_m}{\dot{m}_i k} X \qquad (A\text{-}3)$$

From A-2

$$\frac{\partial \xi}{\partial z} = \frac{1}{X} \qquad (A\text{-}4)$$

$$\frac{\partial \xi}{\partial X} \approx \frac{-z}{X^2} \qquad (A\text{-}5)$$

From A-3

$$c_i = \frac{\dot{m}_i k}{v^* \phi_m} X^{-1} f(\xi) \qquad (A\text{-}6)$$

From A-6

$$\frac{\partial c_i}{\partial z} = \frac{\dot{m}_i k}{v_* \phi_m} X^{-1} \frac{df}{d\xi} \frac{\partial \xi}{\partial z} = \frac{\dot{m}_i k}{v_* \phi_m} X^{-2} \frac{df}{d\xi} \quad \text{(A-7)}$$

From A-7

$$\frac{\partial}{\partial z}\left[z \frac{\partial c_i}{\partial z}\right] = \frac{\dot{m}_i k}{v_* \phi_m} X^{-2}\left[\frac{df}{d\xi} + z \frac{d^2 f}{d\xi^2} \frac{\partial \xi}{\partial z}\right]$$

$$= \frac{\dot{m}_i k}{v_* \phi_m} X^{-2}\left[\frac{df}{d\xi} + \frac{d^2 f}{d\xi^2}\right] \quad \text{(A-8)}$$

Also from A-6

$$\frac{\partial c_i}{\partial X} = \frac{\dot{m}_i k}{v_* \phi_m}\left[-X^{-2} f + X^{-1} \frac{df}{d\xi} \frac{\partial \xi}{dX}\right]$$

$$= \frac{\dot{m}_i k}{v_* \phi_m} X^{-2}\left[-f - \xi \frac{df}{d\xi}\right] \quad \text{(A-9)}$$

Substitution of A-8 and A-9 into A-1 yields

$$\left(\frac{d^2 f}{d\xi^2} + \ln \frac{z}{z_o} \frac{df}{d\xi}\right) + \frac{1}{\xi}\left(\frac{df}{d\xi} + \ln \frac{z}{z_o} f\right) = 0 \quad \text{(A-10)}$$

Let

$$\frac{df}{d\xi} + \ln \frac{z}{z_o} \frac{df}{d\xi} = W,$$

then A-10 becomes

$$\frac{dW}{d\xi} + \frac{1}{\xi} W = 0 \quad \text{(A-11)}$$

The solution of A-11 is

$$W = A_1 \xi^{-1} \quad \text{(A-12)}$$

For finite c_i at $z = 0$ (or finite f at $\xi = 0$), $A_1 = 0$. Then the solution of A-10 is the solution of

$$\frac{df}{d\xi} + \ln \frac{z}{z_o} f = 0 \quad \text{(A-13)}$$

The solution of A-13 is

$$f = A_2 e^{-\ln \frac{z}{z_o} \xi} \quad \text{(A-14)}$$

or

$$\frac{c_i v_* \phi_m}{\dot{m}_i k} X = A_2 e^{-\ln \frac{z}{z_o} \frac{z}{X}} \quad \text{(A-15)}$$

or

$$c_i = A_2 \frac{\dot{m}_i k}{v_* \phi_m X} e^{-\ln \frac{z}{z_o} \frac{z}{X}} \quad \text{(A-16)}$$

for

$$\int_0^\infty c_i \ln \frac{z}{z_o} dz = \frac{\dot{m}_i k}{v_* \phi_m} \quad \text{(A-17)}$$

From A-16 and A-17

$$A_2 \int_0^\infty \frac{\dot{m}_i k}{v_* \phi_m X} e^{-\ln \frac{z}{z_o} \frac{z}{X}} \ln \frac{z}{z_o} dz = \frac{\dot{m}_i k}{v_* \phi_m} \quad \text{(A-18)}$$

or

$$A_2 \int_0^\infty \frac{1}{X} e^{-\ln \frac{z}{z_o} \frac{z}{X}} \ln \frac{z}{z_o} dz = 1 \quad \text{(A-19)}$$

Let $Y = z/X$; then $XY = z$ (A-20)

From A-20

$$X dY = dz \quad \text{(A-21)}$$

Also, at the point of measurement

$$z_o = Y_o X \quad \text{(A-22)}$$

Substitution of A-20, A-21, and A-22 into A-19 results in

$$A_2 = \frac{1}{\int_{Y_o}^\infty e^{-\ln \frac{Y}{Y_o} Y} \ln \frac{Y}{Y_o} dY} \quad \text{(A-22)}$$

For the roughness length commonly encountered, Y_o is small ($Y_o \to 0$); then, the integral in A-22 approaches 0.8.

Hence, the solution of A-1 is

$$c_i = \frac{1}{0.8} \frac{\dot{m}_i k}{v_* \phi_m X} e^{-\ln \frac{z}{z_o} \frac{z}{X}} \quad \text{(A-23)}$$

NOMENCLATURE

C	= correction factor for methane equivalent and instrument response
c	= concentration, gr/cm³
D	= molecular diffusivity, cm²/sec
$D^{(t)}$	= turbulent diffusivity, cm²/sec
d	= thickness of significant concentration, cm
$E_1(x)$	= exponential integral as a function of x
g	= gravitational constant, 980.7 cm/sec²
J_i	= emission rate of component i, gr/cm² · sec
K	= 665 × 10⁻⁶ gr/ppm for methane
k	= von Karman constant, 0.4
L	= Length of area source, cm
$\dot{m}$	= emission rate of line source, gr/cm · sec
N	= non-methane fraction of total hydrocarbons
q	= emission rate of non-methane hydrocarbons, gr/sec
Re	= Reynolds number
Ri	= Richardson number, defined by Equation (3)
R	= receptor point in space
Sc	= Schmidt number, ν/D
S_c	= slope of plot of concentration versus logarithmic height, gr/cm³
S_v	= slope of plot of velocity versus logarithmic height, cm/sec
T	= temperature, °K
v	= wind velocity, cm/sec
v_*	= surface friction velocity, cm/sec
x	= longitudinal distance, cm
y	= lateral distance, cm
z	= height above area source, cm
z_o	= roughness length, cm

Subscripts

i	= component i
H_2O	= water vapor
1	= point 1 with respect to height
2	= point 2 with respect to height
x	= longitudinal direction
y	= lateral direction
z	= vertical direction
o	= surface

Superscripts

t	= turbulent
$-$	= mean

Greek Letters

ϕ_m	= adiabatic velocity-profile correction factor
ν	= kinematic viscosity, cm²/sec

ห้องสมุดกรมวิทยาศาสตร์บริการ

χ = peak concentration of hydrocarbons in Gaussian-fit curve, ppm
σ_y = lateral extent of Gaussian plume, m
σ_z = vertical extent of Gaussian plume, m
τ_o = shear stress, gr/cm · sec.^{2}
ρ = density of air, gr/cm^3

ACKNOWLEDGMENT

This article was reviewed and commented on by Dr. L. J. Thibodeaux, University of Arkansas, Fayetteville, AK 72701.

LITERATURE CITED

1. Thibodeaux, L. J., D. G. Parker, and H. H. Heck, "Measurement of Volatile Chemical Emissions from Wastewater Basins," Report for U.S. EPA-IERL, Cincinnati, Ohio (1981).
2. Thibodeaux, L. J., "Chemodynamics," John Wiley & Sons, New York (1979).
3. Harrison, P. R., "Assessment of Emissions from Petroleum Refinery Wastewater Treatment," Submitted to EPA-IERL, RTP, NC (August, 1981).
4. Herget, W. and D. D. Powell, "Remote Sensing of Gaseous Pollutants by Infrared Absorption and Emission Spectroscopy," Presented at 4th Joint Conference on Sensing of Environmental Pollutants, New Orleans, La. (November 6-11, 1977).
5. Sutton, O. G., Micrometeorology, McGraw-Hill Book Company, New York (1953).
6. Thornthwaite and Holzman, cited in Reference 2.
7. Brooks, R. A. and W. O. Pruitt, "Investigation of Energy, Momentum and Mass Transfer near the Ground," Final Report, 1965, U.S. Army Electronics Command, Atmospheric Sciences Lab., Res. Div., Fort Huachuca, Arizona (June, 1966), pp. 39-42.
8. Thibodeaux, L. J., A.I.Ch.E. meeting, New Orleans, La (November, 1981).
9. Bibbero, R. J. and I. G. Young, "Systems Approach to Air Pollution Control," John Wiley & Sons, Inc. (1974).
10. Li, Wen-Hsiung; "Differential Equation of Hydraulic Transients, Dispersion, and Ground-Water Flow", Prentice-Hall.
11. Eskinazi, S., "Fluid Mechanics and Thermodynamics of our Environment," Academic Press, New York, pp. 83-129.
12. Businger, J. A., "Turbulent Transfer in the Atmospheric Subsurface Layer," *Workshop on Micrometeorology*, Duane A. Haugen, ed., American Meteorological Society, Boston, Mass. (1973), pp. 67-100.
13. Abramowitz, M. and I. A. Stegun, eds., "Handbook of Mathematical Functions," Dover Publications, Inc., New York (1965).
14. Cowherd, C., Jr., "Measurement of Fugitive Particulates," EPA-600/7-77-148, Second Symposium on Fugitive Emissions: Measurement and Control, May, 1977, Houston, Texas.
15. Peters, J. A., K. M. Tackett, and E. C. Eimutis, "Measurement of Fugitive Hydrocarbon Emissions from A Chemical Waste Disposal Site," Proc. Nat. Conf. on Management of Uncontrolled Hazardous Waste Sites, October 28-30, 1981, Wash., D.C.
16. Straus, M. A., "Hazardous Waste Management Facilities in the United States—1977," U.S. EPA, SW-146.3, 1977.
17. U.S. EPA, "Collection and Analysis of Purgeable Organics Emitted from Wastewater Treatment Plant," EPA-600/2-80-017, MERL, USEPA, Cincinnati, Ohio
18. Electric Power Research Institute, "Biogenic Sulfur Emissions in the SURE Region," EA-1516, Palo Alto, California, 1978.

Seong T. Hwang, is a Chemical Engineer with the Office of Solid Waste with U.S. Environmental Protection Agency. He received his B.S., M.S., and Ph.D. in chemical engineering from the University of Michigan.

L. J. Thibodeaux received his B.S. (1962) from the Department of Petroleum Engineering, Louisiana State University, Baton Rouge.

As a teacher, he is involved primarily with the graduate program and teaches advance mass transport and transport processes in the exterior environment. In the latter area he has written a test book entitled "Chemodynamics," published by J. Wiley, appearing in Summer 1979.

He has served as a consultant and has rendered expert service to several state and national chemical companies, mainly in the areas of environmental engineering. He is a member of several professional and honorary organizations and is a Registered Professional Engineer in the States of AK and LA. He served as University of Arkansas Chapter President of Sigma Xi for the years 1977-78.

Coal-Gas Cleanup Facility

An experimental unit employing the Benfield system adequately scrubs sulfur compounds over a wide range of gas compositions and operating conditions.

D. M. Rib, S. G. Kimura, and D. P. Smith, General Electric Corporate Research & Development, Schenectady, N.Y. 12301

The integrated coal-gasification, combined-cycle (IGCC) power-generation concept [*1, 2, 3*] has the potential for achieving high energy efficiency with minimal environmental intrusion. In order to achieve the advantages of the IGCC concept, however, it must be shown that the gas-cleanup process, in which the coal gas is scrubbed of components harmful to the downstream machinery and to the environment, can be performed effectively and efficiently. In this paper, operating results of a PDU-scale gas-cleanup system, which contains all the critical unit operations which will be utilized in a commercial IGCC gas-cleanup system, are described and their ability to meet performance requirements evaluated.

A schematic diagram of an IGCC gas-cleanup plant is shown in Figure 1. The coal gas exiting the gasifier, in the case of a fixed-bed gasifier, or the high-temperature

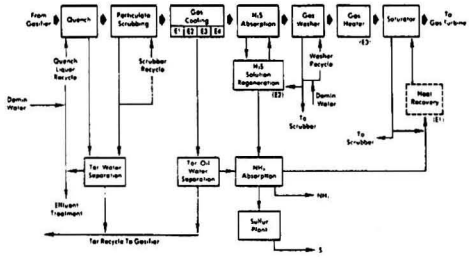

Figure 1. Low-Btu gas-cleanup systems: commercial design.

steam-generation process for an entrained-bed gasifier, is adiabatically quenched and scrubbed of particles and tar-mist. The gas is then cooled in a series of regenerative heat exchangers, which also provide heat to the heat-recovery process which occurs after sulfur scrubbing. The H_2S present in the coal gas is then scrubbed using a liquid absorption process such as the Selexol physical absorbent, Benfield aqueous K_2CO_3, or Stretford redox processes. Desulfurization, of course, is one of the primary reasons for the use of coal gasification for power generation, and it is the area upon which much of this paper will be focused. After desulfurization, the gas may be water-washed to prevent the possibility of carryover of corrosive absorbents during upsets. In the final, critical step, the gas is reheated and resaturated utilizing the condensate formed during the gas-cooling process, which has been heated by indirect heat exchange with the cooling-scrubber exit gas. When hydrocarbons are present, this step also is utilized to recover condensed light hydrocarbons to enable full use of the heating value of these hydrocarbons. It is also possible, however, that prior to use for resaturation, the condensate will need to be stripped of ammonia to prevent the introduction of NH_3, which will be nearly quantitatively converted to NOx upon combustion.

EXPERIMENTAL FACILITY

The General Electric PDU-scale Integrated Gasification Combined Cycle (IGCC) power-plant simulation facility contains the major elements of a commercial IGCC. The gas-cleanup system, which contains all the key elements of the proposed full-scale system, is shown schematically in Figure 2. The major discrepancy between a full-scale design and the PDU simulation is the number of gas-cooling heat exchangers. The experimental unit also does not contain an ammonia-removal system.

The raw coal gas from a 24 ton/day, advanced, fixed-bed gasifier [4] is quenched in a recirculating deluge quench vessel, in which the bulk of the fines and condensed tars are removed. The gas is scrubbed further with a high-energy Venturi fume scrubber to remove the remaining particles and tar. Two heat exchangers are utilized to cool the coal gas to the H_2S-scrubbing temperature. These can be controlled to allow either heat exchanger to take any fraction of the total cooling load. Condensates containing light oils and tars formed during cooling are sent to separate decanters. The H_2S-scrubbing system, which will be

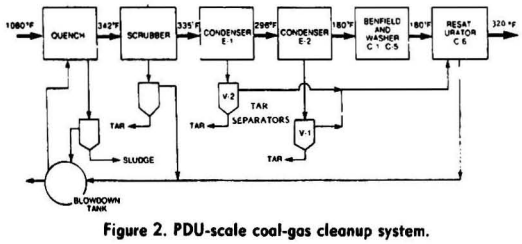

Figure 2. PDU-scale coal-gas cleanup system.

described in greater detail in a later section, is a two-stage Benfield hot potassium-carbonate system. Following the Benfield absorber is a water-wash column to prevent the possibility of absorbent carryover. After slight reheating of the gas in a steam heat exchanger, the gas is reheated and resaturated with the decanted condensate. Typical temperatures of the gas, shown on Figure 2, are set to approximately close the gas-cleanup system water balance.

During operation the gas is sampled on-line with two gas chromatographs and a mass spectrometer. All significant liquid and gaseous process streams are sampled to determine their condensibles composition. The particulate scrubber inlet, outlet, and the gas-cleanup system outlet are also sampled for particulate and alkali-metal loading.

The critical steps in gas cleanup which largely determine the viability of the process—the Benfield H_2S-scrubbing process, resaturation, and particulate scrubbing—have been experimentally evaluated.

OPERATION AND RESULTS

Benfield System

The Benfield acid-gas removal system [5] utilizes an aqueous K_2CO_3 absorbent, operated at elevated temperature. Absorption of the acid gases, H_2S and CO_2, is by the following reactions:

$$H_2S + CO_3^{=} \rightleftarrows HS^- + HCO_3^- \quad (1)$$

$$CO_2 + H_2O + CO_3^{=} \rightleftarrows 2HCO_3^- \quad (2)$$

COS can also be removed through hydrolysis to H_2S and subsequent absorption as H_2S:

$$COS + H_2O \rightarrow H_2S + CO_2 \quad (3)$$

Reactions (1) and (2) proceed in the forward direction during absorption and are reversed in the regenerator by steam stripping or reboiling.

It is known that, at low temperatures (<90°C), H_2S absorption by Reaction (1) is mass-transfer limited since the reaction rate is rapid. CO_2 absorption, however, is reaction-rate limited. Thus, at relatively low temperatures, absorbent selectivity for H_2S over CO_2 can be achieved. As the absorption temperature is increased, the CO_2 reaction rate increases and the selectivity is reduced. Kimura *et al.* [6] have shown this effect dramatically in an absorption-rate study utilizing thin, aqueous carbonate films. Thus, in order to achieve high selectivity, which is desirable from both power-generation and sulfur-conversion considerations, a low operating temperature is utilized.

In order to achieve maximum sulfur removal, however, Reaction (3) for removal of COS must be promoted. The hydrolysis reaction rate is increased with increasing temperature, and COS removal is improved. Since COS typically comprises from 5 to 10% of the total sulfur species in the gas, its removal efficiency may often set a limit on the total sulfur-scrubbing efficiency.

A third consideration in choosing the operating temperature is that of absorbent degradation caused by the formation of formate ion due to the high concentration of CO in the fuel gas. Formate, the anion of formic acid, neutralizes the absorbent, necessitating absorbent replacement. Higher temperatures result in an increased formate-ion formation rate.

Thus, the choice of an operating temperature, typically 85-120°C, for the Benfield system must be made so as to optimize overall performance while achieving overall sulfur-removal goals. The PDU Benfield H_2S-scrubbing system is operated at 85°C to achieve high selectivity.

The PDU Benfield H_2S-scrubbing system is shown schematically in Figure 3. In the split-flow configuration a portion of the absorbent is partially regenerated (semi-lean solution) and is introduced at an intermediate point in the absorber. The remainder of the absorbent is then fully

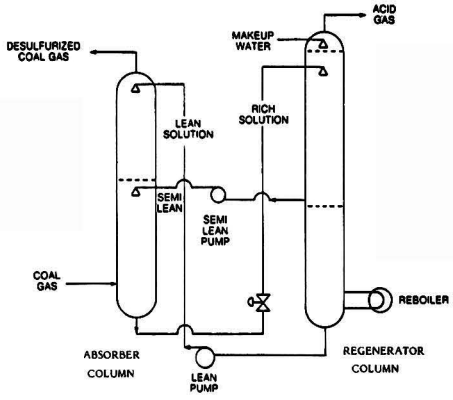

Figure 3. Split-flow Benfield process.

regenerated (lean solution) and introduced at the top of the absorber. Regeneration is accomplished through a combination of pressure reduction and reboiling in a thermosyphon reboiler. In the experimental facility the flow rates of the lean and semi-lean solution and steam flow to the reboiler can be independently varied to enable the characterization of acid-gas scrubbing performance as a function of these operating parameters. Additionally, the inlet gas temperature can be varied if temperature effects are to be investigated.

At nominal design flow and gas-composition conditions (Table 1) the Benfield system was designed to achieve 90% total-sulfur (H_2S + COS) removal. It has been previously reported that sulfur-removal specifications were exceeded under these conditions [5]. During the period of operation described in this paper, the gas flow was approximately 7 to 13% below design flow rate, and the sulfur content was typically 2600 to 3200 ppm, as compared with a design concentration of 6000 to 7000 ppm. Additionally, during this period of operation, the gas composition was varied by changing the steam-to-air ratio.

The effect of varying the three variable operating parameters—lean and semi-lean solution flow and reboiler steam—and the effect of gas composition on Benfield system performance was investigated experimentally. The flow rates are reported as a percent of the design flow, and have been normalized to the actual gas flow rate. Thus, if the total gas flow is 10% below the design flow rate, all operating parameters are reduced by 10% below the design point, and the adjusted conditions are referred to as 100% of design.

TABLE 1

Nominal Design Operating Conditions

Coal feed rate	0.26 kg/sec (1 ton/hr)
Steam/air	0.2 kg/kg
Air/dry coal	2.32 kg/kg
Coal type	Illinois #6
Pressure	21.4 atmospheres

Nominal Gas Composition

H_2	19.4% dry basis
CO	24.3%
CO_2	7.0%
N_2	47.2%
CH_4	3.5%
H_2S	6000 ppmv
COS	500 ppmv
Other	1.6%
Water	12%

The effect of varying the steam-to-air ratio in the gasifier blast on gas composition is shown in Table 2. Of greatest significance to the operation of the Benfield H_2S-scrubbing system is the CO_2 concentration. As the steam-to-air ratio is increased from 0.2 to 0.6 kg/kg, the nominal CO_2 concentration in the coal gas is increased from 6.4 to 17.1%. In Figure 4, the effect of the variations in CO_2 content on H_2S can be seen. At the same absorbent circulation rate and reboiler steam input, increasing the CO_2 content from 7% to 17% at the same H_2S level results in a reduction in H_2S scrubbing efficiency from approximately 95% to 90%. This is not unexpected, since the absorptions of H_2S and CO_2 are competing reactions. Over the range of CO_2 concentrations, CO_2 removal is also an inverse function of CO_2 concentration due to the effect of loading of the absorbent.

Figure 5 shows the variation in H_2S and CO_2 removal with a variation in the reboiler steam flow rate. The CO_2 content was in the range of 11 to 12% for these test points. While solution flows were at 100%, the H_2S removal increased from 88 to 95% over an increase in reboiler steam from 80 to 120%. Over the same range of reboiler steam flow rates, the CO_2 removal increased from 33 to 36%. This increased acid-gas removal efficiency is, of course, due to the increased efficiency of regeneration in increased stripping-steam flow. Thus, it can be seen that improvements in H_2S removal, if required, can be achieved by increasing the reboiler heat input. Similar results were obtained at both 100% lean absorbent flow rate and 60% flow rate, at which the H_2S removal was consistently lower, but affected in a similar manner by reboiler steam input.

The effect of the lean-absorbent flow rate on the acid-gas removal efficiency is shown in Figure 6. For these gas compositions (11.1-11.9% CO_2, 2600-3200 ppm H_2S) the H_2S-removal declines from 92 to 85% as the lean absorbent flow decreases from 100 to 40% of the design flow. Over the same range of lean-absorbent flow rates, the CO_2 removal declines from 33% to 20%. Because of the much higher CO_2 concentration than H_2S concentration in the feed gas, this represents a much larger change in total moles of CO_2 removed.

In Figure 7 the effect of varying the semi-lean solution flow on acid-gas removal is shown. It is particularly interesting to note the difference in response to semi-lean flow for the 60% and 100% lean-solution flow cases. At a lean-solution flow rate which is 100% of the design flow, there appears to be very little effect of semi-lean flow over the range of 60 to 100% of design on either H_2S or CO_2 removal. At a 60% of design lean-solution flow rate, however, there is a substantial effect of semi-lean solution flow rate. This observation may be due to the relative absorbent loadings in the upper and lower sections of the absorber, or simply to the fact that in the 60% lean-flow case, the total absorbent flow is reduced, so that the absorber is operating in the regime in which the sensitivity to flow rate is greater. Further experimentation in which gas compositions at intermediate points in the absorber are measured will be required in order to definitely explain this result.

TABLE 2. GAS COMPOSITIONS FOR RUN PERIOD

	Steam/Air, kg/kg		
	0.2	0.4	0.6
	—	—	—
H_2, %	17.1	20.5	21.6
CO, %	24.6	18.0	9.8
CO_2, %	6.4	11.5	17.1
N_2, %	47.4	45.0	46.1
CH_4, %	3.8	4.2	4.5
H_2S, %	.3	.3	.3
COS, ppm	216	143	106

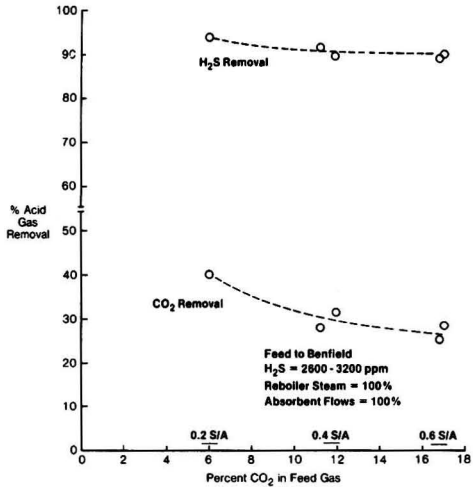

Figure 4. Effect of steam-to-air ratio on Benfield performance.

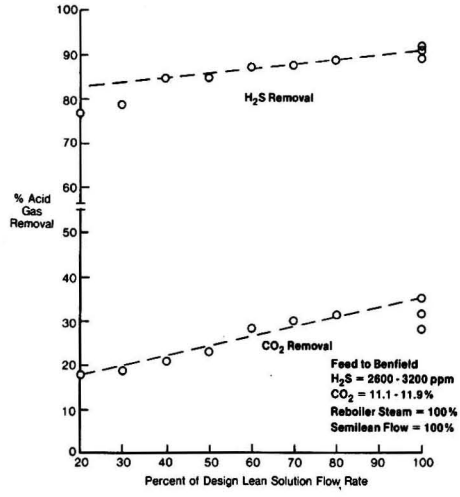

Figure 6. Effect of lean-absorbent flow on acid-gas removal.

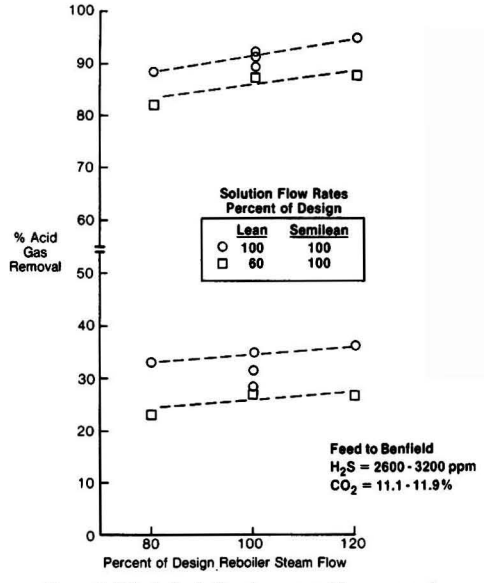

Figure 5. Effect of reboiler steam on acid-gas removal.

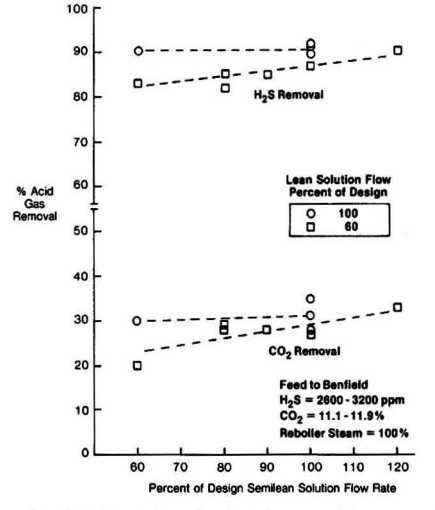

Figure 7. Effect of semi-lean absorbent flow on acid-gas removal.

The results of this experimental investigation permit the optimization of the H_2S-removal process for minimum energy utilization while maintaining acceptable sulfur-discharge levels.

Despite the somewhat reduced H_2S levels during the reporting period, the Benfield process was able to maintain good sulfur removal (~90%) while maintaining better than specified H_2S/CO_2 selectivity. Generally, 70% of the CO_2 was retained in the product gas as compared with a design removal of about 50%.

The COS concentration was generally in the range of 100-250 ppm, or about 3 to 7% of the sulfur species. This seemed to decrease with increasing steam-to-air ratio. It had been expected that about 50% of the COS would be removed by *in-situ* hydrolysis to COS, and removal as H_2S. In general, however, 30 to 40% is removed, thus requiring 91 to 92% H_2S removal to achieve an overall removal efficiency of 90% sulfur.

RESATURATOR PERFORMANCE

The resaturator performance is critical to the overall fuels-plant and power-plant cost and efficiency since it, to a large extent, determines the volume of effluent water requiring treatment, and the recovery of condensed-hydrocarbon heating values in the product gas. The scrubbed H_2S-free, and slightly superheated, gas enters the resaturator at approximately 115°C (240°F), where it is countercurrently contacted with the heated condensate stream (165°C (339°F)). The resultant gas is saturated at a temperature of approximately 160°C (320°F).

The important performance characteristics of the resaturator are its heat and mass efficiency for water, the efficiency of light-hydrocarbons recovery, and fouling tendency, due to the presence of some tar.

The resaturator is shown schematically in Figure 8 with typical operating temperatures. Typical temperature differentials between the entering liquid and product gas are from 1 to 2°C, indicating excellent heat and mass transfer.

A hydrocarbon balance was determined by measurement of the tars, oils, and phenols in the resaturator inlet and exit streams. It was determined that over 90% of the

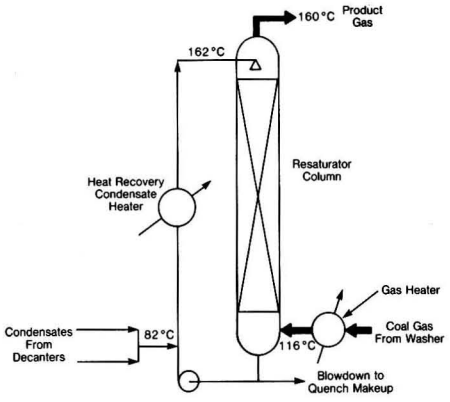

Figure 8. Schematic diagram of resaturator.

phenols in the resaturator feed were evaporated into the product gas. Nearly 100% of the light oils was recovered in the product gas, although substantial quantities of tars were found in the resaturator blowdown stream. This tar was probably a result of incomplete tar separation in the decanter vessel. It is encouraging that, despite the presence of this large quantity of tar, no fouling or loss of performance of the resaturator was observed.

Several samples of the resaturator liquid were tested for pH, and the results were in the range of pH 8-8.5. Although the samples were cooled before depressurization, most of the volatile acid gases, which are mainly CO_2 and H_2S, are flashed. Equilibrium calculations predict that the actual pH of the hot, pressurized resaturator liquid is closer to pH 7. There had been some concern that acid buildup would occur during resaturator operation and cause corrosion problems. This acidity might result from the presence of dissolved acid gases, and from the formation of formic acid due to the carbon-monoxide content in the coal gas. However, the pH of the resaturator samples indicates that this acid buildup did not occur.

PARTICULATE AND ALKALI MEASUREMENTS

Particulate and alkali-metal loadings of the coal gas were determined at the Venturi scrubber inlet and outlet and the resaturator exit. Samples were withdrawn from the main gas stream through heated lines and passed through submicron filters as described by Zarchy [8]. Results are summarized in Table 3.

It can be seen that, despite a considerable range of particulate and alkali-metal loadings, which were caused by wide variations in operating conditions and, in particular, quench variations, in general the final product-gas particulate and alkali-metal loadings are substantially below the gas-turbine specifications of 100 parts per million of particulates and 100 parts per billion of alkali metals (Na + K). Under normal operating conditions, it is expected that the particulate and alkali-metal contents of the gas stream will be at the low end of the ranges shown in Table 3.

CONCLUSIONS

The PDU-Scale Integrated Gasification Combined Cycle experimental facility has been operated, and the critical operations in the gas-cleanup process characterized. The Benfield system has been shown to adequately scrub sulfur compounds over a wide range of gas compositions and operating conditions. The particulate and alkali levels in the product gas are well within the acceptable range for existing gas-turbine fuel specifications. The resaturation process, which is important to minimize effluent water as well as to ensure recovery of light condensible hydrocarbons, has been successfully demonstrated.

ACKNOWLEDGMENTS

The work described in this paper was performed under Department of Energy Contract DE-AC01-80ET14928.

LITERATURE CITED

1. "Energy Conversion Alternatives Study-Phase II," NASA-CR-134949, General Electric Co., (December, 1976).
2. "Economic Studies of Coal Gasification Combined Cycle Systems for Electric Power Generation," EPRI-AF-642, (January, 1978).
3. Kimura, S. G., C. K. Neulander, R. C. Sheldon, and H. A. Quazi, "Low Btu Gas Purification for Combined Cycle Power Generation," Spring 1979 National AIChE Meeting, (April, 1979).
4. Furman, A. H. and N. T. Cankurt, "Effect of Deep Bed Stirring on Fixed Bed Reactor Operation," Spring 1981 National AIChE Meeting, (April, 1981).
5. McCrea, D. H. and J. H. Field, "The Purification of Coal Derived Gases: Applicability and Economics of the Benfield Processes," 78th National Meeting, AIChE, (August, 1974).
6. Kimura, S. G., "Permselection Membranes for Acid Gas Scrubbing for Coal Gas," Proceedings of the Ninth Synthetic Pipeline Gas Symposium, (October, 1977).
7. Neulander, C. K., "A Coal Gas Cleanup Process Evaluation Facility," Spring 1981 National AIChE Meeting, (April, 1981).
8. Neulander, C. K., G. E. Walmet, and A. S. Zarchy, "Particulate Sampling of Low Btu Gas," Proceedings of the 1980 Symposium on Instrumentation and Control for Fossil Energy Processes, (June, 1980).

David M. Rib has been with General Electric for three years. In his present position, Gasification Process Engineer, for the IGCC Process Evaluation Facility, he has been involved in test planning, system operation, and analysis of performance of the coal gas cleanup system. He earned his B.S.Ch.E. at the University of Maryland in 1979 and a M.Eng.ME. from Rensselaer Polytechnic Institute in 1982.

TABLE 3. PARTICULATE SAMPLING RESULTS

	Scrubber Inlet	Scrubber Exit	Resaturator Exit
Total Particulates (ppmw)	394 (150-1000)	119 (20-300)	2.7 (0.4-8)
Potassium:			
Acid soluble	0.43 (0.1-1.4)	0.11 (0.02-0.3)	0.03 (0.005-0.15)
Water soluble	0.12 (0.03-0.2)	0.02 (0.005-0.1)	0.01 (0.005-0.02)
Sodium:			
Acid soluble	0.07 (0.03-0.2)	0.03 (0.005-0.14)	0.005 (0.002-0.02)
Water soluble	0.02 (0.02-0.06)	0.006 (0.002-0.02)	0.002 (0.002-0.005)

Average particulate loadings in parts per million by weight.
Ranges shown in parentheses.

Shiro Gene Kimura has been manager of the Emissions Control Unit since 1975. He had responsibility for the design and construction of the IGCC Process Evaluation Facility gas cleanup system, and is responsible for engineering analysis. He holds seven U.S. patents and has written approximately twenty papers on membrane separations and coal gas purification. He earned a B.S.Ch.E. from the University of California, Berkeley in 1964 and a M.S.Ch.E. from Pennsylvania State University in 1967.

Daniel P. Smith was appointed Manager, Process Operations Unit, at General Electric's Corporate Research & Development Center in 1980 following eight years of managerial responsibility for advanced gas turbine development at G.E. In his present position he directs the operation of the IGCC Process Evaluation Facility and is responsible for engineering system enhancements and modifications. He has authored several papers in the areas of advanced gas turbines, gas turbine fuels, and performance testing and is the holder of one U.S. patent. He received a B.A. in Physics from Cornell University in 1969.

A New Look at Chimney Design

Maximum concentration formulas make it possible to limit ground-level concentrations of pollutants.

Karl B. Schnelle, Jr. and Karl D. Schnelle, Vanderbilt University, Nashville, Tenn. 37235

In the past decade, federal and state air-pollution control regulations have been written which require atmospheric modelling as a part of the permit process for construction of a new source of potential pollution. The main objective of this modelling is the determination of maximum concentration and the location of the maximum. Algorithms have been prepared based on the Gaussian diffusion model and the Briggs plume-rise model. These algorithms have been used to write numerous computer programs to carry out the required calculations. Reasonably large-scale computer facilities are required to use these programs.

In this paper an updated algorithm is presented for a rapid calculation under unlimited mixing conditions of the maximum short-time average ground-level concentrations of air pollutants emitted from a large source in a rural area and the location of the maximum. The models employed are those most currently recommended by the United States Environmental Protection Agency (EPA) [*1*] and used in the MPTER computer program. The information is presented in the form of mathematical equations and plots from which the maximum can readily be determined by use of a hand-held calculator in combination with several charts or graphs. The techniques presented can be used as a screening process to determine if it is necessary to carry out a more thorough analysis. Moreover, the techniques described in this paper could be considered an updating of the work most commonly called "Turner's Workbook" [*2*]. However, unlike the workbook, which designates ten-minute average concentrations, it should be considered that hourly average concentrations are determined by the models presented.

REVIEW OF EARLIER WORK ON MAXIMUM EQUATIONS

Many authors have presented work similar to that reported in this paper. However, no one has carried out the process following the MPTER algorithm. Gifford [*3*] developed an alignment chart or nomograph for similar calculations, and Montgomery *et al.* [*4*] prepared a modified version applicable to emissions from large power plants. The nomographs in these papers were drawn to estimate plume rise and effective emission height from one plot, and then concentration from another. In the case of Montgomery *et al.*, three dispersion models are graphed: coning, inversion breakup, and trapping. "Turner's Workbook" [*2*] presents the Gaussian model for many conditions in analytical and graphical form. In one case Turner presents a plot of maximum-concentration *versus* distance-to-maximum as a function of six stability categories with effective emission height as a parameter. This plot is used as a model for the plots found in this paper.

In his book, "Turbulent Diffusion in the Environment," Csanady [*5*] develops equations for atmospheric diffusion. He finds the critical wind speed (that value which produces the highest ground-level concentration) by first writing dimensionless equations, finding the maximum concentration with respect to distance by differentiation, and then graphically finding the maximum with respect to wind speed. Ragland [*6*] also presents equations for the maximum concentration, and carries out maximization with respect to distance and velocity analytically. However, he uses neither the EPA dispersion coefficients (sigma values) nor the Briggs technique for plume rise. Nevertheless, the maximized equations and graphs developed by Csanady and Ragland agree with those equations which are derived for this paper. Ragland also presents equations for the case of trapping, which is a limited mixing condition.

Baasel [*7*] presents a technique for calculating the maximum concentration, which depends upon linearizing the plume-rise equations. The technique is most certainly an acceptable process, but it is not related to the MPTER algorithm which is followed in this paper.

THE MPTER ALGORITHM AND BASIC FORMULAS

The MPTER (EPA) [*1*] algorithm is a multiple point-source dispersion model for use in rural areas. It employs a Gaussian model, time-averaged in both the horizontal and vertical directions through the dispersing plume. It is assumed that the plumes are continuous and diluted upon release by the wind at chimney top. Concentration estimates are made for each hourly period using the mean meteorological conditions appropriate for each hour. Total concentration at a receptor can be calculated as the sum of the concentrations estimated at the receptor from each source. Concentrations at a receptor for periods larger than an hour can be determined by averaging the hourly concentrations over the period. Equations to estimate the concentration are selected depending upon the stability class

and, for neutral or unstable conditions, depending upon the relation of the vertical dispersion parameter value to the mixing height. The location of the receptor relative to the plume position is a dominant factor determining the magnitude of the concentration.

The dispersion coefficients used are the Pasquill-Gifford values representative of open country where the roughness factor has a value of about 0.3 m. Except for stable layers aloft, which inhibit vertical dispersion, the atmosphere is treated as a single layer in the vertical direction that has the same rate of vertical dispersion throughout. Complete eddy reflection is assumed both from the ground and from the stable layer aloft, which is defined by the mixing height for neutral and unstable stabilities. The entire plume is reflected if the effective plume height is below the mixing height, and is assumed to be within the stable layer aloft if the effective plume height is above the mixing height.

The MPTER algorithm can utilize hourly source emissions which allow for consideration of diurnal, weekday, or weekend source-emission variations. The meteorological data, consisting of wind direction, wind speed, temperature, stability class, and mixing height for each hour, should be representative of the region being modeled. Wind speed is converted from the measured anemometer height to the chimney top using power-law wind-speed profiles with the exponent dependent on stability.

Plume rise is calculated by the methods of Briggs. Although the plume rise from point sources is usually dominated by buoyancy, plume rise due to momentum is also considered. Downwash behind chimneys is calculated from a simple correction formula which compares wind speed and chimney exit velocity. Building downwash is not considered. Chemical reaction in the plume, resulting in a loss of pollutant throughout the entire depth of the plume, can be approximated by MPTER. Depletion is accounted for by an exponential decay and is representative of a realistic loss through the whole plume, without dependence on concentration.

There are four special features as options in MPTER. Terrain adjustment is made by considering the differences between local ground-level elevation at the chimney and at the receptor. The user enters terrain-adjustment factors based on the six Pasquill stability classes. The adjustment is limited to receptors whose ground-level elevation is less than the elevation of the lowest chimney top used in the computation. This terrain adjustment is very simple and does not reflect results from recent model studies by Hunt and Snyder [8] which show an obvious, more sophisticated, relationship to factors directly related to fluid mechanics.

The other three options of MPTER are associated with plume rise. The option to account for chimney downwash has been maintained. Because potentially high concentrations can be found during the initial stages of plume rise, an option to calculate concentrations within this region is provided. Since the plume axis is not horizontal during the rising phase, this option allows dispersion to take place perpendicular to the plume axis. By making calculations with and without this gradual plume rise, it is possible to identify the points of possible high concentrations.

The final option, called buoyancy-induced dispersion, accounts for growth of the plume during the plume-rise phase due to the turbulent motions associated with the conditions of plume release and the turbulent entrainment of ambient air. This dispersion will generally have little effect upon maximum concentrations unless the chimney height is small compared to the plume rise.

Unlimited Mixing Model

Although the MPTER algorithm provides for the presence of a stable layer of air, limiting mixing in the vertical direction, the maximum formulas discussed in this paper do not take limited mixing into account. Thus, the discussion of the mathematical model is begun with the usual bi-gaussian dispersion formula:

$$\bar{C} = \frac{Q}{2\pi \bar{u}_h \sigma_y \sigma_z} \exp\left[-\frac{1}{2}\left(\frac{y}{\sigma_y}\right)^2\right] \left\{\exp\left[-\frac{1}{2}\left(\frac{z-H}{\sigma_z}\right)^2\right] + \exp\left[-\frac{1}{2}\left(\frac{z+H}{\sigma_z}\right)^2\right]\right\} \quad (1)$$

It is this mathematical model which is maximized with respect to distance and wind speed.

Correction of Wind Speed to Stack Height

Wind speeds and directions are those reported by the National Weather Service. The observations are actually averages of a few minutes, usually taken 5 to 10 minutes before the hour and reported as hourly averages.

Emissions from continuous sources are diluted by the wind at chimney top, the concentration being inversely proportional to the wind speed. Measurements of the wind speed are made by anemometer, most usually at an elevation different from that of the chimney top. Thus, it is appropriate to correct the wind speed from anomometer height to chimney top. The MPTER algorithm uses the following power law to accomplish this correction.

$$\bar{u}_h = \bar{u}_z \left(\frac{h_{s\,\mathrm{act}}}{z_a}\right)^P \quad (2)$$

where the exponent P is a function of stability. Since the dispersion coefficients used in MPTER have greatest validity for a surface roughness of approximately 0.3 m, the exponents used in MPTER are based on this roughness and are taken from Irwin [9] and listed in Table 1.

Plume Rise

Plume rise is based on Briggs models and is well documented in the User's Guide (EPA) [*1, p. 150 to 155*]. A flow chart for the MPTER algorithm using Briggs models is given in Figure 1. The initial consideration is to adjust the wind speed to chimney height as discussed previously and given by Equation 2. It is then decided whether the plume is less dense than the ambient air, in which case it may be buoyancy-dominated. The decision is based on the sign of the temperature difference, $\Delta T = (T_s - T_a)$. With $\Delta T > 0$, the plume may be buoyancy-dominated. However, if $\Delta T \leq 0$, then it is assumed that the plume rise is dominated by momentum.

We now define plume rise in terms of a B factor as given by the following four equations:

$$H = h_s + \Delta h \quad (3)$$

$$H = h_s + \frac{B}{\bar{u}_h} \quad (4)$$

$$\Delta h = \frac{B}{\bar{u}_h} \quad (5)$$

$$B \equiv \bar{u}_h \, \Delta h \quad (6)$$

TABLE 1. POWER LAW EXPONENTS FOR WIND SPEED CORRECTION WITH HEIGHT

Surface roughness = 0.3 m

Stability Class	Value of P
A	0.07
B	0.07
C	0.10
D	0.15
E	0.35
F	0.55

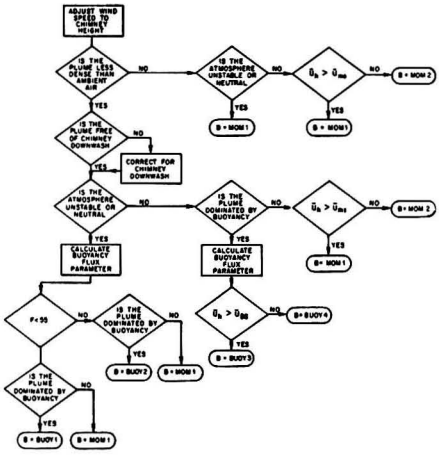

Figure 1. Algorithm for calculation of *B* factor.

For the case where momentum dominates the plume, if the atmosphere is unstable or neutral:

$$\Delta h = \frac{3V_s d_s}{\bar{u}_h} \tag{7}$$

and if the atmosphere is stable we choose either Equation 7 or 8.

$$\Delta h = \frac{1.5}{s^{1/6}} \left[\frac{V_s^2 d_s^2 T_a}{4 T_s \bar{u}_h} \right]^{1/3} \tag{8}$$

whichever gives the lower value for Δh. This equation requires the use of the stability parameter s where

$$s = \frac{g(\Delta\theta/\Delta z)}{T_a} \tag{9}$$

The potential temperature gradient used depends upon the stability category. For the case of E stability, $\Delta\theta/\Delta z = 0.020$ K/m and, for F stability, $\Delta\theta/\Delta z = 0.035$ K/m. A decision between Equations 7 and 8 can be made by setting them equal and solving for the wind speed, $\bar{u}_h$. In this case, $\bar{u}_h$ is defined as $\bar{u}_{ms}$ and given by

$$\bar{u}_{ms} = 5.656\, V_s \left(\frac{d_s T_s}{T_a} \right)^{1/2} s^{1/4} \tag{10}$$

If the actual value of $\bar{u}_h > \bar{u}_{ms}$, then Equation 7 will produce the smaller value of Δh and should be used. Conversely, if $\bar{u}_h \leq \bar{u}_{ms}$, Equation 8 will produce the smaller value of Δh and should be used.

For plumes that may be dominated by buoyancy, a test is first made to determine whether the plume is free of chimney downwash. For chimneys where $V_s \geq 1.5\, \bar{u}_h$, h_s is set equal to $h_{s\text{act}}$. For the case where $V_s < 1.5\, \bar{u}_h$, a reduction in actual stack height is made to correct for the downwash. This correction is given by the following equation:

$$h_s = h_{s\text{act}} + 2[(V_s/\bar{u}_h) - 1.5]d_s \tag{11}$$

Before proceeding, it should be noted that the Briggs plume-rise formula for buoyant plumes depends upon the buoyancy-flux parameter defined by:

$$F = g \frac{V_s d_s^2}{4} \left(\frac{\Delta T}{T_s} \right) \tag{12}$$

The stability of the atmosphere during the expansion of the plume must be determined next. Under stable atmospheric conditions it must then be decided whether the plume is dominated by buoyancy or by momentum. This decision is made by comparing ΔT to the cross-over temperature difference ΔT_c. The cross-over temperature difference in the case of stable conditions is found by setting Equation 8 for momentum plume rise under stable conditions equal to Equation 13 for buoyancy-dominated plume rise under stable conditions and solving for ΔT, which is then designated as ΔT_c.

$$\Delta h = 2.6 \left(\frac{F}{\bar{u}_h s} \right)^{1/3} \tag{13}$$

In this case

$$\Delta T_c = 0.01958\, V_s T_s s^{1/2} \tag{14}$$

If $\Delta T > \Delta T_c$, the plume rise is assumed to be buoyancy-dominated; if $\Delta T \leq \Delta T_c$, the plume rise is assumed to be momentum-dominated. For the case in which the plume is momentum-dominated, Equation 10 is used to select the lower value of Δh in Equations 7 and 8. If the plume is buoyancy-dominated, there is a similar selection process. Plume height is determined by both Equations 13 and 15,

$$\Delta h = 4.0 \frac{F^{1/4}}{s^{3/8}} \tag{15}$$

and the lower of the two values is used. A decision between these two equations can be made by setting them equal and solving for the wind speed, $\bar{u}_h$. This wind speed is designated $\bar{u}_{Bs}$, and is given by

$$\bar{u}_{Bs} = 0.2746\, F^{1/4} s^{1/8} \tag{16}$$

For wind speeds greater than $\bar{u}_{Bs}$ ($\bar{u}_h > \bar{u}_{Bs}$), use Equation 13 for plume rise; for wind speeds less than or equal to $\bar{u}_{Bs}$ ($\bar{u}_h \leq \bar{u}_{Bs}$), use Equation 15.

Proceeding to the unstable and neutral case, first the value of F is calculated. For $F \geq 55$ m^4/s^3, it must be determined if the plume is buoyancy- or momentum-dominated. In this case, the cross-over temperature is found by setting Equation 7, for momentum plume rise under unstable and neutral conditions, equal to Equation 17, for buoyant plume rise under unstable and neutral conditions, with $F \geq 55$ m^4/s^3 and solving for ΔT_c.

$$(F \geq 55 \text{ m}^4/\text{s}^3)\Delta h = 38.71 \frac{F^{3/5}}{\bar{u}_h} \tag{17}$$

$$\Delta T_c = 0.00575 \frac{T_s V_s^{2/3}}{d_s^{1/3}} \tag{18}$$

If $\Delta T > \Delta T_c$, the plume rise is assumed to be buoyancy-dominated; if $\Delta T < \Delta T_c$, the plume rise is assumed to be momentum-dominated. Plume height is given by Equation 17 for buoyancy-dominated plumes and by Equation 7 for momentum-dominated plumes.

A similar process occurs when $F < 55$ m^4/s^3. The buoyant plume rise is given by Equation 19.

$$(F < 55 \text{ m}^4/\text{s}^3)\Delta h = 21.425 \frac{F^{3/4}}{\bar{u}_h} \tag{19}$$

Again, Equation 7 is used for the momentum plume rise under unstable and neutral conditions. Equations 7 and 19 are set equal and the cross-over temperature is calculated.

$$\Delta T_c = 0.0297 \frac{T_s V_s^{1/3}}{d_s^{2/3}} \tag{20}$$

These equations have been summarized in Table 2, where descriptive designations have been given the equations which could be suitable as computer program variable names. Figure 2 is a flow chart of the process for calculating Δh. The flow chart uses the descriptive plume-rise equation names given in Table 2. Table 3 summarizes the data required for use in connection with the flow chart of Figure 2. The differential temperature cross-over equations for determining the plume-rise dependency on momentum or buoyancy are summarized in Table 4. The descriptive variable names in Table 4 are also used in the flow chart of Figure 2.

TABLE 2. PLUME-RISE EQUATIONS AND THE B FACTOR

Type	Stability	Other Conditions	$B = \bar{u}_h \Delta h$	Equation Numbers and Designation
Buoyant	Unstable or neutral	$F < 55\ m^4/s^3$		
	$\Delta h = 21.425 \dfrac{F^{3/4}}{\bar{u}_h}$		$B = 21.425\ F^{3/4}$	Eq. 19 BUOY 1
Buoyant	Unstable or neutral	$F < 55\ m^4/s^3$		
	$\Delta h = 38.71 \dfrac{F^{3/5}}{\bar{u}_h}$		$B = 38.71\ F^{3/5}$	Eq. 17 BUOY 2
Buoyant	Stable	$\bar{u}_h > \bar{u}_{Bs}$		
	$\Delta h = 2.6\left(\dfrac{F}{\bar{u}_h s}\right)^{1.3}$		$B = 2.6\,\bar{u}_h^{1/3}\left(\dfrac{E}{s}\right)^{1/3}$	Eq. 13 BUOY 3
Buoyant	Stable	$\bar{u}_h \le \bar{u}_{Bs}$		
	$\Delta h = 4.0 \dfrac{F^{1/4}}{s^{3/8}}$		$B = 4.0\ \bar{u}_h \dfrac{F^{1/4}}{s^{3/8}}$	Eq. 15 BUOY 4
Momentum	Unstable or neutral			
	$\Delta h = \dfrac{3V_s d_s}{\bar{u}_h}$		$B = 3V_s d_s$	Eq. 7 MOM 1
Momentum	Stable	$\bar{u}_h > \bar{u}_{ms}$		
	Δh = MOM 1		$B = 3V_s d_s$	Eq. 7 MOM 1
Momentum	Stable	$\bar{u}_h \le \bar{u}_{ms}$		
	$\Delta h = \dfrac{1.5\left[\dfrac{V_s^2 d_s^2 T_a}{4T_s}\right]^{1/3}}{s^{1/6}\bar{u}_h}$		$B = \dfrac{1.5\bar{u}_h^{2/3}}{s^{1/6}}\left[\dfrac{V_s d_s^2 T_a}{4T_s}\right]$	Eq. 8 MOM 2

Definitions:

Buoyancy flux Parameter: $F \equiv \dfrac{g V_s d_s^2}{4}\left(\dfrac{\Delta T}{T_s}\right) \qquad \Delta T \equiv T_s - T_a$

Stability parameter: $s \equiv \dfrac{g(\Delta\theta/\Delta z)}{T_a}$

Potential temperature gradient: If measured values are unavailable,

E stability $\dfrac{\Delta\theta}{\Delta z} = 0.020$

F stability $\dfrac{\Delta\theta}{\Delta z} = 0.035$

Velocity parameters for stable conditions:

Buoyant $\bar{u}_{Bs} = 0.2746\ F^{1/4}\ s^{1/8}$ Eq. 16

Momentum $\bar{u}_{ms} = 5.656\ V_s \left(\dfrac{d_s T_s}{T_a}\right)^{1/2} s^{1/4}$ Eq. 10

THE SIGMA DATA

The MPTER algorithm provides for the calculation of dispersion coefficients (sigma values) through a series of analytical equations where the parameters are stability and downwind distance x. The set of sigma values used are those determined by Gifford [*10*] using the methods of Pasquill [*11*]. These dispersion coefficients appear in graphical form in Gifford [*12*] and "Turner's Workbook" [2]. They are most applicable to a surface roughness of 0.3 meters, and are thus consistent with the exponent variation in the wind-speed correction for height, Equation 2.

In order to provide a set of analytical equations that would be simpler to subject to analytical differentiation, both σ_y and σ_z are written in the simple lower-power law, from which follows:

$$\sigma_y = ax^p \tag{21a}$$

$$\sigma_z = ax^q \tag{21b}$$

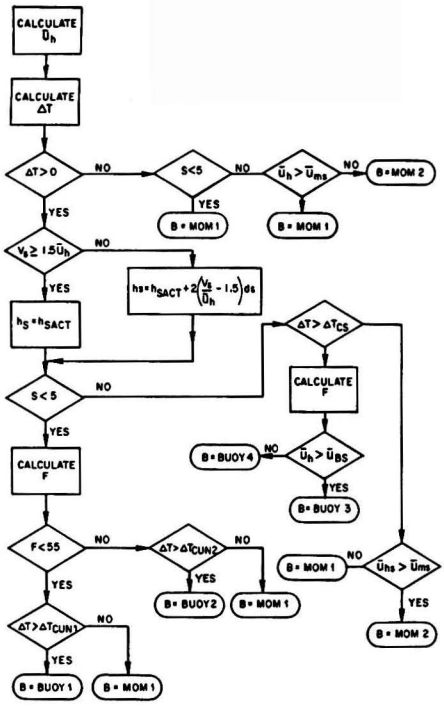

Figure 2. Flow chart for calculation of *B* factor.

The curves from Turner's Workbook were read at a series of downwind distances for each of the six stabilities. The constants a, p, b, and q were determined for each stability from the values read from the Workbook curves. Similar to MPTER, the curves were divided into segments to evaluate the different sets of a, p, b, and q. However, only two or three segments were used as a function of the distance x. The evaluation was carried out through the use of the BASIC computer language CURFIT statistical library program. The constants for Equations 21a and b are reported in Table 5.

It should be noted that the statistical program CURFIT is a linear least-squares parameter-evaluation program that involves a transformation on non-linear equations to the linear form required. Thus, in non-linear equations of the form of Equations 21a or 21b, some data points will be weighted more heavily than others. In order to determine the extent of this bias, and to evaluate the goodness of fit of our equations, values of σ_y and σ_z were calculated at the x distances from which the curves of Turner were originally read, using both our equations and the equations used in MPTER. Comparing the calculated values to the values read, the greatest difference between our calculated values and the values read from the curves was 4.3% (for σ_z at x = 2,000 meters). Most difference values were below ±2.0% with an average difference at about ±1.3%. The MPTER analytical values were a bit better, with the maximum difference from the values read at about 2.7% and the average difference at about ±1.0%. Thus we conclude that the set of parameters in Table 5 for use in Equations 21a and b produce a valid representation of the sigma values used in MPTER.

MAXIMUM FORMULAS AND GRAPHICAL PRESENTATION

Basic Equation

Ground-level concentration is desired, and therefore $z = 0$. Furthermore, the maximum concentration occurs on the center line where $y = 0$. Thus, Equation 1 becomes:

$$\bar{C} = \frac{Q}{\pi \bar{u}_h \sigma_y \sigma_z} \exp\left[-\frac{1}{2}\left(\frac{H}{\sigma_z}\right)\right]^2 \qquad (22)$$

This equation is maximixed first with respect to downwind distance x, where Equations 21a and 21b are used to represent σ_y and σ_z, respectively. The equation is then maximized with respect to wind speed $\bar{u}_h$. It should be noted that the effective emission height given by Equation 3 is directly proportional to the plume rise Δh. In the general case Δh is a function of x. According to theory [13], until the final plume rise is reached $\Delta h \propto x^{2/3}$. Thus, in

TABLE 3. CALCULATION OF *B* FACTOR, DEFINITION AND DATA REQUIREMENTS

Definition:

B Factor

$$H = h_s + \Delta h$$

$$\Delta h = \frac{B}{\bar{u}_h}$$

Thus

$$B \equiv \bar{u}_h \Delta h$$

Data Requirements:

Meteorological

$$T_a,\ \bar{u}_z,\ z_n,\ \frac{\Delta\theta}{\Delta z},\ s$$

Stability by Pasquill-Gifford A B C D E F

$$S \qquad 1\ 2\ 3\ 4\ 5\ 6$$

Source

$$Q,\ h_{sacb},\ V_s,\ t_s,\ d_s$$

Receptor

$$x,\ y,\ z$$

Centerline concentration, y, = 0

Ground-level concentration, z = 0

TABLE 4. DIFFERENTIAL CROSSOVER TEMPERATURE BETWEEN BUOYANCY AND MOMENTUM DOMINATED PLUMES

Unstable or neutral conditions

$$F \geq 55 \text{ m}^4/\text{s}^3$$

$$\Delta T_{crun}1 = 0.0297 \frac{V_s^{1/3} T_s}{d_s^{1/3}} \quad \text{(Eq.20)}$$

$$F \geq 55 \text{ m}^4/\text{s}^3$$

$$\Delta T_{crun}2 = 0.00575 \frac{V_s^{2/3} T_s}{d_s^{1/3}} \quad \text{(Eq. 18)}$$

Stable conditions

$$\Delta T_{cs} = 0.01958\, V_s T_s^{1/2} \quad \text{(Eq. 14)}$$

$\Delta T > \Delta T_{crui}$ plume is buoyant-dominated

$\Delta T \leq \Delta T_{crui}$ plume is momentum-dominated

$$\Delta T \equiv T_s - T_a$$

TABLE 5. CONSTANTS FOR USE IN DIFFUSION PARAMETER EQUATIONS

$$\sigma_y = ax^p \qquad \sigma_z = bx^q$$

Stability Class	Break Points for x	$x <$ first break point				first break point $< x <$ second break point				$x >$ second break point			
		a	p	b	q	a	p	b	q	a	p	b	q
A	300	.4225	.9023	.08930	1.102	.4225	.9023	.006921	1.548	.5904	.8531	2.306 $\times 10^{-4}$	2.098
	500												
B	700	.2800	.9161	.1153	.9805	.4159	.8610	.0573	1 .094	—	—	—	—
C	800	.1739	.9267	.1080	.9171	.2477	.8797	.1170	.9078	—	—	—	—
D	1,000	.1096	.9319	.1054	.8286	.1719	.8744	.4588	.6178	.1719	.8744	1.280	.5118
	10,000												
E	1,000	.09155	.9115	.09962	.7811	.1173	.8842	.5988	.5312	.1173	. 8842	4.564	.3236
	10,000												
F	600	.06072	.9131	.05997	.7960	.07601	.8867	.3062	.5537	.07601	. 8867	3.059	.2984
	7,000												

maximizing Equation 22, we must account for the dependence of H on x.

Maximum with Respect to Downwind Distance x

If Equations 21a and 21b are substituted into Equation 22, and then Equation 22 is differentiated with respect to x and set equal to zero, the following result is obtained:

$$\frac{q}{x}\left(\frac{H(x)}{bx^q}\right)^2 = \frac{p+q}{x} + \left(\frac{H(x)}{(bx^q)^2}\right)\frac{dH(x)}{dx} \quad (23)$$

To proceed, it is assumed that the plume rise has reached its maximum, and thus H is no longer a function of x and $dH(x)/dx = 0$. Equation 23 then becomes

$$\frac{q}{x}\left(\frac{H}{bx^q}\right)^2 = \frac{p+q}{x} \quad (24)$$

which can be solved for

$$\left(\frac{H}{bx^q}\right) = \left(\frac{H}{\sigma_z}\right) = \sqrt{\frac{p+q}{q}} \quad (25)$$

Equation 25 can be solved for the value of x when the concentration is at a maximum.

$$x_{max} = \left[\frac{H}{b\sqrt{\frac{p+q}{q}}}\right]^{1/q} \quad (26)$$

If Equations 21a and b, 25, and 26 are substituted into Equation 22, Equation 27, the maximum concentration with respect to the downwind distance x for any given wind speed $\bar{u}_h$, can be stated:

$$\bar{C}_{max} = \frac{Qb^{(p/q)}\left(\frac{p+q}{q}\right)^{\left(\frac{p+q}{2q}\right)} \exp\left[-\left(\frac{p+q}{2q}\right)\right]}{\pi \bar{u}_h a H^{\left(\frac{p+q}{q}\right)}} \quad (27)$$

This equation can be rewritten:

$$\left[\frac{\bar{C}_{max}\bar{u}_h}{Q}\right] = \frac{b^{(p/q)}\left(\frac{p+q}{q}\right)^{\left(\frac{p+q}{2q}\right)} \exp\left[-\left(\frac{p+q}{2q}\right)\right]}{\pi a H^{\left(\frac{p+q}{q}\right)}} \quad (28)$$

where the right-hand side of this equation and of Equation 26 are functions of the constants π, a, p, b, and q and of the effective emission height H only. Thus x_{max} versus $[\bar{C}_{max}\bar{u}/Q]$ can be plotted with H as a parameter for each stability category for which there is a set of constants. Figure 3 is such a plot and represents the maximum concentration and its location for any given value of the wind speed $\bar{u}$ and the emission rate Q.

Maximum with Respect to Wind Speed

Equation 4 is now substituted for H into Equation 28, with Equation 29 resulting.

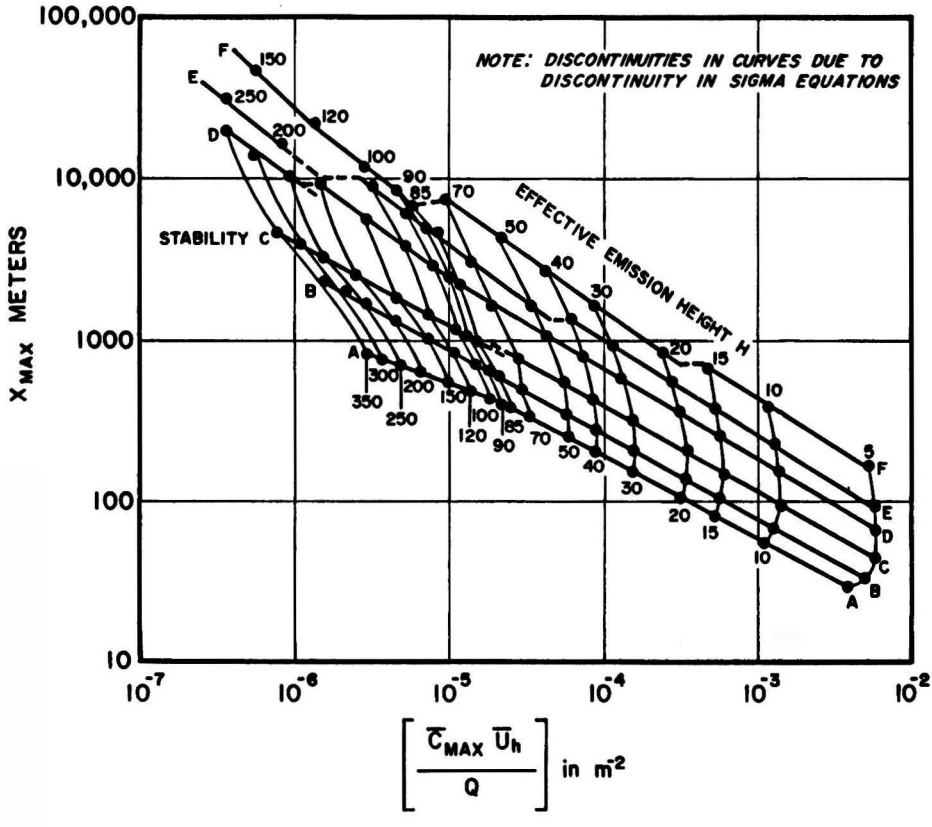

Figure 3. Maximum concentration and downwind distance for any given wind speed and emission rate (Equations 26 and 28).

$$\bar{C}_{max} = \frac{b^{(p/q)}\left(\frac{p+q}{q}\right)^{\left(\frac{p+q}{2q}\right)} \exp\left[-\left(\frac{p+q}{2q}\right)\right]}{\pi a \bar{u}_h \left(h_s + \frac{B}{\bar{u}_h}\right)^{\left(\frac{p+q}{q}\right)}} \tag{29}$$

Note that, in general, B is a power-law function of $\bar{u}_h$, and can be written as follows:

$$B = B_1 \bar{u}_h^n \tag{30}$$

Equation 29 is maximized with respect to $\bar{u}_h$, taking into account Equation 30, setting the derivative equal to zero and solving for $\bar{u}_h$, which is now $\bar{u}_{max}$, the critical maximum wind speed.

$$\bar{u}_{max} = \left\{\left(\frac{h_s}{B_1}\right)\left[\frac{q}{p - n(p+q)}\right]\right\}^{\frac{1}{n-1}} \tag{31}$$

Note that, examining Equation 31 for the case where $p \approx q$, the velocity $\bar{u}_{max}$ becomes:

$$\bar{u}_{max} = \left\{\left(\frac{h_s}{B_1}\right)\left(\frac{1}{1-2n}\right)\right\}^{\frac{1}{n-1}} \tag{32}$$

This equation can produce spurious results if $(1 - 2n) < 0$ or $n > 1/2$. For example, when $n = 2/3, (1 - 2n) = -1/3$ and $(1/n - 1) = -3$. The power of -3 is acceptable but the argument will be negative, thus producing an unacceptable negative value for $\bar{u}_{max}$. This means that using Equation 13 (BUOY 3) or Equation 8 (MOM 2) is questionable. That is, when conditions are stable, this technique fails in some cases for determining the maximum wind speed.

Problems also result when plume rise is not a function of wind speed, as in Equation 15 (BUOY 4) for stable conditions and buoyant plumes. However, Equation 15 is essentially specified for calm conditions, where determining the maximum wind speed is an anomaly. The result of carrying out the differentiation process produces a maximum at infinite wind speed in any case.

Thus, it is apparent that the process for maximizing wind speed using the form of plume rise given by Equation 3 should only be applied in the case where plume rise is inversely proportional to wind speed to the first power. Therefore, Equations 30 and 31 are most applicable when $n = 0$, $B_1 = B$, and

$$\bar{u}_{max} = \left(\frac{B}{h_s}\right)\left(\frac{p}{q}\right) \tag{33}$$

Combining Equation 33 with Equation 4, a maximum value for the effective emission height can be found

$$H_{max} = h_s\left(1 + \frac{q}{p}\right) \tag{34}$$

Equation 34 can be substituted into Equation 26 to find the following equation for location of the maximum

$$x_{max} = \left[\frac{h_s\left(1 + \frac{q}{p}\right)}{b\sqrt{\frac{p+q}{q}}}\right]^{1/q} \tag{35}$$

which can be written for ease of calculation as

$$x_{max} = \left\{\left[\left(\frac{h_s}{b}\right)\frac{1}{(p/q)}\right]^2 2\left(\frac{p+q}{2q}\right)\right\}^{1/2q} \quad (36)$$

One now substitutes Equations 33 and 34 into Equation 27 and rearranges the result into the following equation:

$$\left[\frac{\bar{C}_{max}B}{Q}\right] = \frac{b^{(p/q)}\exp\left[-\left(\frac{p+q}{2q}\right)\right]}{\pi a(p/q)\left[2\left(\frac{p+q}{2q}\right)\frac{1}{(p/q)^2}\right]^{\frac{p+q}{2q}} h_s^{(p/q)}} \quad (37)$$

This equation is similar to Equation 28 and may be plotted as $[\bar{C}_{max}B/Q]$ versus x_{max} from Equation 35 or 36 with h_s as a parameter. The parameter h_s is directly related to chimney height through Equation 11 from $V_s \leq 1.5\ \bar{u}_h$ or $h_s = h_{s\,act}$ for $V_s > 1.5\ \bar{u}_h$. Figures 4a and b are plots of these equations, applicable to all stability conditions with buoyant or momentum-dominated plumes. It should only be applied under stable conditions for the case in which Equation 7 (MOM 1) can be used for calculation of B, to avoid the problem where B is a function of $\bar{u}_h$.

USING THE MAXIMUM FORMULAS FOR DESIGN

The equations developed in this paper can be used to specify chimney height. It is only required to solve the equations for h_s from which $h_{s\,act}$ can be found dependent on the ratio $(V_s/\bar{u}_h)$ as noted previously. It should be recalled that these equations are applicable to single source in a rural setting. All other parameters concerning the chimney must be specified (V_s, T_s, d_s, and 0) as well as the stability conditions and atmospheric temperature, T_a.

Returning to Equation 28, the following definitions are made:

$$A = \frac{b^{(p/q)}\left(\frac{p+q}{q}\right)^{\left(\frac{p+q}{2q}\right)}\exp\left[-\left(\frac{p+q}{2q}\right)\right]}{\pi a} \quad (38)$$

Recall Equation 4,

$$H = h_s + \left(\frac{B}{\bar{u}_h}\right) \quad (4)$$

and substitute Equation 4 into Equation 28 and solve for h_s

$$h_s = \left\{\frac{A}{\left[\frac{\bar{C}_{max}\bar{u}_h}{Q}\right]}\right\}^{\left(\frac{q}{p+q}\right)} - \left(\frac{B}{\bar{u}_h}\right) \quad (39)$$

Equation 39 will give an estimate of h_s for any given value of $\bar{u}_h$ and $\bar{C}_{max}$. The value of $\bar{C}_{max}$ could be chosen to meet some air-pollution standard, for example. Having determined h_s, H can be calculated, and Equation 26 can be used to determine the location of the maximum.

Equation 37 can be used in the same way to determine h_s for maximum wind conditions. In this case A_{max} is defined:

$$A_{max} = \frac{b^{(p/q)}\exp\left[-\left\{\frac{p+q}{2q}\right\}\right]}{\pi a(p/q)\left\{2\left(\frac{p+q}{2q}\right)\left[\frac{1}{(p/q)^2}\right]\right\}^{\frac{p+q}{2q}}} \quad (40)$$

Equation 37 is then solved for h_s:

$$h_s = \left\{\frac{A_{max}}{\left[\frac{\bar{C}_{max}B}{Q}\right]}\right\}^{(q/p)} \quad (41)$$

The maximum wind speed is found from Equation 33 and the location of the maximum from Equations 35 and 36.

INTERACTION WITH GOOD ENGINEERING PRACTICE CHIMNEY HEIGHT

Although the equations in this paper were given for chimneys from which the plumes are unaffected by terrain and building downwash, the chimney height used in these equations or calculated from these equations should be compared to good engineering practice (GEP) chimney height as defined by the EPA [*14*]. The objective of GEP chimney height is to limit the chimney height used in modelling, and not to limit the height of chimney actually constructed. In the case of determining concentration from a given chimney height, the GEP height could be used for $h_{s\,act}$. When calculating chimney height as suggested in the last section from Equations 39 or 41, the reader should recall that the equations developed in this paper were suggested for use only as a screening process to determine whether more sophisticated modelling should be used. Thus it seems reasonable to pursue more sophisticated modelling, especially for the case where Equations 39 or 40 predict chimney heights greater than GEP would allow. In other instances, the use of more sophisticated models would have to be determined on a specific case basis.

ACCURACY AND ERRORS OF THIS ESTIMATE

The "User's Guide for MPTER" [*1*] reports the following possible errors and inaccuracies.

1. Inaccurate source-emission information. Any inaccuracy in chimney-gas exit velocity and temperature and stack diameter will directly affect the calculation of plume rise. Inaccuracies in source strength and chimney height, as well as source and receptor locations, will directly affect the calculation of concentration.
2. Representativeness of the meteorological data. Generally, the greater the distance from the site to be modelled to the location at which the meteorological data are to be measured, the less representative the data. Major terrain features between the modelling site and the measuring site can cause the meteorological data to be quite non-representative (for example, data taken on a plateau and used on a model site in a valley). Wind speed and direction are more subject to terrain induced non-representativeness than are mixing height and stability.
3. Extrapolation of wind speed to chimney top. The exponents used on the wind-speed correction to the chimney height may cause large inaccuracies in concentration. These exponents are functions of stability and, insofar as stability is variable, so will the exponents vary. Since larger vertical variations of the stability are possible, the use of an exponent representing a single stability could introduce large concentration errors. It is noted in the "User's Guide" that, in searching for the maximum, there is less sensitivity to wind-speed differences and power-law exponents than there is to the correct assessment of the stability.
4. Incorrect input of wind direction. The single greatest cause of inaccuracy in the model possibly is the assumption that the direction of wind flow means that direction which is specified by National Weather Service weather-vane measurements taken

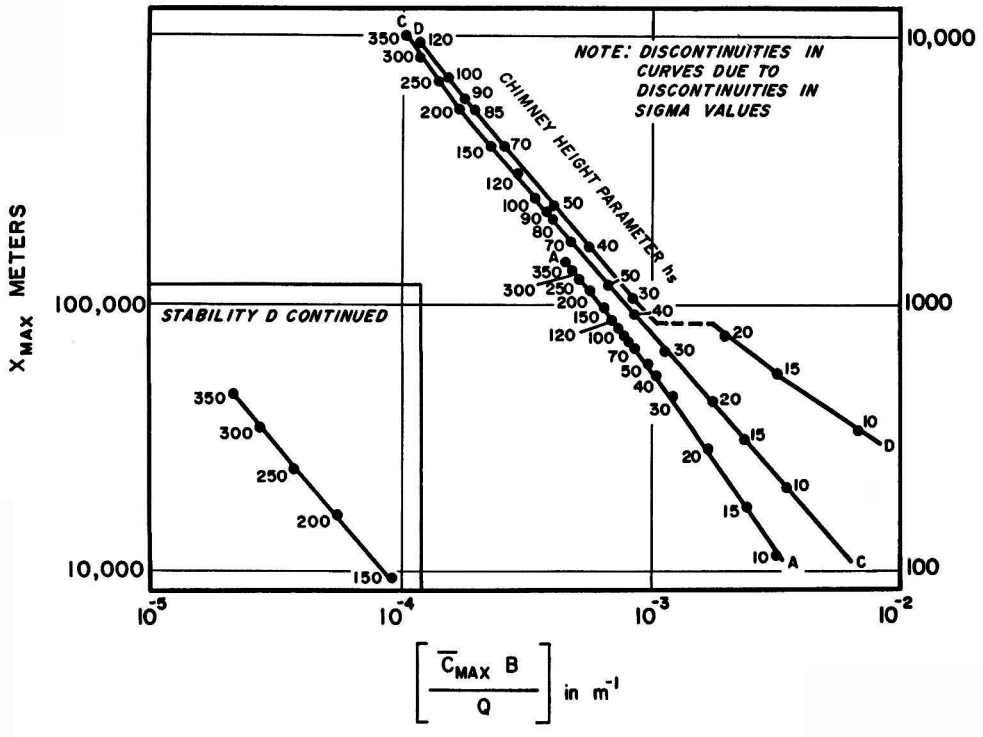

Figure 4a. Maximum concentration and downwind distance at critical wind speed for any given emission rate (Equations 36 and 37) stabilities A, C & D.

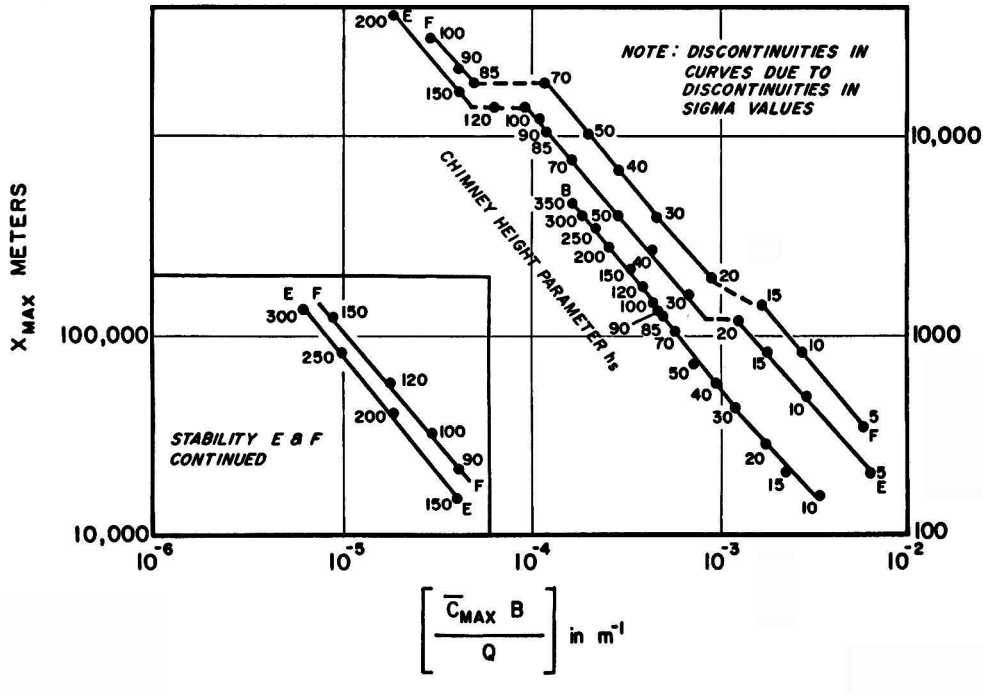

Figure 4b. Maximum concentration and downwind distance at critical wind speed for any given emission rate (Equations 36 and 37) stabilities B, E & F.

near the ground at about the same moment that the wind speed is recorded. In MPTER there is no attempt to account for any wind-directional shear with height due to either the friction-Coriolis force interaction or thermal effects. The greatest inaccuracy caused by neglecting this directional shear is in the hour-to-hour estimates. This potential error would become very important in any attempt to compare short-time average air-quality measurements with model estimates. There may be very little effect on long-time averages (seasonal or annual, for example) and on the estimates of maximum concentration values.

These errors should cause very little inaccuracy in use of the equations presented in this paper for determination of maxima, since this paper does not deal with the direction of the maxima in the calculations, but only with what the magnitude may be. It should be remembered that the techniques presented in this paper are used only as a screening process, or essentially to get first estimates which may be later refined by more sophisticated modelling. Furthermore, even this process is limited in its accuracy by all the factors suggested by the American Meteorological Society's evaluation of atmospheric dispersion models, as reported by Hanna *et al.* [15].

EXAMPLE CALCULATIONS

To illustrate the use of these equations, we can assume that there is a smaller coal-fired power plant with the following data:

Chimney – $h_{s\text{act}} = 84$ m Emissions – 1.890 kg/s of SO_2

$d_s = 4.5$ m

$v_s = 18$ m/s

$T_s = 430$ K

Meteorological data suggest B stability with the following additional required information:

$T_a = 293$ K

$\bar{u}_a = 3.5$ m/s

$z_a = 10$ m

Determine maximum concentration at the given wind speed. (Use of Equation 27)

Following the algorithm and flow sheet given by figures 1 and 2, respectively:

1. Calculate $\bar{u}_h$, B stability, $P = 0.07$ (Table 1).

$$\bar{u}_h = \bar{u}_z \left(\frac{h_{s\text{act}}}{z_a}\right)^P \tag{2}$$

$$\bar{u}_h = 3.5 \left(\frac{84}{10}\right)^{0.07}$$

$$\bar{u}_h = 4.06 \text{ m/s}$$

2. Calculate ΔT

$$\Delta T = T_s - T_a$$

$$\Delta T = 430 - 293$$

$$\Delta T = 137 \text{ K}$$

3. $\Delta T > 0$, therefore determine if $V_s \geq 1.5\ \bar{u}_h$

$$\frac{V_s}{\bar{u}_h} = \frac{18}{4.06} = 4.43 > 1.5$$

4. Set $h_s = h_{s\text{act}} = 84$ m

5. B stability, therefore $S < 5$, calculate F

$$F = g V_s \frac{d_s^2}{4} \left(\frac{\Delta T}{T_s}\right) \tag{12}$$

$$F = \frac{9.80 \times 18 \times (4.5)^2}{4} \left(\frac{137}{430}\right)$$

$$F = 285 \text{ m}^4/\text{s}^3$$

6. $F > 55$ m^4/s^3, therefore calculate ΔT_{run2}

$$\Delta T_{run2} = 0.00575 \frac{V_s^{2/3} T_s}{d_s^{1/3}} \tag{18}$$

$$\Delta T_{run2} = 0.00575 \frac{18^{2/3}\ 430}{4.5^{1/3}}$$

$$\Delta T_{run2} = 10.3 \text{ K}$$

7. Since $\Delta T > \Delta T_{run2}$, B = BUOY 2

$$\text{BUOY 2} = 38.71\ F^{3/5}$$

$$B = 38.71\ (285)^{3/5}$$

$$B = 1150 \text{ m}^2/\text{s}$$

8. Calculate H

$$H = h_s + \Delta h$$

$$\Delta h = \frac{B}{\bar{u}_h}$$

$$\Delta h = \frac{1150}{4.06} = 283 \text{ m}$$

$$H = 84 + 283 = 367 \text{ m}$$

9. Calculate x_{max}

$$x_{max} = \left[\frac{H}{b\sqrt{\frac{p+q}{q}}}\right]^{1/q} \tag{26}$$

From Table 5, assuming $x_{max} > 700$ m

$a = 0.4159$ $p = 0.8610$

$b = 0.0573$ $q = 1.0940$

$$x_{max} = \left[\frac{367}{0.0573\sqrt{\left(\frac{1.9550}{1.0940}\right)}}\right]^{\frac{1}{1.0940}}$$

$$x_{max} = 2.31 \text{ km} > 700 \text{ m}$$

At this point it is well to determine whether the plume has reached its final rise, which is assumed during the derivation of the maximum equations. According to Briggs [13], the final plume rise is reached when

$$x = 3.5x^*$$

where x^* is given by

$$x^* = 14\ F^{5/8} \qquad F < 55$$

$$x^* = 34\ F^{2/5} \qquad F < 55$$

For this case, where $F > 55$

$$x^* = 34\ F^{2/5}$$

$$x^* = 34\ (285)^{2/5}$$

$$x^* = 0.326 \text{ km}$$

$$3.5x^* = 1.14 \text{ km}$$

Since $x_{max} = 2.31$ km, the plume has reached final rise before the maximum point and the equations are valid.

10. Calculate $\bar{C}_{max}$

$$\bar{C}_{max} = \frac{Qb^{(p/q)}\left(\frac{p+q}{q}\right)^{\left(\frac{p+q}{2q}\right)} \exp\left[-\left(\frac{p+q}{2q}\right)\right]}{\pi \bar{u}_h a H^{((p+q)/q)}} \quad (27)$$

$$Q = 1.890 \times 10^9\ ^{+}\mu g/s \qquad H = 367\ m$$

$$\bar{C}_{max} = 674\ \mu g/m^3$$

11. Determine critical wind speed.

By using Equation 27 $\bar{C}_{max}$ can be calculated as a function of $\bar{u}_h$ and the maximum point found. The value of $\bar{u}_h$ at this maximum is the critical wind speed. The following values have been calculated for this case, and are plotted in Figure 5.

$\bar{u}_h$ m/s	$\bar{C}_{max}$ $\mu g/m^3$
2	481
4	669
6	760
8	802
10	817
12	816
14	805
16	789

It should be noted that, when $\bar{u}_h = 14$ m/s, $V_s/\bar{u}_h = 18/14 = 1.29 < 1.50$ and the value of h_s must be reduced due to stack downwash.

$$h_s = h_{s\,act} + 2(V_s/\bar{u}_h - 1.5)d_s$$

$$h_s = 84 + 2(1.29 - 1.50)4.5$$

$$h_s = 82.1\ m$$

For this value of h_s, $\bar{C}_{max} = 822\ g/m^3$ at $\bar{u}_h = 14$ m/s. Carrying on the calculation produces the following results, which are also plotted in Figure 5.

$\bar{u}_h$ m/s	h_s m	$\bar{C}_{max}$ $\mu g/m^3$
14	82.1	822
16	80.6	821
18	79.5	815

Thus, a better maximum concentration might be 822 $\mu g/m^3$. However, this value occurs at very high wind speed where the validity of all the models could be questioned.

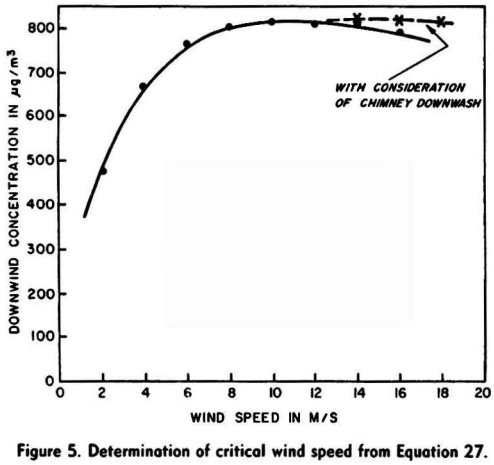

Figure 5. Determination of critical wind speed from Equation 27.

Determine the Maximum Concentration at the Critical Wind Speed (Use of Equation 37)

Assuming all parameters stay the same as in the first illustration, except the wind speed,

1. Determine the critical wind speed

$$\bar{u}_{max} = \left(\frac{B}{h_s}\right)\left(\frac{p}{q}\right) \quad (33)$$

$$\bar{u}_{max} = \left(\frac{1150}{84}\right)\left(\frac{0.8610}{1.0940}\right)$$

$$\bar{u}_{max}\ 10.77\ m/s$$

2. Calculate distance at which the maximum occurs

$$x_{max} = \left\{\left[\left(\frac{h_s}{b}\right)\frac{1}{(p/q)}\right]^2 2\left(\frac{p+q}{2q}\right)\right\}^{1/2q} \quad (36)$$

$$x_{max} = \left\{\left[\left(\frac{84}{0.0573}\right)\frac{1}{\frac{0.8610}{1.0940}}\right]^2 \left(\frac{1.9550}{1.0940}\right)\right\}^{\frac{1}{2.1880}}$$

$$x_{max} = 1.27\ km$$

Thus, x_{max} is within the range of the a, p, b, q values and beyond the point of final plume rise, and all equations are valid.

3. Calculate $\bar{C}_{max}$

$$\bar{C}_{max} = \frac{Qb^{(p/q)} \exp\left[-\left(\frac{p+q}{2q}\right)\right]}{\pi a(p/q)B\left[2\left(\frac{p+q}{2q}\right)\frac{1}{(p/q)^2}\right]^{\frac{p+q}{2q}} h_s^{(p/q)}} \quad (37)$$

$$Q = 1.890 \times 10^9\ \mu g/s \qquad B = 1150$$

$$\bar{C}_{max} = 818\ \mu g/m^3$$

This valve agrees with the maximum found from Equation 27 and Figure 5.

Using the Maximum Formulas for Design (use of Equation 39 and 41).

Assume that an hourly average SO_2 ambient air-quality standard has been set at 2,000 $\mu g/m^3$, not to be exceeded more than once per year. It has also been determined that the worst-case meteorological conditions are B stability and $\bar{u}_h = 9.0$ m/s. Thus, the values of a, p, b and q previously selected are good for this example, and all the chimney parameters are assumed to be the same except for the height, which is calculated. From Equation 38, $A = 0.055429$, with $Q = 1.89 \times 10^9\ \mu g/s$ and $B = 1150$,

$$h_s = \left[\frac{A}{\frac{\bar{C}_{max}\bar{u}_h}{Q}}\right]^{\left(\frac{q}{p+q}\right)} - \frac{B}{\bar{u}_h} \quad (39)$$

$$h_s = \left[\frac{0.055429}{\frac{2000 \times 9}{1.98 \times 10^9}}\right]^{\frac{1.0940}{1.9550}} - \frac{1150}{9}$$

$$h_s = 127.88 = 127.78$$

$$h_s \approx 0$$

which implies that no stack is needed. Under this condition a good engineering practice chimney height is called for. However, it should be remembered that maximum (i.e., critical) wind speed might result in a different answer.

The calculation of chimney height is now needed at the critical wind speed of 10.77 m/s. From Equation 40, $A_{max} =$

0.016262 is calculated. Then, Equation 41 is used to calculate h_s.

$$h_s = \left[\frac{A_{max}}{\frac{\bar{C}_{max}B}{Q}}\right]^{(q/p)} \quad (41)$$

$$h_s = \left[\frac{0.016267}{\frac{2000 \times 1150}{1.89 \times 10^9}}\right]^{\left(\frac{1.0940}{0.8610}\right)} = 27 \text{ m}$$

Thus, to satisfy the maximum conditions where chimney downwash is not a problem requires a substantial chimney.

These calculations can be extended with the same critical velocity to show the effect of the choice of hourly standard on chimney height. The following table illustrates this point; the data are plotted in Figure 6.

C_{max} g/m³	h_s m
2000	27
1500	39
1000	65
500	157
250	379

ACKNOWLEDGEMENT

One author (KBS) wishes to acknowledge the assistance provided by Professor André Berger and the Université Catholique de Louvain, Institut d'Astronomie et de Géophysique Georges Lemaitre, Louvain-la-Neuve, Belgium. It was during the author's appointment as Visiting Professor in May 1982 that the paper was completed. The assistance of the National Science Foundation in providing a short-term visit award as part of the United States-Belgium Cooperative Science Program is gratefully acknowledged. It should be noted that any opinions, findings, and conclusions, or recommendations expressed in this publication are those of the authors and do not necessarily reflect the views of the National Science Foundation.

NOMENCLATURE

A = Maximization factor defined by Equation 38
A_{max} = Maximization factor defined by Equation 40
B = Plume-rise factor defined by Equation 6, m²/s
$\bar{C}$ = One-hour average concentration, $\mu g/m^3$
$\bar{C}_{max}$ = Maximum one-hour average concentration, $\mu g/m^3$
F = Buoyancy-flux parameter, m^4/s^3
H = Effective emission height, m
P = Wind-speed power-law exponential
Q = Emission strength, $\mu g/s$
T_a = Atmospheric temperature, K
T_s = Chimney gas temperature, K
V_s = Chimney gas velocity, m/s
a = Sigma equation coefficient, defined by Equation 21a
b = Sigma equation coefficient, defined by Equation 21b
d_s = Chimney diameter, m
g = Acceleration due to gravity, m/s^2
h_s = Chimney-height parameter, m
h_{sact} = Actual chimney height, m
p = Sigma equation exponent, defined by Equation 21a
q = Sigma equation exponent, defined by Equation 21b
s = Stability parameter, defined by Equation 9
$\bar{u}_{Bs}$ = Buoyancy wind-speed factor defined by Equation 16
$\bar{u}_h$ = Average wind speed at chimney height, m/s
$\bar{u}_{max}$ = Critical or maximum wind speed for any stability category, m/s
$\bar{u}_{ms}$ = Momentum wind-speed factor defined by Equation 10
$\bar{u}_z$ = Wind speed at anemometer height, m/s
x = Downwind coordinate, m
y = Crosswind coordinate, m
z = Vertical coordinate, m
z_a = Height of wind-speed anemometer, m
Δh = Plume rise, m
ΔT = Difference between chimney gas and atmospheric temperature, K
ΔT_c = Cross-over temperature, K
$\Delta\theta/\Delta z$ = Potential temperature gradient, K/m
σ_y = y-directed dispersion coefficient, m
σ_z = z-directed dispersion coefficient, m

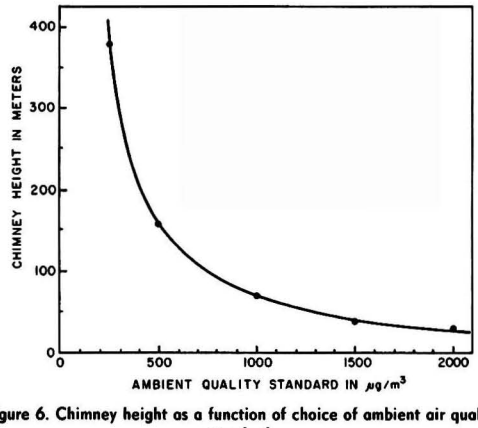

Figure 6. Chimney height as a function of choice of ambient air quality standard.

LITERATURE CITED

1. Environmental Protection Agency, "User's Guide for MPTER: A Multiple Point Gaussian Dispersion Algorithm with Optional Terrain Adjustment," EPA-600/8-80-016 (April, 1980).
2. Turner, D. B., "Workbook of Atmospheric Dispersion Estimates," Office of Air Programs Publication AP-26. U. S. Environmental Protection Agency, Research Triangle Park, N.C., 84 pp (1970).
3. Gifford, F. A. Jr., "An Alignment Chart for Atmospheric Diffusion Calculations," *Bull. Amer. Meteorol. Society*, **34**, (3) and (5), 101-105 and 216 (1953).
4. Montgomery, T. L. W. B. Norris, F. W. Thomas, and S. B. Carpenter, "A Simplified Technique Used to Evaluate Atmospheric Dispersion of Emissions from Large Power Plants," *Journal of the Air Pollution Control Association*, **23**(5), 388-394 (May, 1973).
5. Csanady, G. T., "Turbulent Diffusion in the Environment," Reidel, Dordrecht, Holland (1973).
6. Ragland, K. W. "Worst-Case Ambient Air Concentrations from Point Sources Using the Gaussian Plume Model," *Atmospheric Environment*, **10**, 371-374 (1976).
7. Baasel, William D. "A Simple Technique for Determining the Maximum Ground Level Concentration of an Elevated Gaseous Release," *Journal of the Air Pollution Control Association*, **31**, 866-870 (August, 1981).
8. Hunt, J. C. R., W. H. Snyder, and R. E. Lawson, Jr., "Flow Structure and Turbulent Diffusion around a Three-Dimension Hill-Fluid Modeling Study on Effects of Stratification. Part 1. Flow Structure," EPA-600/4-78-041, U.S. Environmental Protection Agency, Research Triangle Park, N.C., 84 pp (1978).

9. Irwin, J. S., "A Theoretical Variation of the Wind Profile Power-Law Exponent as a Function of Surface Roughness and Stability," *Atmos. Environ.*, **13**, 191-194 (1979).
10. Gifford, F. A., Jr., "Atmospheric Dispersion Calculations Using the Generalized Gaussian Plume Model," *Nucl. Saf.*, **2** (2), 56-59 (1960).
11. Pasquill, F., "The Estimation of the Dispersion of Windborne Material," *Meteorol. Mag.*, **90**, (1063) 33-49 (1961).
12. Gifford, F. A., Jr., "Turbulent Diffusion-typing Schemes: A Review," *Nucl. Saf.*, **17**(1), 68-86 (1976).
13. Briggs, Gary A., "Plume rise predictions," *Lectures on Air Pollution and Environmental Impact Analysis*, Duane A. Haugen, ed., Amer. Meteorol. Soc., Chapter 3, pp. 59-111, Boston, Mass., 296 pp. (1975).
14. Environmental Protection Agency, "Guideline for Determining Good Engineering Practice Stack Height" (Technical Support Document for the Stack Height Regulation) EPA-450/4-80-023 (July, 1981).
15. Hanna, S. R., G. A. Briggs, J. Deardorff, B. A. Egan, F. A. Gifford, and F. Pasquill, AMS Workshop on Stability Classification Schemes and Sigma Curves—Summary of Recommendations," *Bull. Amer. Meteorol. Society*, **58**(12), 1305-1309 (December, 1977).

Karl B. Schnelle, Jr. earned his B.S., M.S. and Ph.D. in Chemical Engineering at Carnegie-Mellon University. He has been employed by the Pittsburgh Plate Glass, Chemical Division, as a Chemical Engineer and by the Instrument Society of America as Manager of Education and Research. He has been a faculty member in the School of Engineering at Vanderbilt University, Nashville, TN for 21 years where he currently is Professor of Chemical and Environmental Engineering and serves as Chairman of the Chemical Engineering Department.

Karl D. Schnelle is a senior student in the Chemical Engineering Department at Vanderbilt University. He has been a summer employee of the Monsanto Corp., at the Chocolate Bayou Plant in Alvin, TX in the Manufacturing Technical Service Group, and has served Vanderbilt University as a student assistant in the Chemical Engineering Department Computer Laboratory.

Air Permit Applications for Boilers

A case history of the construction permitting process for a wood refuse/coal-fired boiler.

Perry W. Fisher and Herbert A. Weidemann, Dames & Moore, Park Ridge, Ill. 60068
Eric J. Larson, Flambeau Paper Corp., Park Falls, Wis.

Flambeau Paper Corporation operates a calcium sulfite paper mill in Park Falls, Wisconsin. The mill has been serving the Park Falls area since 1898 and is one of the few mills of its kind in the United States. The present paper discusses Flambeau Paper Corporation's application for construction permits to operate a steam generating plant located approximately 500 meters south-southwest of the Park Falls mill. This project was initiated due to the planned retirement of the Lake Superior District Power Company gas-fired peaking unit in Park Falls, which has served the electrical power and steam needs of the Flambeau Paper mill. A mill modernization project will be implemented coincident with the proposed steam plant.

PLANT DESCRIPTION

Existing Facility

The mill presently processes approximately 207,000 tons of pulp wood annually. The mill's three paper machines produce an average of about 300 tons of uncoated fine-printing and specialty paper products each work day. The pulp mill, operated in conjunction with the paper manufacturing facilities, has an average daily output of 120 tons of sulfite pulp. Spent liquor from the sulfite pulp mill is recovered and sold for use as an ingredient in a variety of products, including cattle-feed supplements.

The mill is located in the city of Park Falls, Wisconsin, along the west bank of the North Fork of the Flambeau River. Figure 1 presents a general site layout showing major existing and proposed structures.

Major emission sources at the existing mill include the power plant, sulfur burner, digester blow tank, and six-stage evaporator. Each of the mill's four boilers is equipped to burn more than one type of fuel. The rated capacity for each fuel type and the stack height for the existing boilers is summarized in Table 1. Table 2 presents a summary of stack height and SO_2 emission rate for the existing sulfur burner, digester blow tank, and the six-stage evaporator.

Proposed Boiler Project

The maximum heat input to the boiler, which will have a maximum design capacity of 150,000 pounds per hour of steam, will be limited to 249 million Btu per hour when 100-percent wood-fired and 222.7 million Btu per hour when 100-percent coal-fired. Other design and operating parameters, for 100-percent coal and 100-percent wood-firing, are summarized in Table 3. The proposed boiler will replace Boiler No. 2, which will be shut down, and either Boiler No. 4 or No. 5 will be used as an emergency stand-by boiler.

Mill Modernization Project

The mill modernization project, which will be implemented simultaneously with the operation of the proposed steam plant, will produce significant reductions in atmospheric emissions of SO_2 from the sulfur burner, digester blow tank, and six-stage evaporator. The objective of the mill modernization project is to increase production in the wood room and sulfite mill.

Increased SO_2 emissions resulting from the increased production will be controlled by venting all sulfite mill sources (i.e., six-stage evaporator, sulfur burner, and digester blow tank) through a wet scrubber with a 90-percent collection efficiency. Furthermore, the scrubber stack will be of Good Engineering Practice (GEP) design to alle-

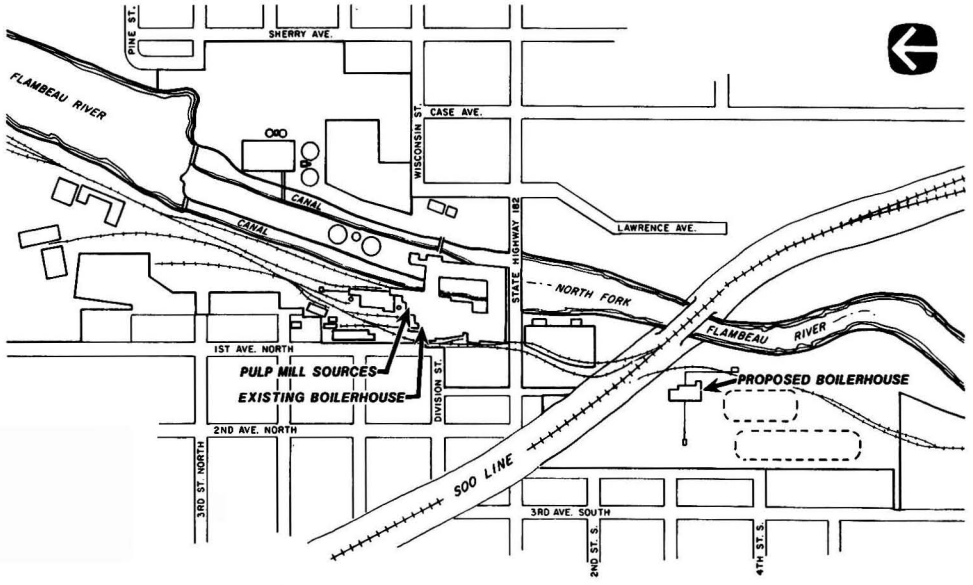

Figure 1. General site layout at the Flambeau Paper Company Park Falls mill.

viate the potential for high ground-level concentrations due to aerodynamic downwash from the facility complex. The installation of the new scrubber system will substantially reduce SO_2 emissions from the existing mill operations (as well as from the proposed modernized portions of the mill).

STUDY AREA CHARACTERISTICS

Topography

The topography of the study area is best described as gently rolling. Many of the relief features are located adjacent to the Flambeau River and its many small tributaries.

TABLE 1. RATED CAPACITY AND STACK HEIGHT FOR EXISTING BOILERS

Boiler	Fuel Type	Rated Capacity (10^6 Btu/hr)	Stack Height (m)
Boiler No. 2	Sub-bituminous coal	50.5	57.9
	Waste wood	43.5	
Boiler No. 3	Sub-bituminous coal	82.5	32.6
	No. 6 oil & natural gas	82.5	
	Waste wood	60.0	
Boiler No. 4	No. 6 oil	80.5	21.3
	Natural gas	97.5	
Boiler No. 5.	No. 6 oil	166.7	16.2
	Natural gas	176.4	

TABLE 2. STACK HEIGHT AND SO_2 EMISSION RATE FOR EXISTING SULFUR BURNER, DIGESTER BLOW TANK, AND SIX-STAGE EVAPORATOR

Parameter	Sulfur Burner	Digester Blow Tank	Six-stage Evaporator
Stack height (m)	30.8	19.8	12.8
Maximum SO_2 emission rate* (tons/yr)	79.6	2126.5	86.2

* SO_2 emission rates presented are 1979 emission rates computed by the Wisconsin Department of Natural Resources based upon an annual average throughput of 39,614 tons of air-dried pulp per year.

The elevation at the plant site is approximately 457 meters above mean sea level. Since there are only gradual changes of slope and terrain between the various land forms, the variation of the topography will not be an important factor in the transport and dispersion of air pollutants throughout the study area. The Wisconsin Department of Natural Resources (WDNR) agreed that terrain elevations need not be included in the dispersion model.

Rural/Urban Description

A technique was developed by Irwin [2] to classify a site as either rural or urban. This classification can be based on either average heat flux, land use, or population density within a 3-km radius circle surrounding the plant sources. Of these, the EPA has specified that land use is the most definitive criterion [3]. The rural/urban classification based on land use is as follows:

Using the meteorological land-use typing scheme established by Auer[4], an urban classification of the

TABLE 3. DESIGN AND OPERATING PARAMETERS FOR PROPOSED COAL/WOOD-FIRED BOILER

Parameter	100 Percent Coal-Fired	100 Percent Wood-Fired
Maximum heat input to boiler (10^6 Btu/hr)	222.7	249
Rated steam load (lb/hr)	150,000	143,000
Heating value (Btu/lb)	8,615	4,350
Boiler efficiency (%)	79.84	67.88
Stack height (m)	--------53.3--------	
Maximum sulfur content of fuel (%)	0.78	0.1
Maximum ash content of fuel (%)	7.79	4.20
Maximum SO_2 emission rate (tons/yr)	1170[a]	89[b]
Maximum PM emission rate (tons/yr)[b]	80	89
Maximum NO_x emission rate (tons/yr)[c]	679	267
Maximum CO emission rate (tons/yr)[d]	57	270

[a] Based on 1.2 lb/10^6 Btu heat input.
[b] Based on 0.1 lb/10^6 Btu heat input.
[c] Based on 0.7 lb/10^6 Btu heat input for coal usage and 2 lb NO_x per ton of bark burned.
[d] Based on 2 lb CO per ton of coal burned, and 2 lb CO per ton of bark burned [1].

site area requires more than 50 percent of the following land-use types: heavy industrial [I1], light-moderate industrial [I2], single compact residential (R2), and multi-family compact residential (R3). Otherwise, the site area is considered rural.

Using the land-use typing scheme for an area of 3-km radius around the mill site, urban land-use types comprise, at most, 20 percent of the total land area. It is evident that the site and surrounding area must be classified as rural; thus, modeling with rural dispersion coefficients is appropriate for the air quality assessment.

Current Air Quality Status

Flambeau Paper's mill is located in an attainment area for all criteria pollutants. Further, there are no SO_2, PM, NO_2, or CO nonattainment areas within 50 kilometers of the paper mill site. However, violations of both the primary and secondary NAAQS for SO_2 were recorded by the WDNR in 1980. These violations were measured at monitoring sites near the Flambeau Paper mill.

REGULATORY REQUIREMENTS

Because of the measured violations of the SO_2 NAAQS in the vicinity of the mill during 1980, WDNR and Flambeau Paper agreed that the proposed boiler should undergo nonattainment area New Source Review with respect to SO_2. Since its potential SO_2 emission rate when burning 100 percent coal is 1170 tons per year, this boiler was reviewed as a major SO_2 emission source and, as a consequence, was subject to the following requirements with respect to SO_2:

- Lowest Achievable Emission Rate (LAER) technology;
- All of the applicant's facilities in Wisconsin must be in compliance or on a compliance schedule;
- Emission offsets from other sources must be greater than the proposed emission increases; and
- Emission offsets will provide a net air quality benefit in the area to assure reasonable further progress toward attainment of NAAQS.

In addition to these requirements, the WDNR specified that Flambeau Paper demonstrate in its permit application that the SO_2 NAAQS will be attained following startup of the proposed boiler (this includes coincident shutdown of Boiler No. 2 and completion of the mill modernization project). WDNR's requirement was made because Flambeau Paper is the only major SO_2 emission source in the Park Falls area.

Because the net increases of PM, NO_x, and CO emissions, following startup of the proposed boiler, exceed EPA's significant emission rates (25, 40, and 100 tons per year, respectively), the proposed boiler was subject to PSD review for these pollutants. This required for each pollutant:

- A case-by-case Best Available Control Technology (BACT) demonstration, taking into account energy, environmental, and economic impacts as well as technical feasibility;
- An ambient air quality impact analysis to determine if the allowable emissions from the proposed source, in conjunction with all other applicable emission increases or reductions, would cause or contribute to a violation of the applicable PSD increments and NAAQS (refer to Table 4); and
- An assessment of the direct and indirect effects of the proposed source on general growth, soil, vegetation, and visibility.

Because the permit application was submitted prior to June 7, 1981, no air quality monitoring data were required by the WDNR. Further, sufficient monitoring data were collected by the WDNR in Park Falls to represent existing air quality.

BACT AND LAER DEMONSTRATIONS

BACT for PM

The use of a multicyclone and a variable-throat Venturi scrubber followed by an impingement separator for continuous removal of fly ash in the flue gas stream will result in an outlet PM grain loading not exceeding 0.1 pounds per million Btu heat input. This constitutes BACT for PM.

Three alternate control strategies were considered for the proposed boiler's PM emissions. Although a baghouse offers the advantage of very high PM removal efficiency, a baghouse is not suited for use with a wood-fired boiler because of the likelihood of fire due to the presence of hot char particles in the baghouse. Dry scrubbing was rejected, since it is not considered a proven control technique when used in conjunction with a wood-fired boiler.

An electrostatic precipitator (ESP) was also considered as a PM control device for the proposed boiler. An ESP offers the advantage of being able to handle a large volume of gas with comparatively little pressure drop and, therefore, lower energy consumption. However, this advantage is outweighed by several disadvantages associated with this potential application. ESPs must be shut down completely for maintenance or repairs. They must be bypassed during boiler startup to avoid the dangers of fire or explosion. The installation of an ESP would require a high initial capital expenditure. ESP performance is sensitive to many variables, including flue gas velocity, temperature, moisture content, dust loading, particle size, and resistivity to an electric charge. The use of low sulfur fuels reduces the amount of sulfur trioxide (SO_3) in the flue gas, thereby reducing the electric conductivity of the particles to be collected by the ESP. Instead of moving rapidly from the ESP's negatively charged electrodes to the positively charged collecting plates, the particles move comparatively slowly, thus resisting capture. Therefore, the potential exists that the required 0.1 pounds per million Btu heat input PM emission limitation would not be consistently met due to either the variability in the percentages of coal- and wood-firing rates or due to the total reliance on readily available low sulfur fuels to limit SO_2 emissions.

In contrast to the three rejected alternative PM control strategies, the proposed PM control system offers these advantages: The multicyclone is a simple and reliable mechanical device. It has comparatively low capital and maintenance costs, draft loss, and space requirements. The wet Venturi scrubber and impingement separator can handle varying dust loads and particle sizes. Their collection efficiency does not vary with flue gas temperature, moisture content, or SO_3 content. Space requirements are also acceptable.

With respect to the PM control strategies proposed for the fuel handling and storage facilities, bag filters, having a PM collection efficiency of 99.9 percent, will be installed on the roof-top vents associated with the crusher house, hogging and screening structure, and all coal and wood bunkers in the powerhouse.

The coal stockout pile will be fenced on three sides. Coal will be unloaded into an underground hopper from bottom dump railcars. The coal unloading area will be an open-ended shed. Wood will be delivered by semitrailers and unloaded by truck dumpers. All coal and wood conveyors will be enclosed on three sides. Haul roads leading to the wood dumping area will either be paved or gravel-covered. These measures will adequately minimize fugitive PM emissions from fuel handling and storage operations.

BACT for NO_x

The control of NO_x emissions by limiting NO_x formation in the combustion zone and by controlling flame temperature and excess air during the combustion process will

TABLE 4. NATIONAL AMBIENT AIR QUALITY STANDARDS, MAXIMUM ALLOWABLE PSD INCREMENTS, AND SIGNIFICANT IMPACT INCREMENTS

Pollutant	Averaging Period	Ambient Air Quality Standards ($\mu g/m^3$)[a]		PSD Increments ($\mu g/m^3$)[b]			Significant Impact Increments ($\mu g/m^3$)[b]
		Primary	Secondary	Class I	Class II	Class III	
Sulfur dioxide (SO_2)	Annual (arith. mean)	80	—	2	20	40	1
	24-hour	365	—	5	91	182	5
	3-Hour	—	1300	25	512	700	25
Particulate matter (PM)	Annual (geom. mean)	75	60[c]	5	19	37	1
	24-Hour	260	150	10	37	75	5
Nitrogen dioxide (NO_2)	Annual (arith. mean)	100	Same as primary	—	—	—	1
Carbon monoxide (CO)	8-Hour	10,000	Same as primary	—	—	—	500
	1-Hour	40,000	Same as primary	—	—	—	2,000
Ozone (O_3)	1-Hour	235	Same as primary	—	—	—	—
Lead (Pb)	Calendar quarter	1.5	Same as primary	—	—	—	—

Note: The ambient air quality standards and maximum allowable PSD increments with averaging periods of 24 hours or less are not to be exceeded more than once per year.
[a] 40 CFR 50.
[b] 43 FR 26399, date June 19, 1978.
[c] Guideline, not a formal enforceable standard.

limit NO_x emissions to 0.7 pounds per million Btu heat input. This constitutes BACT for No_x. Limiting excess air in the combustion zone reduces the amount of oxygen and the temperature in this zone, which limits the formation of NO_x.

Excess air will be controlled with a zirconium oxide O_2 analyzer. The capability for automatic control will be built into the system but, from a practical standpoint, considering the varying moisture and Btu quality of waste wood materials, the regulation will probably be manual, using the O_2 analyzer as an indicator. The overfire air will also be controlled manually for varying firing conditions.

BACT for CO

A deficiency of combustion air is the usual cause of excessive CO emissions. The exact amount of CO depends on several factors, including the degree of mixing and turbulence during combustion. However, the most critical operating variable is the quantity of excess air supplied. Controlling the amount of excess air should provide sufficient control to minimize the amount of CO produced. The proposed boiler is being designed to operate with 30 percent excess air. The percentage of oxygen in the boiler exhaust gas will be monitored. This will assure minimum formation of CO and constitutes BACT for this application.

LAER For SO_2

The use of low sulfur coal and waste wood, having respective sulfur contents of approximately 0.78 and 0.1 percent, to assure that SO_2 emissions will not exceed 1.2 pounds per million Btu, constitutes LAER for the proposed coal/wood-fired boiler with respect to SO_2. This emission limitation will be met when burning a normal fuel mix of 80% wood/20% low sulfur coal without scrubbing. When burning 100% coal, a caustic injection system will be utilized to scrub SO_2 from the flue gas. A continuous pH monitor will be utilized to determine the quantity of caustic to add to the scrubbing liquid in order to meet the emission limitation.

Since the mill itself is a source of large quantities of low sulfur wood fuel from debarking operations, and Flambeau Paper is confident of obtaining additional quantities of supplemental low sulfur coal, no specific flue gas desulfurization (FGD) system will be necessary in meeting the 1.2 pounds per million Btu limitation. At present, the majority of FGD systems for industrial applications are of the throwaway type. Such an FGD system for the proposed boiler is undesirable for the following reasons:

1. The high investment cost for an FGD system;
2. The high operating costs and energy requirements;
3. Sludge disposal problems; and
4. Reduced plume buoyancy due to lower flue gas temperature.

DISPERSION MODELING METHODOLOGY

Dispersion Model

The air quality modeling analysis employed the U.S. EPA's Industrial Source Complex (ISC) model [5]. This model has been recommended as a guideline model for assessing the air quality impact of aerodynamic downwash and fugitive particulate emissions [3]. Aerodynamic downwash of the proposed boiler's plume may occur, since the stack height of 53.3 meters is slightly less than the Good Engineering Practice stack height of 56.4 meters. Existing sources of the mill also have stacks less than GEP stack height.

The ISC model consists of two programs: a short-term model (ISCST) and a long-term model (ISCLT). The difference in these programs is that the ISCST program utilizes an hourly meteorological data base, while ISCLT is a sector-averaged program using a frequency of occurrence based on categories of wind speed, wind direction, and atmospheric stability. The ISCLT model was used to assess NO_2 impacts, since only an annual average standard exists for this pollutant. The ISCST model was employed to assess both short-term and long-term impacts of SO_2, PM, and CO.

Emission Inventory Data

Flambeau Paper Corporation is the only major emission source in the study area. Dispersion modeling analyses to assess air quality impact used only the existing and proposed sources of Flambeau Paper. Impacts due to distant background sources were included by the determination of a background concentration based on the WDNR monitoring data.

Since each of the existing boilers uses multiple fuels, the SO_2 emission rates for the existing boilers were represented by the maximum emission rate for the fuel producing highest SO_2 emissions. The proposed steam generating plant was conservatively assumed to operate at its maximum design capacity using coal continuously throughout the year.

Table 5 presents the emission inventory for the SO_2 net air quality benefit demonstration. The proposed SO_2 emission increases are from the steam plant boiler and the scrubber stack of the digester blow tank. Reductions of SO_2 emissions will occur from venting the six-stage evaporator, sulfur burner, and digester blow tank emissions through the proposed scrubber stack as part of the mill modernization project. Boiler No. 2 is included as an emission offset, since this unit will be retired prior to the operation of the proposed steam plant.

Meteorological Data Base

The dispersion model simulations were based on 5 years (1973-1977) of surface data at the Eau Claire Municipal Airport and coincident upper air observations recorded at the Green Bay Austin Straubel Airport.

Receptor Grid

The selection of receptor points for the dispersion modeling analyses for PSD review was based on the following considerations:

1. Locations of predicted maximum ground-level concentrations for the proposed steam plant and existing emission sources;
2. Locations along the plant property boundary of the existing paper mill and the proposed steam plant;
3. Locations of predicted maximum ground-level concentrations from fugitive emission sources;
4. Locations of air quality monitoring sites; and
5. Sufficient area coverage within the study area.

Air Quality Monitoring Data

Air quality monitoring data for the period from July 1979 to July 1980 were obtained from the WDNR for two monitoring van site locations in Park Falls. Each van was equipped to measure wind speed, wind direction, SO_2, NO_2, PM, and O_3.

The monitoring data were used to determine the background concentrations of SO_2, NO_2, and PM in Park Falls. Background concentrations represent the contributions to ambient air quality from sources other than the Flambeau Paper mill. Background determination procedures for each pollutant were performed as follows:

TABLE 5. EMISSION INVENTORY FOR SO_2 NET AIR QUALITY BENEFIT DEMONSTRATION

Source	Stack Height (m)	SO_2 Emission* Rate (tons/yr)
Proposed Increases		
Steam plant boiler	53.3	1170
Digester blow tank (with scrubber)	40.4	287
Proposed Reductions		
Six-stage evaporator	12.8	86
Sulfur burner (acid plant)	30.8	80
Digester blow tank	19.8	2127
Boiler 2	57.9	300

* Proposed increases total 1457 tons/year and proposed reductions total 2593 tons/year. A total reduction of 1136 tons/year SO_2 will result after the boiler and mill modernization projects are completed.

Sulfur Dioxide—Since Flambeau Paper is a major source of SO_2, the procedure to determine a background concentration must avoid time periods in which the paper mill impacts the monitors. The EPA recommends a screening procedure to invalidate all concentrations for wind directions which are within a 45° angle on either side of the direction aligning an emission source with the monitor [3]. Since the Park Falls mill consists of multiple SO_2 emission sources, a sector greater than 90° was used to account for the extent of the paper mill source locations. The wind direction screening model excluded monitored concentrations for wind directions from the sector 241°-354° for one of the WDNR vans and from the sector 165°-272° for the other van.

Background SO_2 concentrations for 3-hour and 24-hour running averaging periods were determined for each monitor using the corresponding meteorological data recorded at each monitor. An annual average background concentration was also calculated. The calculation of background concentrations excluded 1) hourly periods in which the measured wind speed was less than 0.4 meter per second (1 mile per hour); and 2) 3-hour and 24-hour average concentrations which had more than 25 percent of the hours from the wind direction sector including the Flambeau Paper mill.

Particulate Matter—The background PM concentration for a 24-hour period was defined as the highest of the second highest concentration at each monitor. As a conservative approach, all PM concentrations were considered as valid background concentrations (that is, a screening procedure eliminating PM concentrations during periods in which the monitors were impacted by Flambeau Paper was not utilized). The background PM concentration for an annual average was defined as the arithmetic average of the annual geometric means at both monitors.

Nitrogen Dioxide—Limited NO_2 monitoring was performed in the Park Falls area. The background NO_2 concentration was defined as the highest of the arithmetic average of all measured concentrations at the two sample locations.

Based on the procedures described above, background SO_2, PM, and NO_2 concentrations were determined for each averaging period in which an NAAQS exists. These concentrations, presented in Table 6, were added to the maximum predicted concentrations from the mill to assess compliance with the NAAQS.

Net Air Quality Benefit Analysis

The net air quality benefit analysis used a single "worst year" of meteorological data selected from the 5-year meteorological data base, since it was evident that a substantial air quality benefit would result by reducing SO_2 emissions over 87 percent from the digester blow tank and increasing its stack height from 19.8 to 40.4 meters (GEP).

TABLE 6. AIR QUALITY BACKGROUND CONCENTRATIONS FOR THE STUDY AREA

Pollutant	Background Concentration ($\mu g/m^3$)	NAAQS ($\mu g/m^3$)	Percent of NAAQS
Sulfur Dioxide			
3 Hour	109.3	1,300	8.4
24 Hour	54.6	365	15.0
Annual	6.0	80	7.5
Particulate			
24 Hour	100.0	150	66.7
Annual	34.0	75	45.3
Nitrogen Dioxide			
Annual	10.5	100	10.5

Note: Second highest concentration is given for short-term averaging periods.

The worst year was chosen by performing dispersion model simulations of the air quality impact of the proposed steam plant and ranking the 5 years based on maximum predicted concentrations for 3-hour, 24-hour, and annual averaging periods. From this procedure, the year 1975 was selected.

The proposed sources (new boiler and increased emissions due to increased productive capacity of the mill modernization) and offset sources (existing sources whose emissions are reduced or eliminated following startup of the new steam plant and mill modernization) were modeled simultaneously using the ISCST model. Offset sources were assigned negative emission rates to reflect the reduction in air quality impact due to emission reductions. The guideline for receptor placement was that no bias should be given to either the proposed or offset source air quality impact which might compromise the validity of the net air quality benefit demonstration. This objective is achieved through use of a completely symmetrical receptor grid. Since several offset sources are involved, an ideal symmetrical grid cannot be achieved and the best approximation was to center the grid between the major source of emission increase (proposed steam plant) and the major source of emission reduction (digester blow tank). The receptor grid used for the net air quality benefit modeling is illustrated on Figure 2.

The adequacy of the emission offset was evaluated by Dames & Moore's NETCON post-processor program. Net air quality benefit for an emission offset scenario is demonstrated if the following conditions are met in the ISCST model results:

a. The average of all predicted concentrations at all receptors must be less than zero.
b. The highest predicted concentration for all pertinent averaging times (3 hours, 24 hours, annual) at any receptor must be lower in absolute value than the lowest predicted concentration at any receptor. For example, if the highest predicted 3-hour average SO_2 concentration was 200 $\mu g/m^3$, the lowest 3-hour average SO_2 concentration would have to be less than -200 $\mu g/m^3$. Predicted concentration maxima and minima need not occur at the same receptor locations.
c. In the same manner described in condition b., the highest second-highest 3-hour, and 24-hour average concentrations must be lower in absolute value than the corresponding lowest second-lowest concentrations.
d. For each pertinent averaging time, the highest 100 and lowest 100 concentrations for all receptors combined are ranked by NETCON. The 1st, 2nd, 5th, 10th, 20th, 50th, and 100th highest-ranking and lowest-ranking concentrations are used together to test for net air quality benefit at the extreme ends of the predicted concentration frequency distributions. The condition:

Extreme Value Factor (EVF)

$$= \frac{-1}{7}\left[\frac{H(1)}{L(1)} + \frac{H(2)}{L(2)} + \frac{H(5)}{L(5)} + \frac{H(10)}{L(10)} + \frac{H(20)}{L(20)} + \frac{H(50)}{L(50)} + \frac{H(100)}{L(100)}\right] < 1$$

must be met, where H(n) is the nth highest predicted concentration and L(n) is the nth lowest predicted concentration.

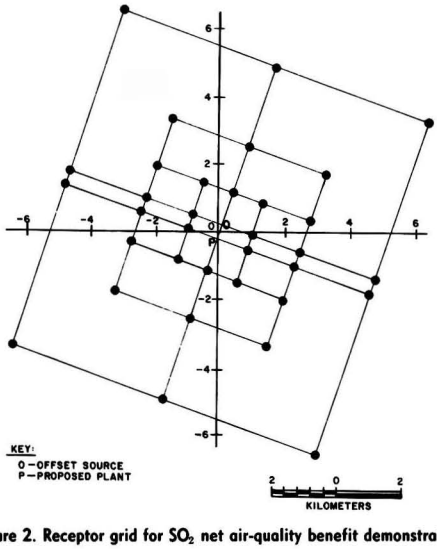

Figure 2. Receptor grid for SO_2 net air-quality benefit demonstration.

AMBIENT AIR QUALITY IMPACT ASSESSMENT

PSD Increment Assessment

Since the requirement to demonstrate net air quality benefit for SO_2 is more stringent than conformance with the PSD increments, the PSD increment demonstration was only performed for PM. In this regard, discussion with the WDNR revealed that the proposed steam plant is the only emission source consuming PSD increments within the proposed plant's impact area. Predicted PM concentration increases due to the proposed steam plant were used to determine if the maximum allowable PSD Class II air quality increments for PM can be met.

Predicted annual average PM impact is less than 1 $\mu g/m^3$, far below the PSD increment of 19 $\mu g/m^3$, while the highest 2nd highest 24-hour PM concentration from the proposed plant is less than 6 $\mu g/m^3$, consuming only 15 percent of the PSD increment of 37 $\mu g/m^3$. The maximum predicted concentrations occur very close to the plant site as a result of simulating fugitive dust emissions.

The only PSD Class I area near the Flambeau mill is the Rainbow Lake Wilderness Area, located 85 km northwest of the site. The predicted PM concentrations indicate that the steam plant's impact on the Class I area is well below the Class I increments.

Comparisons with Applicable Ambient Air Quality Standards

One of the PSD review requirements is to determine whether a new source will cause the NAAQS to be exceeded. To determine compliance with the NAAQS, the SO_2, PM, and NO_2 ambient concentrations following startup of the proposed boiler were compared with the applicable NAAQS.

Although the total existing SO_2 emissions will be reduced by over 1,136 tons per year as a consequence of installing an SO_2 scrubber in the pulp mill, projected SO_2 ambient concentrations following startup of the proposed boiler indicate a highest second-highest 24-hour SO_2 concentration of 506 $\mu g/m^3$ as compared to the NAAQS of 365 $\mu g/m^3$. Flambeau Paper's existing boilers No. 4 and No. 5 using 3.5 percent-sulfur oil contributed 449 $\mu g/m^3$ of the 506 $\mu g/m^3$. By limiting the fuel oil fired in these boilers to 2.4 percent sulfur, conformance with the 24-hour SO_2 NAAQS was demonstrated. Flambeau Paper committed to

this as a permit condition for their proposed boiler. With this permit condition, compliance with the 3-hour and annual average SO_2 NAAQS is easily demonstrated.

The PM air quality in Park Falls is predicted to be attained after the proposed project is in operation. The highest 2nd-highest 24-hour PM concentration is predicted to be 137 $\mu g/m^3$, about 91 percent of the NAAQS of 150 $\mu g/m^3$. This is a result of using a conservatively high background concentration of 100 $\mu g/m^3$, accounting for over 67 percent of the NAAQS. The maximum annual geometric mean is predicted to be 36 $\mu g/m^3$ (45 percent of the annual standard).

The maximum annual average NO_2 concentration in Park Falls following startup of the proposed boiler is estimated to be 13 $\mu g/m^3$. This is well below the NAAQS of 100 $\mu g/m^3$.

Dispersion modeling analysis of the CO impact from the proposed boiler indicated a highest second-highest 3-hour CO concentration of less than 10 $\mu g/m^3$, demonstrating that the boiler will have an insignificant impact on ambient CO concentration since the 8-hour and 1-hour CO significant impact increments of 500 and 2,000 $\mu g/m^3$ will not be approached.

Net Air Quality Benefit Demonstration

The proposed steam plant and mill modernization project will result in increased SO_2 emissions of 1,457 tons per year and reductions of 2,593 tons per year (not taking into account reduced SO_2 emissions from Boilers 4 and 5 in converting from 3.5 to 2.4 percent sulfur oil) for an SO_2 emission reduction ratio of 1:1.78, i.e., SO_2 emissions will be reduced 78 percent more than increases from the proposed steam plant and mill modernization. The proposed emission increases and reductions were modeled using ISCST for one year of meteorological data and a symmetric receptor grid about the proposed steam plant and the existing digester blow tank. Table 7 presents the results of the modeling based upon the net air quality benefit criteria. All four conditions necessary to establish a net air quality benefit are met. Prior to the mill modernization project, the digester blow tank, which is the predominant SO_2 emission source at the mill, vented emissions from a short stack. The building influence on the dispersion of the digester emissions leads to predicted concentrations exceeding the NAAQS. Venting the digester emissions through a GEP stack height, complemented by a 90-percent reduction of SO_2 emissions from a scrubber, will result in significant improvements of SO_2 air quality in the study area. The dominance of negative predicted concentrations as presented in Table 7 represents a net air quality benefit.

PROJECT TIMEFRAME

The first step in the permit process was the development of a Project Plan for the proposed project. This plan included the following; a description of the proposed project, estimated emission rates, applicable air quality regulations, proposed BACT and LAER technologies, and methodology for completing the necessary air quality impact assessments. It was presented and discussed with the WDNR to minimize potential delays in submitting an incomplete permit application. Preparation of a Project Plan considerably expedited the permit process. The time period between submittal of a draft Project Plan to Flambeau Paper for review and receipt of the air construction permit from the WDNR and PSD permit from EPA was 8 months. Table 8 presents the key project milestones during this period.

LITERATURE CITED

1. U.S. Environmental Protection Agency, "Compilation of Air Pollution Emission Factors," AP-42, Office of Air Quality Planning and Standards, Research Triangle Park, North Carolina (1973).
2. Irwin, J. S., "Proposed Criteria for Selection of Urban Versus Rural Dispersion Coefficients," Meteorology and Assessment Division, U.S. Environmental Protection Agency, Research Triangle Park, North Carolina (1979).
3. U.S. Environmental Protection Agency, "Guidelines on Air Quality Models-Proposed Revisions," Office of Air Quality Planning and Standards, Research Triangle Park, North Carolina (October, 1980).
4. Auer, A. H., "Correlation of Land Use and Cover with Meteorological Anomalies," *Journal of Applied Meteorology*, **17**, 636-643 (1978).
5. U.S. Environmental Protection Agency, "Industrial Source Complex Dispersion Model User's Guide," Volume 1, EPA-450/4-79-030, Office of Air Quality Planning and Standards, Research Triangle Park, North Carolina (1979).

TABLE 8. PROJECT MILESTONES

Event	Date	Time (months)
Draft project plan to Flambeau Paper	09/05/80	0
Final project plan to WDNR	09/20/80	0.5
Meeting with WDNR to discuss project plan	09/25/80	0.6
Draft PSD permit application submitted to Flambeau Paper	12/16/80	3.4
Final PSD permit application submitted to WDNR	12/29/80	3.8
WDNR initial requests by telephone for additional information	01/26 and 01/29/81	4.8
D&M response to initial WDNR questions	02/02/81	4.9
WDNR final request by letter for additional information	02/11/81	5.2
D&M response to final WDNR questions	02/20/81	5.5
Flambeau submits additional information to WDNR	02/25 and 03/05/81	6.0
WDNR's preliminary approval	03/13/81	6.3
Public comment period commences	03/14/81	6.3
Joint WDNR/EPA public hearing	04/15/81	7.3
Public comment period ends	04/23/81	7.5
WDNR issues air construction permit	04/28/81	7.7
EPA issues PSD permit	05/05/81	8.0

TABLE 7. SO_2 NET AIR QUALITY BENEFIT DEMONSTRATION

Proposed Sources: Steam plant boiler and scrubber stack of digester
Offset Sources: Boiler No. 2 and sulfite mill sources
Proposed to existing source emission offset ratio: 1:1.78

	Predicted Concentration, $\mu g/m^3$					
	Highest	Lowest	Highest 2nd-Highest	Lowest 2nd-Lowest	Overall Average	Extreme Value Factor
3-Hour average	93	−2783	71	−2447	−11.5	.03
24-Hour average	14	−786	14	−539	−11.5	.02

Perry W. Fisher, who specializes in air quality permitting and regulations, received a Ph.D. in meteorology at the University of Michigan, a M.S. in mathematics at the University of Michigan and a Bachelor of Engineering Physics at Cornell University. He is a Certified Consulting Meteorologist and a partner of Dames & Moore.

Eric J. Larson, received a B.S. in chemical engineering at Michigan Technological University. He is currently a utilities manager at Flambeau Paper Corp.

Hebert A. Weidemann, received a B.S. in mathematics at Pennsylvania State University. He specializes in air quality analyses, permitting and regulations and is currently a project environmental scientist at Dames & Moore.

Industrial Wastewater Treatment With a New Biological Fixed-Film System

The Biological Aerated Filter System—an innovative fixed-film secondary wastewater-treatment system for industrial application.

H. David Stensel and Steven Reiber, University of Utah, Salt Lake City, Utah 84112

Removal of industrial wastewater organic pollutants by biological degradation is considered to be a most cost-effective method, provided that unmanageable biological toxicity problems are not present. Various types of biological reactor designs have been applied, with due consideration for oxygenation methods, mixing and contact between the biomass and wastewater, and liquid-solids separation techniques.

An evaluation of trickling-filter and activated-sludge-system reactor designs *versus* bacteria doubling time and substrate-removal rates exhibits some interesting differences. Although aerobic microorganisms used in wastewater treatment have doubling times less than 4-6 hours, their actual average doubling rate is in excess of 5-10 days, due to the biological reactor designs employed. Substrate removal due to biological absorption and metabolism has been observed to occur within minutes, yet many reactor designs employ detention times in the range of hours. These differences between biological removal capability and reactor design are due to: 1) oxygen transfer-rate limitations, 2) reactor configuration, 3) secondary clarifier liquid-solids separation problems, especially for high biological growth-rate systems, and 4) limitations on the ability to thicken and concentrate and microorganisms.

High-rate fixed-film systems have been developed in the 1970's in an attempt to take advantage of microorganism removal capabilities and to reduce reactor volumes. Examples of these systems are: 1) An upflow activated-carbon bed termed the Integrated Physico-Chemical System [*1*]. This system uses pure oxygen to presaturate the influent with oxygen. Activated carbon supports a relatively dense biological population and also adsorbs nondegradable organic compounds. 2) An upflow sand or coal media bed with air injected into the influent stream [2]. 3) the Ecolotrol [3] upflow fluidized-sand-bed system. This system also requires influent oxygenation using pure oxygen.

BIOLOGICAL AERATED FILTER SYSTEM DESCRIPTION

All of these systems, though promising, have some drawbacks due to the economics of using pure oxygen or the occurrence of high effluent suspended solids due to limited solids-removal mechanisms. A recently developed packed-bed system which eliminates the need for influent preoxygenation and provides efficient suspended-solids removal has been described at EPA Innovative Technology Assessment Seminars [*4*]. The system, termed the Biological Aerated Filter (BAF)* as shown in Figure 1, was developed since 1975 by OTV in Paris, France. Air is sparged in the bottom section of the bed counter-current to the influent wastewater flow, which is applied at the top of the bed. A 3-5-mm fixed-clay medium making up a 5-6-foot bed is used as the biological support medium. The size is small enough to accomplish filtration and absorption of influent solids and biologically produced solid without creating excessive operating headlosses. An 8,000-20,000 mg/liter reactor biomass suspended-solids concentration based on total bed volume has been observed in University of Utah BAF-column experiments. The high biomass concentration results in reactor detention times of 40-80 minutes to achieve 90-percent BOD removal. Volumetric organic loadings are usually in the range of 3-5 kg BOD/m^3 day (200-310 lb BOD/1,000 ft^3 day).

* Eimco PMD, Salt Lake City, Utah, has licensed the BAF system from OTV for U.S. applications.

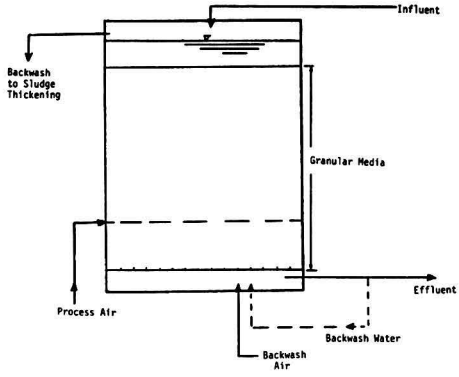

Figure 1. Biological aerated filter system.

No secondary clarification is required after the BAF system. Effluent solids concentrations of less than 10 mg/liter are typically achieved at normal loadings. Periodic backwashing is required to eliminate excess biological growth and suspended solids captured in the bed. A BAF system consists of a number of cells to maintain treatment during backwashing. The backwash frequency is a function of influent BOD concentration and suspended solids. The backwash operation consists of an air scour, an air and water agitation, a water flush, and, finally, removal of backwash water from the top of the bed by a siphon pipe. When flow through the siphon pipe has been initiated by the increased water level above the bed, the backwash pumps are turned off. The backwash water may be returned to a pretreatment solids-removal unit process or may be sent to a surge tank. Solids are then removed from the surge tank to a thickener prior to further stabilization. The above cycle is repeated 4-5 times during a backwash operation. The backwashing is initiated by a liquid-level sensor above the media or by a timer.

The backwash cycle is automatically carried out by a microprocessor controller. The BAF is regarded as an automatically operated secondary treatment system in view of the backwash controls and lack of operator decisions required.

INDUSTRIAL WASTEWATER TREATMENT APPLICATION

As Figure 2A shows, the BAF system is used as an alternative to other secondary wastewater-treatment processes. Common industrial-wastewater design considerations such as nutrient requirements, equalization needs, and toxicity problems must be addressed. Influent suspended-solids concentrations should be low enough to minimize backwash frequency. Influent suspended-solids concentrations of less than 100-150 mg/liter are usually desired. Influent oil and grease concentrations should be reduced to minimal levels to prevent coating of the biological slime layer on the media and interference with BOD-removal capabilities. Present data on the BAF system indicates that wastewater-equalization considerations are similar to those for other secondary systems.

Table 1 summarizes BAF-system pilot-plant results for industrial wastewater applications. A secondary effluent quality was achieved at volumetric organic loadings that were 8-9 times greater than those used for conventional activated-sludge treatment.

For influent wastewater strengths above 300-350 mg/liter BOD_5 concentrations, effluent recycle is used. This is done to maintain a sufficient liquid velocity through the bed to prevent accumulation of biological and influent solids at the top of the bed, which may cause plugging problems. Typical hydraulic application rates may range from 1.0-4.0 m/hr (0.4-1.6 gpm/ft²). As the

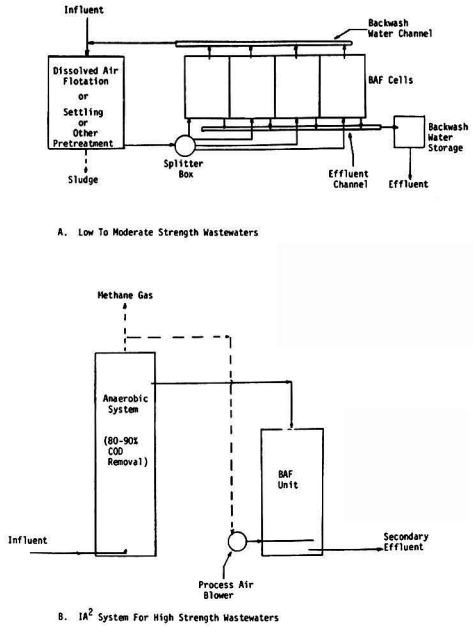

Figure 2. BAF-system industrial-wastewater applications

influent wastewater BOD_5 concentration increases, the solids production per unit of wastewater flow applied increases. This results in the use of a greater percentage of treated water for backwashing. This does not affect the size of the BAF reactor volume, but may increase the size of backwash water processing equipment and backwash storage water tanks, as well as backwash energy requirements.

An integrated anaerobic—BAF (IA²) system (Figure 2B) has been advocated* for cost-effective treatment of high-strength industrial wastewaters to achieve a high-quality effluent. After 85-90 percent BOD removal in an upflow sludge-blanket reactor, the BOD is decreased to below 20 mg/liter concentration by a BAF reactor. Methane gas produced in the anaerobic reactor is used to drive blowers to supply air to the BAF reactor. Laboratory studies on synthetic wastewaters indicate that a 2,500 mg/liter degradable COD wastewater could be treated to produce an effluent BOD_5 concentration of less than 10 mg/liter by the IA² system. This was demonstrated with a 15-hour anaerobic reactor detention time and a 45-minute BAF reactor detention time. The organic loadings were 4 kg COD/m³·day and 8 kg COD/m³·day, for the anaerobic and BAF reactors, respectively. The anaerobic reactor detention could be reduced further, since the system was not at steady-state operation. The advantages of this two-stage system include minimal energy requirements, land area, capital cost, and sludge production.

COMPARISON TO CONVENTIONAL SECONDARY TREATMENT SYSTEMS

Figure 3 compares the BAF-design volumetric organic loadings to achieve a secondary effluent equal to those used for conventional systems. A significant difference in reactor size requirements is apparent.

The BAF-system costs were evaluated for secondary treatment [4] and compared to other conventional secondary-treatment costs to determine if the high-rate

* IA² (Integrated Anaerobic-Aerobic) System using the BAF reactor has been introduced by Process Dynamics Inc., Jacksonville, Florida

TABLE 1. INDUSTRIAL WASTEWATER PILOT PLANT RESULTS

Wastewater	Pretreatment	Loading (kg $BOD_5/m^3 \cdot day$)	Influent BOD_5 (mg/liter)	Effluent BOD_5 (mg/liter)
Domestic & meat packing	Primary clarification	5.6	360	22
Brewery	Primary clarification	5.9	1,500	23

Temp. = 15°C

system could indeed offer cost savings. The secondary systems evaluated were Rotating Biological Contactors, Plastic Media Trickling Filters, and Activated Sludge. All systems were assumed to follow the same pretreatment steps, and sludge handling and disposal costs were assumed to be equal. An influent BOD_5 concentration equal to 140 mg/liter, a flow of 11,368 m^3/d (3MGD), and a wastewater temperature of 15°C were assumed for all systems. All four systems were designed to achieve an effluent BOD_5 concentration of 20 mg/liter. After sizing the unit processes, the costs for each conventional secondary-treatment system were obtained from the EPA I/A Technology Assessment Manual [5]. All costs were updated to 4th quarter 1981 costs using the ENR construction cost index. The BAF costs were based on Eimco PMD equipment quoted selling prices plus installation and miscellaneous equipment costs obtained from the I/A manual.

Table 2 summarizes the important design parameters assumed and the unit process sizing for each of the four secondary-treatment systems. Figure 4 shows that, for the design example evaluated, the BAF system is about 40-50 percent lower in capital cost than the conventional secondary-treatment systems. The energy requirements for this example are about equal to that for the Rotating Biological Contactor as shown in Figure 5. The Plastic Media Trickling Filter system had the lowest energy requirements. A comparison of secondary treatment system land-area requirements, shown in Figure 6, show that the BAF system offers considerable savings in land use for wastewater treatment. The area requirements are about one-fifth of the trickling filter and one-tenth of the activated sludge land-area requirements. The lower BAF area requirements are due to the high design organic loadings possible and the elimination of secondary clarifiers and sludge-recycle systems. Though this evaluation was done at only one set of wastewater conditions, it serves to indicate that the BAF system is an attractive economical alternative for secondary treatment.

INDUSTRIAL WASTEWATER DESIGN PARAMETERS

Design of the BAF system requires determining the reactor volume, oxygen requirements to size the blowers, sludge production to size the sludge-handling units, and backwash requirements to determine the backwash-water storage requirements and backwash flows for sludge thickening and removal hydraulic designs. Volumetric organic loadings (kg $COD/m^3 \cdot d$) determined from pilot-plant studies to achieve a desired effluent quality are used to determine the reactor volume. Pilot-plant studies are recommended to determine the effect of influent solids on operating headloss and backwash frequency. Oxygen needs can be determined in pilot-plant studies by measuring the air flow used to remove a certain amount of organic material at a given loading. This is a gross overall measurement of oxygen used per unit of BOD removed, oxygen-dissolution efficiency, and liquid dissolved-oxygen concentration maintained in the unit. Oxygen-utilization efficiencies of 8-12 percent have been claimed for the BAF system [6]. The air flow in and out of a pilot-plant unit can be evaluated by ORSAT analysis to determine the actual oxygen-utilization efficiency under a given set of operating conditions.

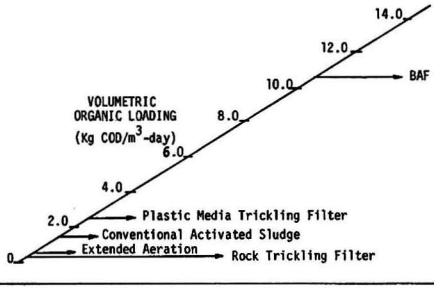

Figure 3. Comparison of aerobic biological systems loadings.

Pilot-plant studies are also needed to determine the type of microorganisms developed in the fixed-film system. The type of microorganisms, as well as the influent solids removed, will determine the settling and thickening characteristics of the backwashed solids. The biofilm thickness and density in the medium may also be affected by the type of microorganisms developed. This will determine the total reactor biomass solids concentration which affects the rate of BOD removal. In one BAF-column study at the University of Utah a very thick fungi biofilm was developed when treating a synthetic sucrose wastewater. The biofilm thickness could not be controlled by backwashing and excessive operating headlosses occurred. The type of microorganisms developed should be affected by the type of industrial wastewater treated. The fixed-film system may also encourage the acclimation of microorganisms to poorly degraded wastewater compounds.

The pilot-plant data described above are useful to generate overall BAF-system design data. Fundamental studies are needed to develop a more rational design approach that can be based on fundamental mass-transfer and biological kinetic rates occurring in the BAF media. Such a model is under development and evaluation using laboratory BAF-column operating data. Factors affecting the BAF-system substrate-removal rates and design are:

1. Liquid velocity
2. Substrate
   a. Concentration
   b. Diffusion rates
   c. Biological reaction rates *versus* the substrate concentration in the biofilm
   d. Particulate *versus* soluble substrate
3. Biofilm thickness and density
4. Flow-distribution pattern in BAF system
5. Oxygen transfer
   a. Oxygen-transfer efficiency in the sparged bed
   b. Oxygen-diffusion rates to the biofilm
6. Wastewater temperature
7. Inhibitory substances in the wastewater

LABORATORY CONTINUOUS FLOW FIXED FILM RESPIROMETER

A laboratory Continuous Flow Fixed Film Respirometer (CFFFR) has been developed at the University of Utah to evaluate oxygen-transfer mechanisms in high-rate biolog-

TABLE 2. COST EVALUATION DESIGN ASSUMPTIONS AND UNIT SIZING FOR 3 MGD APPLICATION

System	Assumptions	Design
BAF	5 kg $BOD_5/m^3 \cdot day$ 0.85 kg O_2/kg BOD removed 10.5% O_2 utilization efficiency $\alpha = 0.83, \beta = 0.95$	Volume = 320 m^3 4 tanks @ 3.7 m × 12.8 m Media depth = 1.8 m 4 cells/tank 2.4 m/hr hydraulic appl. Backwash storage (76 m^3)
RBC	101.7 L/d·m^2 media area (2.5 gpd/ft^2) Clarifier, 1 m/hr 4.85 Hp. shaft	12 shafts, 9302 m^2 area/shaft (12′ dia. × 10′ shafts) 2-17 m dia. clarifiers
Trickling Filter	0.53 kg $BOD_5/m^3 \cdot day$ Recirculation 1:1 Media depth, 6.4 m Clarifier, 1 m/hr	2-17 m dia. towers 2-17 m dia. clarifiers
Activated Sludge	SRT, 8 days FLM, 0.25 MLSS, 2,500 mg/liter 1.0 kg O_2/kg BOD_5 $\alpha = 0.83, \beta = 0.95$ Aerator eff., 1.4 kg O_2/hp·hr Clarifier, 1 m/hr	Detention time = 6 hours Aeration volume = 2842 m^3 2-50 Hp aerators 2-17 m dia. clarifiers 150% sludge recycle 1-3 m dia. DAF sludge thickener

ical fixed-film systems. The device, shown in Figure 7, can also be used for BAF-system treatability studies. The principal function of the CFFFR is to provide a direct, continuous, and accurate measurement of the oxygen utilized in the biological degradation of substrates continuously fed to the fixed-film reactor. Continuous measurements can be obtained under steady-state or non-steady-state operating conditions. The CFFFR system can be described by the following features:

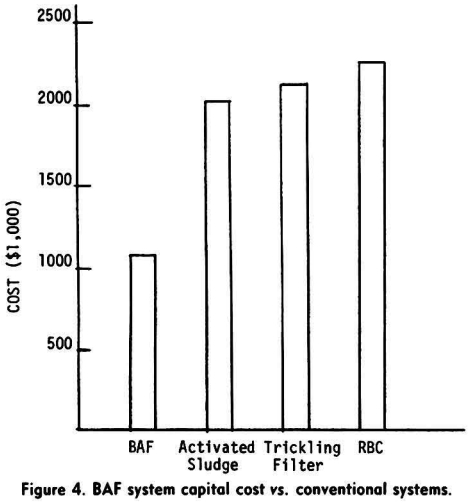

Figure 4. BAF system capital cost vs. conventional systems.

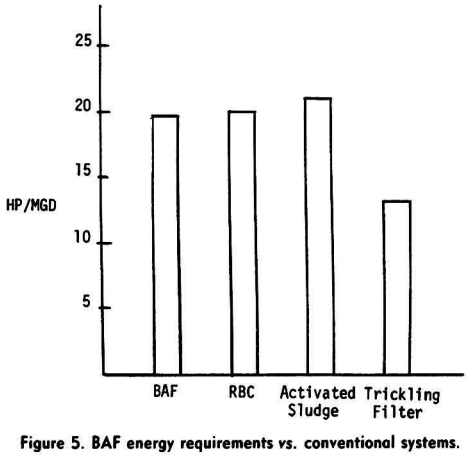

Figure 5. BAF energy requirements vs. conventional systems.

1. Reactor

A variety of reactor configurations can be used for the reactor section. A small simulation of the BAF reactor is shown. Wastewater is continuously pumped to the reactor from a feed reservoir at a controlled rate. Baffles are placed along the sidewalls of the reactor to minimize wall effects, that could cause short circuiting. Air is sparged into the bed through a perforated tube. Effluent is collected in a reservoir for use during periodic backwashing of the system. The backwash water is collected for determination of solids-production and solids-settling and thickening characteristics. A separate air line is used to provide air agitation during the backwashing cycle. Backwashing is done manually. The air-sparging line is closed off during backwashing.

The reactor configuration can also be modified for an upflow fixed, expanded, or fluidized-bed operation.

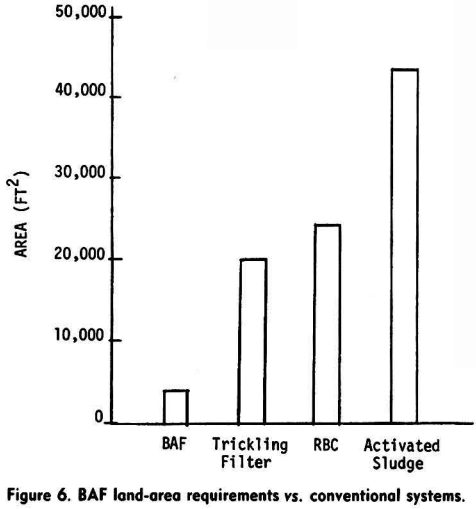

Figure 6. BAF land-area requirements vs. conventional systems.

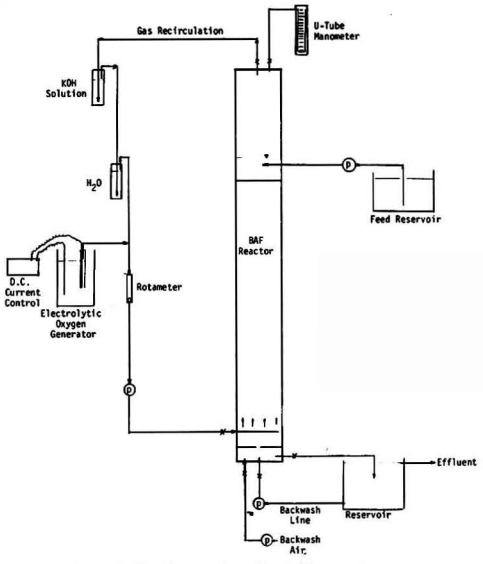

Figure 7. Continuous-flow fixed-film respirometer.

2. Oxygenation

A unique feature of the laboratory CFFFR system is a closed gas-recycle loop used for oxygenation. Oxygen is introduced using an in-bed gas-sparging technique. The gas collects at the top of the reactor and is passed through a KOH solution to remove carbon dioxide produced in the reactor during oxygen dissolution and depletion. The reactor gas-recycle flow and sparge rate is controlled by a rotameter and a pinch valve. The oxygen tension of the closed-loop gas stream is determined by dissolved oxygen measurements in a small distilled-water reservoir, through which the recycled gas passes continuously.

3. Oxygen Consumption Measurements

Oxygen utilized in the respirometer is replaced by the electrolysis of water in an isolated generator. Carbon dioxide produced in the respirometer is removed in a separate potassium-hydroxide trap. The entire gas volume is continually recycled without any outside gas makeup, aside from the oxygen produced by the electrolytic generator.

With this technique, the production of oxygen by the electrolytic generator is controlled to equal the oxygen-utilization rate in the respirometer. When the oxygen-production rate of the generator does not match the consumption rate in the reactor, a pressure imbalance within the closed gas-recycle loop occurs, which is in turn registered by the attached manometer. The rate of oxygen production by the generator is controlled simply by varying the D.C. current amperage or the time-on at a fixed amperage. Thus, the oxygen-utilization rate in the respirometer is directly proportional to the D.C. amperage supplied to the electrolytic generator. A correction is made to account for the influent and effluent dissolved-oxygen concentrations of the liquid stream. This technique for measuring oxygen utilization is considerably simpler than that required using the ORSAT analysis and can be performed with greater accuracy and on a continuous basis. This approach is also applicable for non-steady-state conditions where a fluctuating oxygen demand due to variable substrate loading may exist.

In general, steady-state oxygen-utilization patterns can be established rapidly enough so that the oxygen production of the electrolytic generator can be set manually through direct observation of the internal respirometer pressure. However, the oxygen generator current can be automatically controlled by a mechanical pressure-sensing device in the manometer. In this way, the oxygen uptake could be recorded on a strip-chart device measuring the current supplied to the electrolytic generator.

The innovative CFFFR system provides a simple laboratory treatability device. Bio-acclimation to industrial wastes can be judged by observing increasing daily oxygen consumption rates until a steady-state oxygen-consumption level is reached. Suspended solids-removal and headloss build-up can be observed in the small BAF reactor. Effluent quality, oxygen consumption per unit of BOD removed, and sludge production per unit of BOD removed can be observed at various organic loadings. Evaluation of toxic or inhibitory feed streams can be made quickly from the continuous oxygen-consumption measurements.

SUMMARY AND CONCLUSIONS

The Biological Aerated Filter System is a new innovative fixed-film biological secondary wastewater-treatment system for industrial wastewater treatment. The innovative fixed-film packed-bed design results in a high biomass concentration per unit volume to provide secondary treatment at greatly reduced reactor detention times. Effluent BOD_5 concentrations less than 30 mg/liter have been achieved at volumetric organic loadings of 4-6 kg $BOD_5/m^3 \cdot d$ when treating industrial wastewater. Industrial wastewater applications using the BAF system must consider nutrient addition and equalization requirements, as well as pretreatment steps to minimize influent suspended solids, oil, and grease concentrations to the BAF unit.

The BAF system is best suited for applications requiring moderate to high-quality effluents. For high-strength industrial wastewaters (COD >1,000 mg/liter), the IA[2] system, consisting of integrated anaerobic—BAF units, has been shown to produce a secondary effluent quality.

A secondary treatment application cost example showed that the BAF system offers the potential for significant capital-cost and land-area savings as compared to Rotating Biological Contactors, Plastic Media Trickling Filters, and Activated Sludge Systems. For the example used, the BAF system offered a 40-50 percent reduction in capital cost. The BAF-system energy requirements are similar to that reported for Rotating Biological Contactor Systems. Land-area requirements for the BAF system may be one-tenth of Activated Sludge System requirements.

The BAF-system design approach is empirical at this time and must be based on pilot-plant studies. Volumetric organic loadings and air-application rates are determined to achieve a desired effluent quality. A more fundamental bench-scale treatability study approach is under investigation with the aid of the Continuous Flow Fixed Film Respirometer System. The CFFFR system may be used to determine oxygen-utilization rates, bio-acclimation levels, potential toxicity problems, and fundamental design data.

LITERATURE CITED

1. Ying, W. and W. J. Weber, Jr., "Bio-Physicochemical Adsorption Model Systems for Wastewater Treatment," *Journal Water Pollution Control Federation*, **53**, 2661 (1979).
2. Young, J. C. and M. C. Stewart, "PBR—A New Addition to the AWT Family," *Water and Wastes Engineering*, **20** (August, 1979).

3. Jeris, J. S. *et al.*, "Biological Fluidized-Bed Treatment for BOD and Nitrogen Removal," *Journal Water Pollution Control Federation*, 48, 816 (1977).
4. Stensel, H. D., "Biological Aerated Filter," "EPA Assessment and Evaluation of Emerging I/A Technologies," Center for Environmental Research Information (March, 1982).
5. "EPA I/A Technology Assessment Manual," EPA-430/9-78-009, Cincinnati, Ohio (February, 1980).
6. Leglise, J. P., P. Gilles, and H. Moreaud, "A New Development in the Biological Aerated Filter Bed Technology," Presented at the 53rd Annual Water Pollution Control Federation Conference, Las Vegas, Nevada (October 2, 1980).

H. D. Stensel is an associate professor of environmental engineering at the University of Utah. A registered engineer in Pennsylvania, he holds a B.S.C.E. degree from Union College, and M.S. and Ph.D. degrees in environmental engineering from Cornell University. He has extensive experience in biological wastewater treatment processes and has authored several technical articles on wastewater treatment-systems design and applications.

S. Reiber is a doctoral student in environmental engineering at the University of Utah. He holds an M.S. in environmental engineering degree from the University of Michigan and an M.S. in public health from Johns Hopkins University.

Optimized Effluent Treatment—Implementation and Management

An actual case history account of the development of an optimized effluent-treating system at Amoco's Whiting, Indiana, refinery.

David C. Kloeckner, Amoco Oil Co., Whiting, Ind. 46394

Practical application of an optimized effluent-treatment system and implementation of a significant program of best-management practices is exceptionally effective in maintaining good refinery effluent-water quality. Although no major new operations or practices are employed over the known conventional treatment the resultant effect is phenomenal when these two areas are controlled for mutual effects. When these are applied in plant-wide operations, i.e., at Amoco Oil Company's Whiting refinery, the concept demonstrates major effluent improvements such that compliance with imposed regulatory requirements is feasible.

Amoco's Whiting (Indiana) refinery, located at the southern tip of Lake Michigan, is a modern, fully integrated, EPA Subcategory D facility. The major refinery processes utilized are crude desalting, distillation, hydrotreating, catalytic cracking, platinum reforming, alkylation, hydrodesulfurization, treating, lube oil manufacture, etc. The refinery's origin dates back to 1889. It is the oldest in the Amoco Oil Company system, and the second largest. Of approximately 280 refineries in the United States, it is the sixth largest.

For the petroleum refining industry, meeting best practicable control technology currently available (BPCTCA) goals for 1977 requires an end-of-pipe treatment sequence involving primary, intermediate, and secondary treatment. Oil-water separators are involved in primary treatment; equalization, pH control, reduction of immediate oxygen demand, chemical destabilization and filtration, or air flotation in intermediate treatment; and the activated-sludge process (ASP) or its performance equivalent in secondary treatment [*1,2*].

Proposed 1984 best available technology economically available (BATEA) includes add-on granular activated-carbon facilities. Amoco views the use of the combination optimized treatment system and best management practices as a possible viable alternative to granular activated carbon for meeting proposed 1984 effluent-quality standards.

The objective of a granular activated-carbon facility is the same as for existing secondary treatment facilities, that is, the removal of soluble organics [3]. The large costs involved for granular carbon provide an incentive to investigate the improvement in performance of the existing BPCTCA treatment sequence with the objective of eliminating the need for costly add-on granular activated-carbon facilities.

Over the years, the ASP has proved its wide applicability and tremendous capacity for water purification. Often, the role of the ASP is identified solely with secondary treatment. Current work [*4,5*] has demonstrated that viewing the ASP solely as a secondary treatment process is shortsighted and, in fact, that the ASP provides the preferred means for achieving future BATEA water-quality goals when compared to alternatives. A cost-effective route for using the ASP to achieve BATEA effluent quality requires that the ASP be operated at an unusually high sludge age. In order to accomplish this objective, the treatment complex must be supplemented and reinforced by an established comprehensive program of best management practices. A best management practices program includes an interfacing of numerous refinery disciplines (i.e., management, maintenance, engineering, technical support groups, and the ultimate team key-hourly employees). A management program is required as part of the BPCTCA goals for 1977; however, if a comprehensive, tough refinery-wide program of good management practices is implemented, BATEA may be reachable.

Amoco Oil's Whiting refinery environmental operating program has three principal phases:

1. System optimization by limiting the role of the activated-sludge process to one of removing chiefly soluble contaminants.
2. Optimization of each unit operation, both treatment

plant and in-refinery control equipment, to new performance goals consistent with the newly defined function of the ASP.
3. Development and implementation of a strong management program to further promote enhancement of the ASP toward meeting EPA's 1984 goals.

SYSTEMS OPTIMIZATION

Optimizing a refinery effluent-treatment sequence requires recognition of the fact that each of the end-of-pipe process steps has a principal function. Whiting's sequence of process steps consists of in-plant treatment with controlled disposal of select antagonistic streams, primary, intermediate, secondary, and tertiary treatment. Whiting's end-of-pipe treatment complex consists of existing wastewater-treatment processes currently available and used in industry.

Figure 1 is a schematic representation of Whiting's process wastewater-treating facilities. It consists of pre- or in-plant equipment, bar screen, API separators, equalization and storm surge, dissolved-air flotation (DAF), mixed-liquor aeration tanks, clarifiers, and final filters. The average theoretical hydraulic retention times, in hours, for the sequence are: 2 to 3, separation; 10 to 12, equalization; 1/2, DAF; 10, aeration; 3, setting; and a 4.3 GPM/ft^2 filtration rate.

Amoco has identified the ASP as the key treatment unit for NPDES compliance. The workhorse role of the ASP has been deleted, and the prime function redefined as the removal of essentially only soluble contaminants. The beneficial effects realized are [3]:

1. The settling (SVI) characteristics of the activated sludge mass are excellent at very high sludge ages, i.e., over 40 days.
2. Process control is greatly simplified by operating at a very high sludge age, i.e., greater than 40 days.
3. Using a very high sludge age for process operation eliminates the need for many process-control tests.
4. Operating at a very high sludge age produces an exemplary effluent very low in total organic (TOC) and other contaminants.
5. Biological cell yield is remarkably low at a very high sludge age.
6. At a very high sludge age, the population dynamics of the sludge mass improve.
7. Maximum ASP capacity for purification is achieved by operating at high sludge ages.

Recent kinetic expressions [6,7,8] predict that the lowest residual organics will be produced by the ASP with the lowest feed strength. For example, in the Adams *et al.* expression:

$$S_e = S_i(S_i - S_e)/KMt \qquad (1)$$

Where,

S_e = Soluble organics in effluent (mg/liter)
S_i = Organics in influent (mg/liter)
K = Kinetic constant
M = Biomass (mg/liter)
t = Time

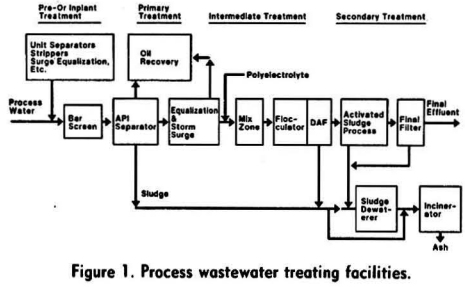

Figure 1. Process wastewater treating facilities.

The authors point out that $S_i/Mt = F/M$, and , letting $F = S_i/Mt$, Equation 1 becomes:

$$S_e = S_i(KF^{-1} + 1) \qquad (2)$$

Equation 2 clearly points out that a low F/M ratio (high sludge age) and low feed strength are associated with optimized ASP effluent quality.

Thus, removing colloids and solids in pretreatment facilities serves the purpose of minimizing the organics in the influent, which typically reduces the waste strength by 50 percent or more [1] and corresponds to the kinetic equations. When operated chiefly for soluble organics removal, the ASP can be operated easily in existing facilities in the unusual operating mode of very high sludge age [4,5,9,10,11].

PRETREATMENT FACILITIES

Restricting the operating objective of secondary treatment to the removal of soluble contaminants means that pretreatment to remove colloidal and suspended matter is a prerequisite. Dissolved-air flotation (DAF) units and filter are widely used in this service. Typically, however, the physical function of this equipment for phase separation is stressed and, therefore, optimum performance is not achieved. The key to obtaining optimum performance from DAF units and filters lies in chemical preteatment of water [12].

The use of chemicals in the treatment of industrial wastewaters is not a new concept. Field-application techniques generally are haphazard, with beaker tests forming the scientific basis. As it became apparent that more stringent effluent goals would have to be addressed, coupled with the new role assignment for the ASP, it was determined that a more systematic scientific approach must be used in wastewater chemical-application technology. Optimization of phase-separation equipment is vital to the successful implementation of high-sludge age/activated-sludge process operation.

Phase-separation efficiency requires recognizing that most solids in the presence of water have a negative electrical surface charge (zeta potential). Also, flotation air bubbles and the surface of the granular media in a filter have a negative electrical potential. Maximized phase-separation efficiency requires that these coulombic repulsive forces be controlled by controlling the properties of the dispersed phase. Destabilization of colloidals by chemical treatment has the objective of neutralizing or reducing a particle's electrical charge so that mutual repulsion is reduced to the extent that individual particles can approach each other close enough for van-der-Waals and/or chemical forces to become effective. The attractive van-der-Waals forces cause the particles to aggregate into agglomerates, which facilitate their removal by sedimentation, air flotation, or filtration processes. The surface charge on colloidal particles may be estimated by electrophoretic, electroosmotic, streaming, and sedimentation-potential techniques.

Amoco found that the electrophoretic procedure and equipment of Riddick permit a rapid determination of colloidal charge to be made, and our investigations involved the use of a zeta meter. Accordingly, the electrokinetic values reported herein are zeta potentials (ZP).

Figure 2 is a comparison of polyelectrolyte performance on Whiting wastewater prior to liquid/solid phase separation by dissolved-air flotation (DAF). These ZP-cationic polyelectrolyte titration curves quantify the amount of polyelectrolyte needed to reduce the repulsive coulombic forces to levels that permit total destabilization by attractive forces.

By running titration curves, the effectiveness of cationic polyelectrolytes can be quantified for specific applications. Sometimes the titration "end-point" (zero zeta po-

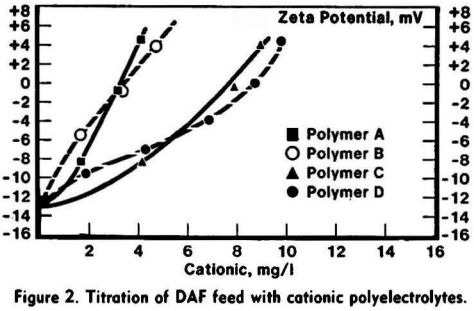

Figure 2. Titration of DAF feed with cationic polyelectrolytes.

tential) is exact, and at times it is somewhat arbitrary. We find that most colloid systems are destabilized adequately for phase removal when the ZP is only reduced to −5 or −3 mV. This seems to depend on particle size and hydrophilicity. At optimum dosage, the colloidal charge is reduced to an acceptable end-point (−3 to+3 mV), while extreme overdosing can result in charge reversal and deterioration or failure of the liquid/solid phase separation facilities.

The use of solely the zero ZP "end-point" for system-cost evaluation should be avoided. Comparative ZP rankings, slope of the ZP titration curve, effect of potential system antagonism or synergisms, manpower, and educational ability of plant operators to vary dosages to prevent and control what otherwise would result in upsets, etc., must all be given due consideration in a total-system cost analysis in conjunction with base material prices.

IMPACT OF INTERMEDIATE TREATMENT ON SECONDARY TREATMENT

The importance of good primary treatment and optimized intermediate treatment on design and operating considerations for a following secondary treatment facility can be visualized by taking waste-load data and plotting it on probability paper. Figures 3 thru 7 are probability plots of typical Whiting refinery data for total suspended solids (TSS), oil and grease (O & G), total organic carbon (TOC), ammonia (NH_3), and phenol, respectively.

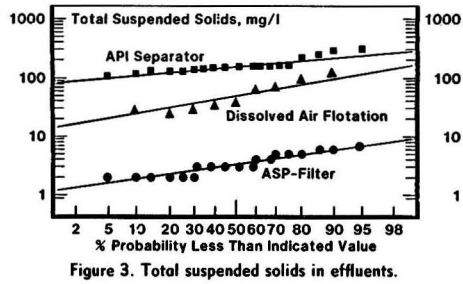

Figure 3. Total suspended solids in effluents.

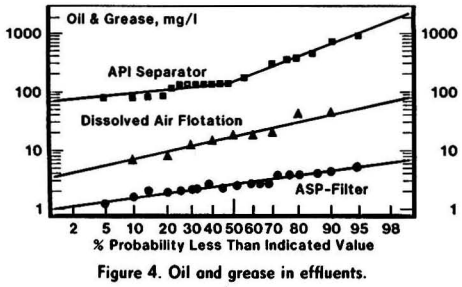

Figure 4. Oil and grease in effluents.

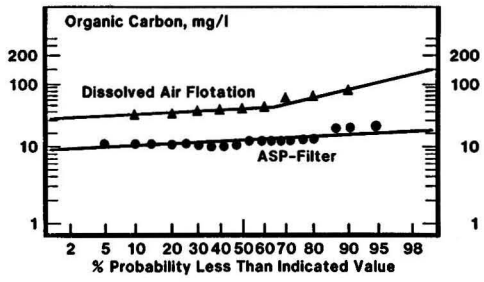

Figure 5. Organic carbon in effluents.

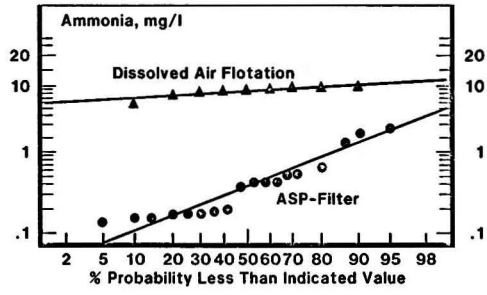

Figure 6. Ammonia in effluents.

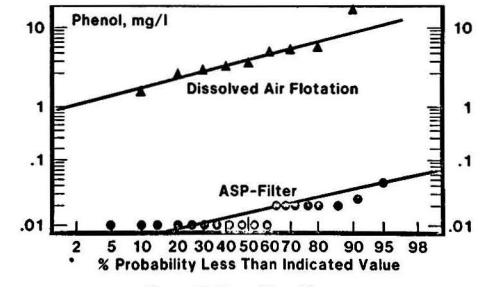

Figure 7. Phenol in effluents.

As repeatedly stated, the maintenance of a high sludge age in the ASP requires a feed that is significantly depleted of oil and inerts that accumulate in the activated-sludge mass. Raw-feed concentrations vary considerably over a year's time (Figures 3 and 4) whereas, after pretreatment, the slope of the probability curve decreases, providing an equalized feed quality. The equalizing effect of the intermediate treatment step is indicated by reviewing the 50-percentile level: the dissolved—air flotation unit removed 69 percent of the TSS and 84 percent of the O & G. At the 95-percentile level, the respective percent removals were 52 percent and 94 percent—a significant fraction of the raw-waste load. Also, removing oil from the process water effluent prior to biological treatment recovers oil in a sludge much easier and less costly to handle than if the oil is commingled in a waste activated sludge.

Equalized feed quality in terms of organic loading can be achieved in the intermediate treatment section, as shown for chemical oxygen demand (COD) data in Figure 8. Colloidal and suspended matter contributes significantly to total COD.

Intermediate treatment reduced the raw-feed organic load by 45 and 68 percent for the 50- and 95-percentile levels, respectively. Equalized organic loading results in substantial savings in capital and operating costs, simpler operations, and better effluent quality with less variability

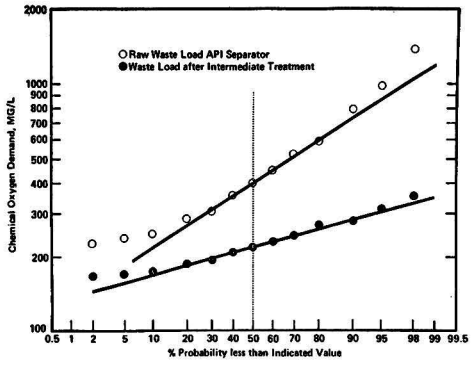

Figure 8. Feed quality in terms of organic loading.

in water quality leaving the secondary treatment facilities, as predicted by the kinetic equations. The design engineer now has a less variable feed quality for a design base.

Figures 3 thru 7 illustrate the exemplary effluent quality achieved by the Whiting treatment complex. Typically, the ASP operates at 35 to 40 days sludge age.

On close examination, it is obvious that high sludge age operation of Whiting's ASP results in a lightly loaded treatment plant by industry comparison. The plant is accomplishing what the kinetic equations predict, but what must be recognized is that 1) it takes a continuous enthusiastic and cooperative environmental effort by all refinery employees to minimize variability in feed quality, and 2) management practices have a dominant impact.

BEST MANAGEMENT PRACTICES

EPA has recognized from the onset in its regulatory policy that in-refinery management operating practices can have a substantial impact on waste loads discharged to an end-of-pipe wastewater-treatment facility. BPCTCA, as defined by the EPA for petroleum refineries, suggests that in-plant controls should include:

- Installation of sour-water strippers to reduce sulfide and ammonia concentrations entering the treatment plant.
- Elimination of once-through barometric-condenser water by using surface condensers or recycle systems with oily-water cooling towers.
- Segregation of sewers, so that uncontaminated storm runoff and once-through cooling waters are not treated normally with process and other contaminated waters.
- Elimination of polluted once-through cooling water by monitoring and repair of surface condensers, or by use of wet and dry recycle systems.
- Employment of good housekeeping practices and precautionary measures during operating unit turnarounds.

Provided under the "Management Requirements" part of most NPDES permits is a broad provision reading: "The permittee shall at all times maintain in good working order and operate as efficiently as possible all treatment or control facilities or systems installed or used by the permittee to achieve compliance with the terms and conditions of this permit" [*13*].

Broadly viewed, EPA has authority to mandate not only the in-plant equipment controls necessary to insure permit compliance, but also included therein could be monitoring, operator training, maintenance, and personnel provisions. Amoco's Whiting refinery management has adopted a tough in-plant management program to reduce the possibility of future potential EPA intrusion into in-plant operations.

Such a management program is easily applied on paper, but application requires an intense, sincere effort refinery-wide. Employees and managers in environmentally responsible positions must be trend setters.

PROGRAM SEQUENCE

The Whiting refinery's in-plant "Best Management Program" involves a sequence of program steps (Figure 9) intended to fulfill the following objectives:

- Assure NPDES permit compliance.
- Assure total environmental cooperation and consciousness by each and every employee.

These objectives point to the fact that just having in-plant and end-of-pipe control equipment in place and operating does not assure NPDES permit compliance.

Each program sequence focuses on preventing the discharge of gross quantities of contaminants to the sewer system. A well operated end-of-pipe treatment system has a vast potential to assimilate a broad cross-section of contaminants while yielding an excellent quality effluent, provided it is not abused. Ammonia, phenol, monoethanolamine (MEA), etc., can be discharged and treated successfully when volume and time of discharge are controlled. Potential water pollution is minimized when all elements in the refinery are controlled for mutual effects.

Whiting refinery management has clearly reaffirmed the importance and support of an effective environmental program to all its supervisors, professional, and hourly refinery personnel. In-plant environmental infractions are defined not only as those resulting in regulatory attention, but include any actions which are contrary to good environmental practices.

Environmental training has been intensified to increase and improve in-refinery environmental operations. The principal thrust is to familiarize each operating division as to how their operations affect the refinery's NPDES permit. Also, we strive to broaden the understanding between divisions as to the interdivisional impact of operations.

Regardless of precautions taken (i.e., design, training, operations, etc.), surges in the contaminant concentration of wastewater streams requiring treatment will occur. To protect waste-treatment plant operations from contaminant surges, thus preventing most violations, requires an intensive ALERT monitoring program. At Whiting, wastewater-treatment operating personnel provide the initial monitoring key.

A review of historic operations pinpointed the fact that surges in hydrocarbons, ammonia, phenolics, pH, MEA, turbidity, and flow volume exhibited the greatest potential for hindering or upsetting treatment-plant efficiencies. Any one of these contaminants is removable if the influent concentration is kept reasonable.

On-site monitoring by treatment-plant operators provides a means of rapidly detecting changes so that in-refinery response can be activated to control the surge discharge. On-site monitoring procedures require the use of analytical techniques which are quite basic, for they will be implemented and used by non-technical personnel.

The Whiting treatment complex uses a six-site sampling, monitoring, and evaluation program that is performed routinely every two hours. The frequency is increased when surges and upsets are detected, until conditions stabilize. Excessive hydrocarbons are checked by visual observation of the inlet-channel water surface. Ammonia and phenolic level is determined by colorimeter techniques. Chemets, manufactured by CHEMetrics, Inc., are used to develop a color intensity which is then compared to a known contaminant concentration color reference. If contaminant levels exceed comparison ranges, on-site dilutions are carried out. The pH is measured by glass elec-

Program	Group	Method	Purpose
Amoco policy	All refinery personnel	Management position statement	Reaffirm management's commitment and support of an effective environmental program
Training	All refinery personnel	Person-to-person and videotape	Provide detailed understanding of how each operating area impacts the refinery's NPDES permit
Monitoring	Treatment plant	Environmental inspection team	Develop an early detection system to detect, trace, and curtail discharges of gross pollutant loads
		Treatment plant operators	
	Laboratory Services	Training covering NPDES permit considerations	Provide laboratory personnel with working knowledge of NPDES limitations, thus assuring rapid communication of possible excursions
Operations Planning Coordination	Supervisors & professional personnel	Establish areas of joint responsibilities	Reduce impact of inplant control equipment outages (covers both major and extremely minor problems), thus preventing simultaneous discharge of gross contaminant loads from unrelated operating areas
Maintenance Coordination	Maintenance & Operations	Daily meeting	Establish repair priorities and assure maintenance personnel understand potential environmental impact if things are mishandled
Communication	All refinery personnel	Environmental inspection team	Provide 24-hr. continuous monitoring of refinery operations impacting on environmental compliance
		Radio (open channel)	Provides environmental inspector with a good overview of on-going refinery activities and promotes quick communication access between inspector and refinery units in responding to calls for assistance and review
Pre- or Inplant Treatment	Refinery	Equipment, training and environmental inspection team	Provides equipment and procedures to minimize gross contaminant discharges to process sewer

Figure 9. Best management program sequence.

trode. Turbidity is determined by conventional light-scattering instrumentation. Turbidity is important in evaluating the efficiency of liquid-solid phase-separation facilities (i.e., dissolved-air flotation, clarifiers, and filters) and provides a secondary basis for evaluating polyelectrolyte dosages in the field.

Whiting's raw-waste load process water inlet, due to its historic design, is not provided with flow measurement, but this does not prevent operator evaluation of significant flow changes. Observation of left-station operation and bypass control-loop settings provide a key to flow changes. Subsequent downstream treatment sequences are equipped with flow-measurement equipment for NPDES reporting. No "quickie" field technique has been found for detecting shock MEA losses. Routine inlet samples are delivered to Laboratory Services for total nitrogen and ammonia-as-nitrogen concentration determination. From historical operating experience, we assume that all total nitrogen in excess of the ammonia component represents MEA. We have been successful in establishing a base total-nitrogen range below which, we are confident, MEA can be easily oxidized by the activated-sludge.

When operating personnel sampling detects any values that fall outside acceptable levels, communication is established with the refinery environmental inspector (EI).

The environmental inspection team provides a close surveillance of all in-refinery environmental matters on a full-time, 24-hour basis. This team serves as the eyes and ears of the environmental supervisors. They oversee any activities which remotely affect the refinery's environmental position (i.e., flares, oil, and sour-water pipeline repairs, tank cleaning, stripper upsets, all types of leaks, etc.). The list is unending. When contaminant excursions are reported to the EI, he conducts a check of pre-established refinery sewer locations for the contaminant of concern. Given a process-unit discharge map, detailing which units discharge upstream of the test point, the EI can narrow the source down to a few possible candidates. Once the exact unit source is established, a review of the situation is made to establish what type of corrective action will be undertaken.

Laboratory Services also provides a vital service in minimizing NPDES permit excursion. At times, quick analytical evaluations are requested to track troublesome upset incidents. Technicians are trained to recognize potentially contaminated samples. They alert operating personnel of any significant changes in effluent quality, so a maximum opportunity exists to take corrective action or to evaluate the need to question sampling procedure. Laboratory personnel take all samples used for NPDES permit compliance, reporting independently of treatment-plant personnel.

Interdivisional planning coordination of scheduled abnormal operating practices is important for controlling gross contaminant discharge. Environmental control supervisors are kept informed of planned unit activities in other divisions. These supervisors oversee, review, and coordinate major and relatively minor activities which have related environmental overtones (i.e., tank and exchanger cleaning, line repairs, proposed water use and tie-in projects, in-refinery control-equipment outages and repairs). The list can be endless. Jobs may be postponed days or weeks if necessary. Consideration must be given to the performance level existing at the waste-treatment complex. It must be established whether the plant is at optimum or if it is being hindered by temperature or storm constraints, or whether a major equipment outage has

occurred, hindering optimum biological efficiency. It is impossible to overemphasize or overstress the importance of this area. Almost anything within reason is achievable, but CONTROL is the key.

Maintenance procedures must provide for prompt attention to the equipment required to maintain environmental compliance. Whiting's waste-treatment complex has a complement of maintenance personnel whose sole assigned area of responsiblity is maintenance of environmental facilities. Daily maintenance job assignment priority meetings are used to coordinate critical control-equipment repair. Some limited cross-familiarization and job training between operations and maintenance is done to develop an understanding of job capability and limitations. Certain critical equipment is placed on a preventive-maintenance checkout list; thus, night-shift and weekend outages are minimized.

Communication provides a vital link between a good, effective environmental program and an inefficient one. To foster and accomplish communication, refinery environmental personnel encourage telephone and radio communication with respect to intended activities, regardless of how insignificant they seem. The refinery operates a plant-wide radio system, on which the environmental personnel maintain an open-channel policy. This policy promotes quick access to environmental representatives, especially the environmental inspector. Additionally, this provides environmental supervisors with an overview of all refinery activities and how their environmental subordinates are responding and handling situtations. This provides an added level of assurance that inquiries will be coped-with skillfully and quickly so that work can progress in a timely manner.

As previously noted, EPA has recognized that certain in-refinery conventional pollution-control equipment is required as part of an end-of-pipe water-treatment facility. These conventional equipment components are well known and broadly used throughout the oil industry (i.e., sour-water strippers, segregated sewers, oil-water separators, good housekeeping practices, etc.). At Amoco's Whiting refinery it was found that this typical equipment proved inadequate if NPDES permit compliance was to be assured. Whiting determined that extremely high losses of MEA to the process sewer proved to be a compliance problem. It was found that a very few gallons of MEA shocked the nitrification reaction of the ASP biological culture. It was determined that surge MEA sewer losses must be control-discharged. Whiting's treatment facility is equipped with a 12-hour-retention equalization basin, but this has proved to be inadequate. An in-refinery toxic-shock surge tank was needed. All upset pumpages from the Sulfur Recovery Unit (SRU) MEA-circulation system and condensate collections from fuel-gas knockout drums are discharged to the shock tank. Then, under the auspices of the EI, the tank's contaminant stream is drained to the process sewer at a controlled rate (normally 5 to 20 gpm), depending on concentration. Surge volumes which used to find their way to the sewer in a mattter of minutes are now control-discharged over weeks or months. This tank, given proper control, has proved invaluable in advancing the refinery toward its goal of zero NPDES excursions.

OBSERVATIONS AND RECOMMENDATIONS

- The role of the ASP in treatment of refinery effluents should be limited to removal of soluble contaminants.
- The ASP should be operated at conditions of high sludge age to achieve maximum biological oxidation.
- It is the responsibility of all refinery employees to exercise good environmental judgment and caution at all times.
- Any environmental conditions or questions that arise should be brought to the attention of environmental personnel for quick, safe handling.
- Frequently there is little difference between environmental compliance *vs.* violations, except employee attitude.

LITERATURE CITED

1. Grutsch, J. F. and R. C. Mallatt, "Intermediate Treatment," Hydrocarbon Processing **55**, No. 4, 213 (1976).
2. "U. S. Environmental Protection Agency (Draft) Development Document for Effluent Limitations, Guidelines and New Source Performance Standards for the Petroleum Refining Point Source Category," USEPA, Washington, D.C. 20460 (April, 1974).
3. Grutsch, J. F. and D. C. Kloeckner, "Optimizing the Role of the Activated Sludge Process to Meet BATEA," *Industrial Water Engineering*, 10-14 January/February (1979).
4. Grutsch, J. F. and R. C. Mallatt, "A New Perspective on the Role of the Activated Sludge Process and Ancillary Facilities," First Open Forum on Management of Petroleum Refinery Wastewaters, USEPA, API, NPRA, University of Tulsa, Tulsa, Oklahoma (January, 1976).
5. Grutsch, J. F. and R. C. Mallatt, "Design and Operation: Bases for an Activated Sludge Route to BAT (1983) Water Quality Goals," Second Open Forum on Management of Petroleum Refinery Wastewaters, USEPA, API, NPRA, University of Tulsa, Tulsa, Oklahoma (June, 1977).
6. Grady, C. P. L. *et al.*, "Effects of Influent Substrate Concentration on the Kinetics of Natural Microbial Populations in Continuous Culture," *Water Research* **9**, 171 (1975).
7. Sykes, R. M., "Microbial Product Formation and Variable Yield," *JWPCF* **48**, 2046 (August, 1976).
8. Adams, C. E., W. W. Eckenfelder, and J. C. Hovious, "A Kinetic Model for Design of Completely Mixed Activated Sludge Treating Variable Strength Industrial Wastewaters," *Water Research* **9**, 37 (1975).
9. Grieves, C. G., M. K. Stenstrom, J. D. Walk, and J. F. Grutsch, "Powdered Carbon Improves Activated Sludge Treatment," *Hydrocarbon Processing*, 125-130 (October, 1977).
10. Grieves, C. G. *et al.*, Powdered Carbon Enhancement versus Granular Carbon Adsorption for Oil Refinery BATEA Waste Water Treatment," WPCF Meeting, Anaheim, California (October, 1978).
11. U. S. Patent 4,104,163
12. Grutsch, J. F., "Wastewater Treatment: The Electrical Connection," *Environmental Science and Technology*, 712, No. 79, p. 1022.
13. "Whiting Refinery NPDES Permit—Management Requirements, Part II."

David C. Kloeckner is Superintendent, Reclamation, for Amoco Oil Company's Whiting (Indiana) refinery. He has 14 years of experience in research, design, construction, and operation of environmental facilities for refineries. He is a registered professional engineer and holds a certified state wastewater treatment plant operator's license.

Reverse Osmosis of Blast-Furnace Scrubber Water

In conjunction with cellulose-acetate membranes, reverse osmosis shows significant advantages in scrubber applications.

M. E. Terril, U.S. Steel Corp., Monroeville, Pa. 15146
and
R. D. Neufeld, University of Pittsburgh, Pittsburgh, Pa. 15213

Entrained dust in blast-furnace off-gas must be removed before the gas can be used as fuel. Wet scrubbing is the standard method for cleaning blast-furnace gas. As illustrated in Figure 1, the scrubber water is contained in a recycle system. A sidestream (blowdown) is discharged to prevent scaling or corrosion in the recycle system.

Presently, wastewater discharged from the gas-scrubber recycle system is subject to Best Practical Control Technology Currently Available (BPT) limitations. Compliance with Best Available Technology Economically Achievable (BAT) and Best Available Conventional Control Technology (BCT) limits will be required by July, 1984. These limits have been proposed by the U.S. Environmental Protection Agency (EPA) and are shown in Table 1. Additional treatment will be required to achieve BAT limits. Alkaline chlorination is, currently, the treatment method recommended by the EPA. For those systems that have blast-furnace-slag quenching facilities, the gas-scrubber recycle-system blowdown may be disposed of by evaporation on hot slag. Prior research was conducted by Osantowski and Geinopolos [*1*] who investigated ozonation, alkaline chlorination, and reverse osmosis (RO) with polyamide membranes followed by alkaline chlorination or ozonation of the RO concentrate as treatment approaches for gas-scrubber blowdown water. Our study was based on the use of RO for treatment of waters discharged from cooling-water recycle systems [*2, 3*], and advanced the work of Osantowski and Geinopolos by investigating spiral-wound cellulose acetate membranes. The use of conventional spiral-wound cellulose-acetate-membranes represents a significant potential capital-cost savings. Figure 2 is a sketch of a typical spiral-wound membrane. A second reason for selecting cellulose acetate was that it displays low rejections of cyanide and phenol at pH values below 7.

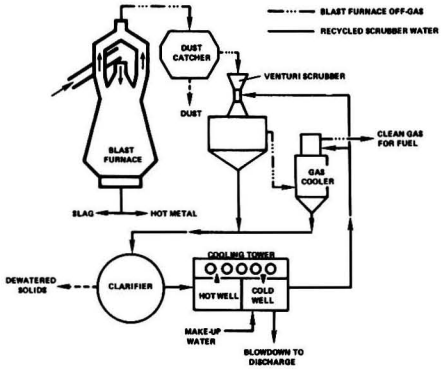

Figure 1. Blast-furnace gas-scrubber recycled-water system.

Consequently, these contaminants should enter the RO permeate, which would be recovered for reuse within the gas-scrubber recycle system. This concept is shown in Figure 3. The EPA [*4*] has indicated that gas-scrubber recycle systems reduce the discharge of contaminants over a once-through system. This would indicate that some mechanism, perhaps biological, exists to limit contaminant (cyanide and phenol) loadings. Return of these contaminants to the recycle system via an RO permeate stream would be expected to cause no increase in the recycle-system loadings.

Cellulose acetate rejects calcium, magnesium, and sulfate, which are scaling components, and chloride, a corrosive component. It is expected that these substances would be removed via the concentrate stream where they are discharged.

Table 2 is a partial listing of the contaminants found in the blast-furnace gas scrubber recycle-system water used in this study.

EXPERIMENTAL METHOD

The test device utilized in this research was an OSMO-1960-SS97PES pilot-scale unit manufactured by Osmonics Inc. It is rated for a permeate flow of 12.4 gallons per hour (gph), [46.9 liters per hour (l/h)] and a concentrate flow of 87.2 gph (330.1 l/h) at a 600 pounds per square inch, gage (psig) [4.1 × 10^6 Pa] operating pressure with an Osmonics SEPA-97 membrane. This membrane was used in the evaluation and its characteristics are detailed in Table 3.

Scrubber-water samples [55 gallons (208 liters) each] were obtained from a local blast-furnace facility. The pH was adjusted to 5.0 ± 0.2 units with sulfuric acid prior to testing to destroy alkalinity, and to shift the dissociation equilibrium for cyanide and phenol to their unionized state. Operating pressures investigated ranged from 350 to 450 psig (2.4 × 10^6 to 3.1 × 10^6 Pa), and feed temperatures were varied between 74 to 86°F (296.5 to 303.1°K). Permeate flux rates [gallons per day per square foot, gpd/ft² (liters per day per square meter, l/d/m²)] were measured as a function of water-volume recovery level. A flow diagram of the experimental set-up is shown in Figure 4. Recovery levels ranged from 10 percent to approximately 80 percent. Two control runs with distilled water were made before each experimental run. The first control was run at an

TABLE 1. GAS-SCRUBBER RECYCLE-SYSTEM PROPOSED DISCHARGE LIMITATIONS LB/1000 LB[a] IRON PRODUCED (mg/l)[b]

	BPT	BAT	BCT[c]
Total suspended solids	0.0260 (50)	—	0.00438 (15)
Cyanide (total)	0.00782 (15)	0.000292 (1)	—
Phenol	0.00210 (4)	0.0000292 (0.1)	—
Ammonia as nitrogen	0.0537 (103)	0.00292 (10)	—
Oil & grease	—	—	0.00292 (10 max)
Zinc	—	0.0000876 (0.3)	—
Lead	—	0.0000730 (0.25)	—

[a] lb/1000 lb = kg/kkg
[b] Concentration calculated based on 125 gallons per ton (gpt) iron produced for BPT limits, and 70 gpt iron produced for BAT and BCT limits.
[c] These are proposed limitations, and have not yet been promulgated.

operating pressure of 400 psig (2.8×10^6 Pa) and a feed temperature of 74°F (296.5°K) to detect changes in membrane performance. The second control was run at the experimental conditions to determine the scrubber-water osmotic pressure. A series of six tests was conducted to determine membrane rejection values of the contaminants listed in Table 1. All the test work as conducted in a batch mode. Data were analyzed according to the solution-diffusion model describing RO water and solute transport [5, 6] as outlined below.

EXPERIMENTAL AND THEORETICAL APPROACH AND RESULTS

Water Transport

Membrane water-flux rate is a function of the effective pressure applied across the membrane, described by the following equation:

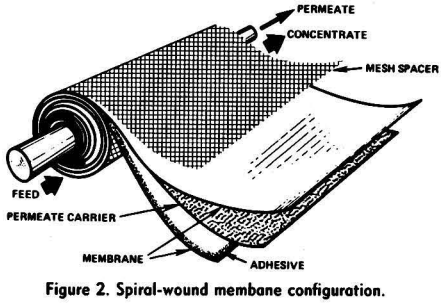

Figure 2. Spiral-wound membane configuration.

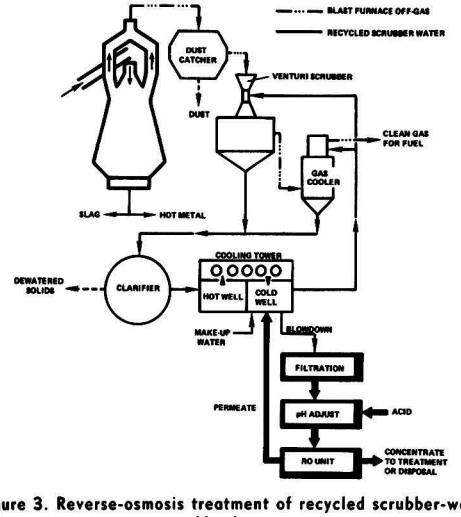

Figure 3. Reverse-osmosis treatment of recycled scrubber-water blowdown.

$$F_w = W_p(\Delta P - \Delta\pi) \quad (1)$$

where

F_w = membrane water flux rate, gpd/ft² (l/d/m²)
w_p = water permeability coefficient, gpd/ft²/psig (l/d/m²/Pa)
ΔP = differential applied pressure across membrane, psig (Pa)
$\Delta\pi$ = differential osmotic pressure across membrane, psig (Pa)

Membrane water-flow rates declined with increasing water-recovery levels due to increasing solution osmotic pressure caused by membrane solute rejection. Observed flux declines with water recovery are presented in Figures 5 and 6. Operating pressures were varied at 350, 400, and 450 psig (2.4×10^6, 2.8×10^6, and 3.1×10^6 Pa) levels with feed-water temperatures ranging from 74°F to 86°F (296.5 °K to 303.1°K).

Water-flux rates are also influenced by temperature because of the dependence of the water-permeability coefficient on this parameter. Water-permeability coefficients for the scrubber-water samples were determined by plotting water-flux rates against effective applied pressure in accordance with Equation (1). These results are shown in Figure 7. Water-permeability coefficient values determined in this manner are listed in Table 4.

Good agreement was obtained between values of each control run at 400 psig (2.8×10^6 Pa) and 74°F (296.5°K), indicating no significant decline in membrane water-flux rates over the test period. Agreement was also obtained between values of the control run at experimental conditions and the experimental runs. This indicates that differences observed between each of the experimental runs were due to temperature effects and not to differences in the individual samples. This temperature dependence is displayed in Figure 8. Using linear regression, the magnitude of the water-permeability coefficient temperature dependence was determined as 5.4×10^{-4} gpd/ft²·°K (2.2×10^{-2} l/d/m²·°K) for the control runs at the experimental conditions, and 6.2×10^{-4} gpd/ft² · °K (2.5×10^{-2} l/d/m² · °K) for the gas-scrubber water samples. These values agree within experimental error.

Water-flux rates for a model full-scale RO unit were estimated by determining median flux rates from each of the flux-decline runs. These rates were corrected for the observed temperature range (60°F to 90°F (16°C to 32°C)) of the gas-scrubber recycle system using the relationship derived above and are presented in Table 5.

Solute Transport

Membrane solute-flux rate is a function of the solute-concentration differential across the membrane, as shown by the following equation:

$$F_i = k_p(C_c - C_p) \quad (2)$$

where

TABLE 2. CONTAMINANT CHARACTERIZATION OF BLAST-FURNACE GAS-SCRUBBER RECYCLE SYSTEM

Contaminant	Average Concentration mg/liter	Standard Deviation mg/liter	Maximum mg/liter	Minimum mg/liter	Number of Observations
Calcium as $CaCO_3$	358	76	728	190	91
Magnesium	47	10	60	34	9
Zinc	27	24	79	5	9
Conductivity, siemens/m	465	133	820	188	91
Total cyanide	3.4	2.8	9.0	0.42	9
Free cyanide	3.4	3.2	9.1	0.33	7
Thiocyanate	0.4	0.6	0.8	<0.01	2
Phenol	0.8	0.8	2.3	0.08	9
Ammonia as nitrogen	128	31	158	55	9
Fluoride	25	6	38	19	9
Chloride	1125	278	1621	815	9
Sulfate	554	348	1265	186	7
Sulfide	0.2	0.2	0.3	<0.05	2

TABLE 3. OSMONIC SEPA-97 MEMBRANE CHARACTERISTICS

Membrane material	Cellulose acetate
NaCl rejection	94-97%
Permeate flux, gpd/ft² [a] (tap water)	10-14@ 400 psig [b]
Maximum operating pressure	800 psig
Normal operating pressure	400-500 psig
pH Range	2-8
Surface area	19 ft² [c]

[a] 1 gpd/ft² = 40.7l/0/m²
[b] 1 psig = 6894.8 Pa
[c] 1 ft² = 0.093 m²

F_i = solute flux, g/d/ft² (g/d/m²)
k_p = solute-permeability coefficient liter/d/ft² (l/d/m²)
C_c = concentrate solute concentration, g/liter
C_p = permeate solute concentration, g/liter

Total dissolved solids (TDS) measurements were made to determine solute-flux rates across the membrane in accordance with Equation (2). TDS flux rates were calculated in accordance with Equation (3).

$$F_i = \frac{F_w C_p}{C_{w,p}} \qquad (3)$$

where
F_w = membrane water flux, g/d/ft² (g/d/m²)
C_p = permeate solute concentration, mg/liter
$C_{w,p}$ = permeate pure-water concentration, assumed to equal 10^6 mg/liter

TDS permeability coefficients were calculated by plotting TDS flux rates against the membrane concentration difference, as shown in Figures 9 and 10. The permeability coefficients obtained in this manner ranged from 1.10 liters per day per square foot (liter/d/ft²) [11.8 liters per day per square meter (l/d/m²)] to 1.83 liter/d/ft² (19.7 l/d/m²). As the solute permeability coefficient is dependent on the composition of the solute, and the type and condition of the reverse-osmosis membrane, the values listed above are valid only under these experimental conditions.

Tests to determine rejection values for various wastewater contaminants were also conducted. These results are presented in Table 6. Negative rejections were obtained for cyanide, phenol, and sulfide, indicating preferential sorption of these materials across the membrane. Thiocyanate also displayed low rejection levels. Rejection values obtained for other contaminants examined were found to compare favorably with ranges reported in the literature.

PERMEATE WATER QUALITY

Permeate solute-concentration increases directly with feed solute concentration and water-recovery level. Figures 11 and 12 display these relationships for the gas-scrubber recycle-water samples. Initial TDS concentrations of the samples ranged from approximately 2800 mg/liter to 6100 mg/liter, resulting in permeate concentrations from 300 mg/liter to 600 mg/liter at a 70-percent

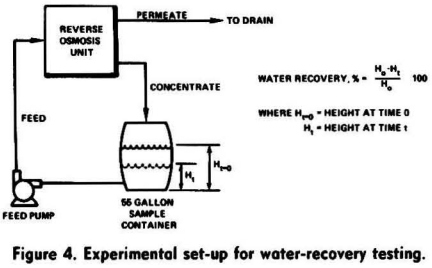

Figure 4. Experimental set-up for water-recovery testing.

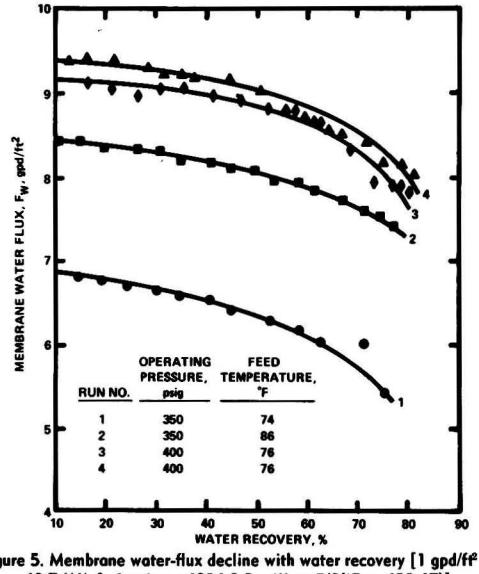

Figure 5. Membrane water-flux decline with water recovery [1 gpd/ft² = 40.7 l/d/m², 1 psig = 6894.8 Pa, °K = 5/9(°F + 459.67)].

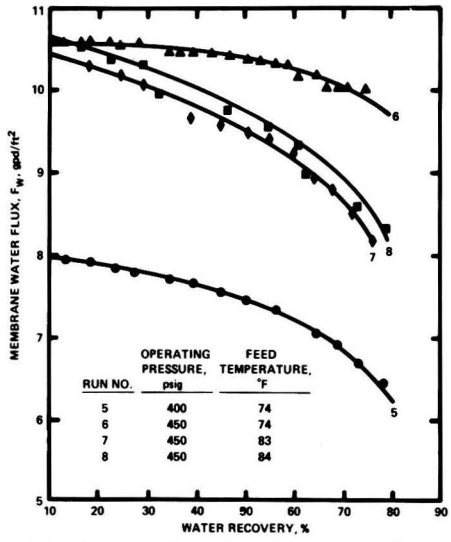

Figure 6. Membrane water-flux decline with water recovery [1 gpd/ft² = 40.7 l/d/m², 1 psig = 6894.8 Pa, °K = 5/9(°F + 459.67)].

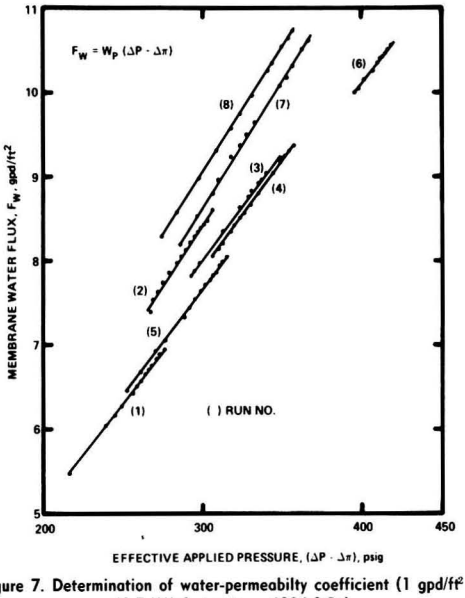

Figure 7. Determination of water-permeabilty coefficient (1 gpd/ft² = 40.7 l/d/m², 1 psig = 6894.8 Pa).

water-recovery level. For water-recovery levels above about 70 percent, permeate concentrations increased dramatically.

Concentration Polarization and Fouling Effects

Concentration polarization is defined as the ratio of solute concentration at the membrane surface to solute concentration in the bulk solution. This may be expressed mathematically by

$$B = \frac{C_m}{C_B} \qquad (4)$$

where

B = concentration polarization
C_m = solute concentration at membrane surface
C_B = average bulk-solute concentration

It is caused by concentrate solute concentration building up at the membrane surface, exceeding the bulk-solution concentration. When this occurs, the solute tends to back-diffuse away from the membrane into the bulk solution. Concentration polarization increases the local osmotic pressure at the membrane surface, reduces membrane water-flux rates, increases permeate solute concentration, and allows the concentration increase of sparingly soluble solutes, possibly causing precipitation onto the membrane. It is enhanced by high recovery levels, but may be minimized by recirculation of the concentrate stream. The magnitude of concentration polarization cannot be determined directly because measurement of the membrane surface solute concentration is required. However, the presence of concentration polarization or fouling may be detected experimentally. As the solute concentration at the membrane surface increases, so does the local osmotic pressure. Osmotic pressure increases more rapidly as a result of concentration polarization or fouling than would be expected simply from increases in concentrate solute concentration.

A plot of osmotic pressure *vs.* concentrate solute concentration can be used to detect concentration polarization or fouling, as shown in Figure 13. Figure 14 is a similar plot for each of the scrubber-water samples. Linear relationships were established for each of the samples, indicating that concentration polarization and fouling effects were negligible.

APPLICATION OF RESULTS TO HYPOTHETICAL DESIGN

Calculations were made of the permeate and concentrate water quality from a model full-scale RO unit treating 200 gallons per minute (gpm) [757 liters per minute (l/min)] of gas-scrubber blowdown water. The rejection data contained in Table 6 were used instead of determining median rejection values, since it was desired to obtain a conservative estimate of the contaminant loadings in the concentrate stream. These calculations are based on the average concentration values shown in Table 2.

Calculated contaminant loadings are presented in Table 7. Using conservative rejection values, we find that total cyanide and phenol (at 90% water recovery) loadings are within BAT limits, while zinc and ammonia loadings exceed these limits.

Calculated reductions in contaminant discharge loadings, for a single pass through the RO unit and various water-recovery levels, are presented in Table 8.

SUGGESTIONS FOR THE TREATMENT OF REVERSE OSMOSIS CONCENTRATE

Disposal of a portion of the RO concentrate may be accomplished by evaporation by quenching hot blast-furnace slag.

Treatment by alkaline chlorination and ozonation has been investigated by Osantowski and Geinopolos [*1*]. Both processes were found capable of achieving proposed BAT limitations and are outlined in Figure 15. Ammonia was found to be the critical parameter for both processes; if the ammonia concentrations were reduced below BAT limits, all other oxidizable pollutants were also reduced below their respective limitations.

RESULTS AND CONCLUSIONS

Based on the results of this research, we can conclude that:

1. Reverse osmosis with cellulose-acetate membranes appears capable of effecting significant reductions in discharge volume and contaminant loadings from a blast furnace gas-scrubber recycled-water system. Cellulose-acetate membranes displayed preferen-

TABLE 4. WATER PERMEABILITY COEFFICIENTS, W_p, FOR CONTROL AND EXPERIMENTAL RUNS

Run Number	Distilled Water; 74°F, 400 psig (gpd/ft²/psig)[a]	Distilled Water, Experimental Condition (gpd/ft²/ psig)	Gas-Scrubber Water, Experimental Conditions (gpd/ft²/psig)
1	0.0251	0.0251	0.0251
2	0.0258	0.0281	0.0286
3	0.0267	0.0267	0.0268
4	0.0263	0.0263	0.0263
5	0.0255	0.0255	0.0256
6	0.0264	0.0264	0.0258
7	0.0257	0.0289	0.0295
8	0.0261	0.0301	0.0300

[a] 1 gpd/ft²/psig = 0.006 l/d/m²/Pa

tial sorption of phenol (−14%), free cyanide (−3%), and sulfide (−14%) with low rejection of thiocyanate (8%).

2. Hypothetical plant calculations indicated that phenol (at 90% water recovery) and cyanide discharge loadings were below BAT limits.
3. High rejections of zinc (>99%) and ammonia (93%)

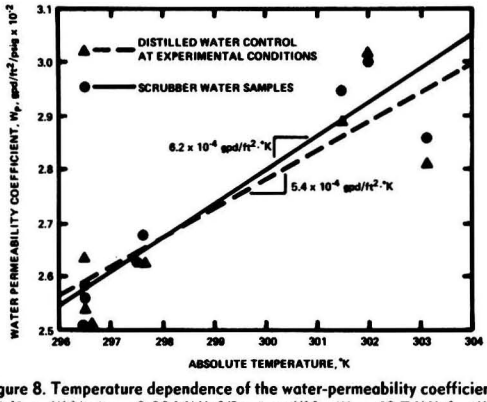

Figure 8. Temperature dependence of the water-permeability coefficient, W_p (1 gpd/ft²/psig = 0.006 l/d/m²/Pa, 1 gpd/ft² · °K = 40.7 l/d/m² · °K).

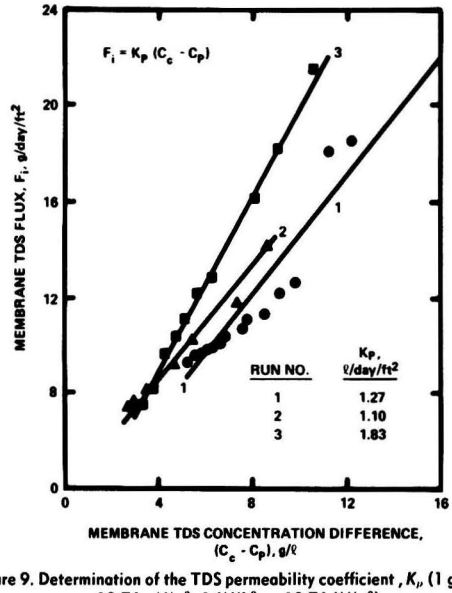

Figure 9. Determination of the TDS permeability coefficient, K_p (1 g/d/ft² = 10.76 g/d/m², 1 l/d/ft² = 10.76 l/d/m²).

TABLE 5. ESTIMATED WATER FLUX RATES FOR A MODEL FULL-SCALE RO UNIT

Operating Pressure psig[b]	Water Flux[a] Rate, gpd/ft²[c] 60°F	90°F
350	5.1 —	9.0
400	5.9 —	10.4
450	6.8 —	12.6

[a] Osmotic pressure of the gas-scrubber water samples ranged from 40 psig to 90 psig which is accounted for in the stated water flux ranges.
[b] 1 psig = 6894.8 Pa
[c] 1 gpd/ft² = 40.7 l/0/m²

were obtained, indicating a need for additional treatment for their removal prior to discharge. It should be noted that zinc concentrations in the samples collected were unusually high because of the composition of sinter and scrap used as blast-furnace charge. Rejections of calcium, magnesium, sulfate (>99%) and chloride (94%) were also high,

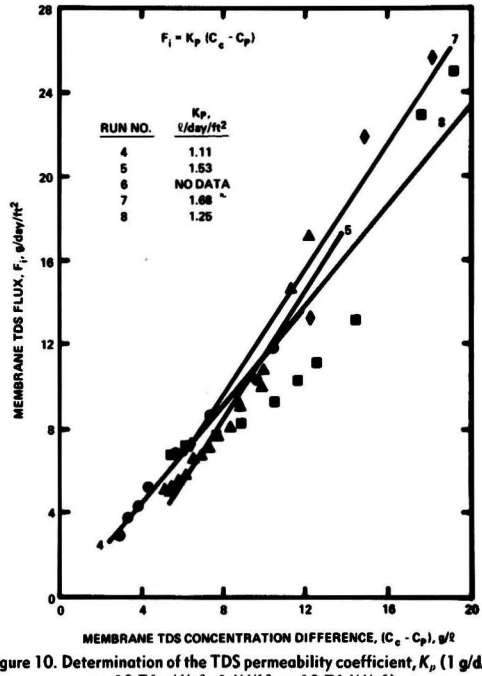

Figure 10. Determination of the TDS permeability coefficient, K_p (1 g/d/ft² = 10.76 g/d/m², 1 l/d/ft² = 10.76 l/d/m²)

TABLE 6. OBSERVED CONTAMINANT MEMBRANE REJECTION

Solute	Average Rejection, %	Observed Rejection Range, %	Reported Rejection Range, %
Calcium as $CaCO_3$	>99	>99	96.3 to 99.7[6]***
Magnesium	>99	>99	93 to 99.9[6]
Zinc	>99	>99	
Total dissolved solids	97	96 to 98	89 to 99[6]
Total cyanide*	−1	−12 to +12	—
Free cyanide*	−3	−7 to +6	0 for pH <7[7]
Thiocyanate*	8	−10 to +24	—
Phenol	−14	−18 to −10	−20 to −10[8]
Ammonia	93	91 to 94	77 to 95[6]
Fluoride	91	89 to 92	88 to 98[6]
Chloride	94	92 to 96	86 to 97[6]
Sulfate	>99	>99	99 to 100[6]
Sulfide**	−14	—	—

* Low concentrations responsible for broad rejection range.
** Only one observation was above maximum analytical sensitivity limits (0.05 mg/liter).
*** See References.

assuring the reusability of the permeate stream in the recycle system.

4. Water recoveries ranging from 70 percent to 80 percent appear to be possible, although permeate water quality decreases dramatically for water recoveries exceeding 70 percent.
5. Water-flux rates appeared to be adequate [(5.9 to 10.4 gpd/ft² (240 to 423 l/d/m²) at 400 psig) (2.8 × 10^6 Pa)] although, because of the temperature dependence of these flux rates, sizing of a full-scale unit should carefully take temperature variations into

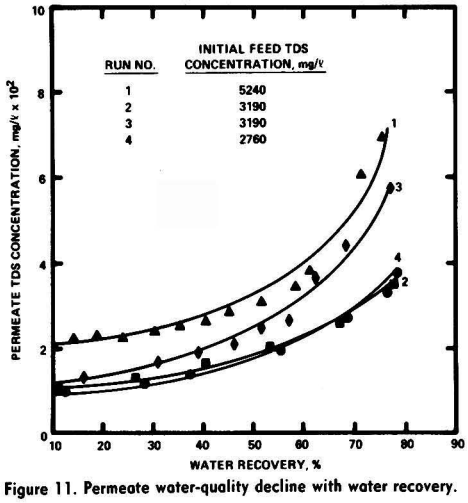

Figure 11. Permeate water-quality decline with water recovery.

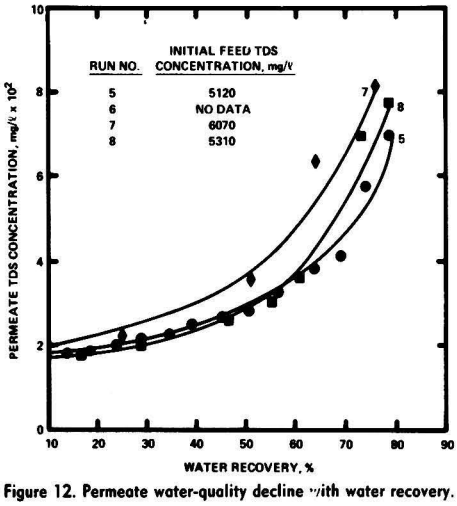

Figure 12. Permeate water-quality decline with water recovery.

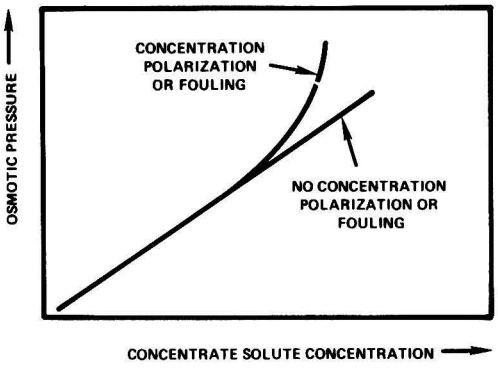

Figure 13. Detection of concentration polarization or fouling.

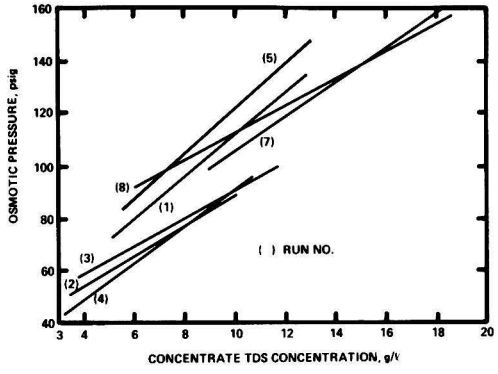

Figure 14. Evaluation for the presence of concentration polarization of fouling (1 psig = 6894.8 Pa).

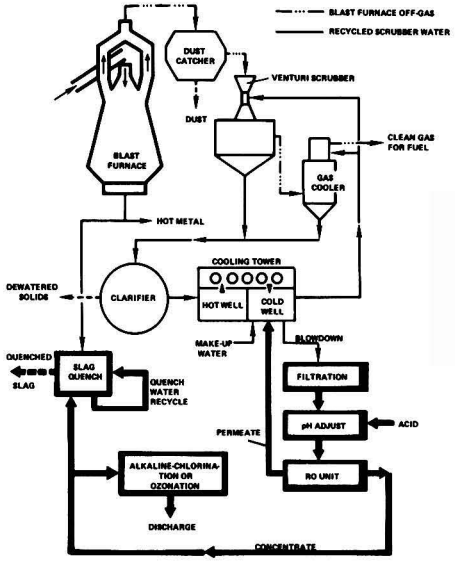

Figure 15. Treatment of reverse-osmosis concentrate.

TABLE 7. CALCULATED DATA: APPLICATION OF RO TO BLAST-FURNA CE GAS-SCRUBBER RECYCLE-SYSTEM BLOWDOWN TREATMENT

Contaminant	Permeate Contaminant Mass Flow Rate lb/day[a]			Concentrate Contaminant Mass Flow Rate lb/day[a]			Contaminant Mass Discharged lbs./1000 lbs.[b] Hot Metal × 10^{-4}			BAT Limitations lbs./1000 lbs.[b] Hot Metal × 10^{-4}
Water recovery	70%	80%	90%	70%	80%	90%	70%	80%	90%	
Calcium as $CaCO_3$	19	33	71	841	827	789	837	824	786	—
Magnesium	2.6	4.3	9.3	110	108	103	110	108	103	—
Zinc	1.5	2.5	5.4	63	62	59	63	62	59	0.876
Total cyanide	5.7	6.6	7.4	2.5	1.6	0.8	2.5	1.6	1.3	2.92
Free cyanide	5.8	6.6	7.4	2.4	1.6	0.8	2.4	1.6	1.3	—
Thiocyanate	0.66	0.76	0.86	0.30	0.20	0.10	0.9	0.9	0.9	—
Phenol	1.4	1.6	1.8	0.5	0.3	0.1	0.5	0.3	0.1	0.292
Ammonia as nitrogen	43	67	119	265	241	189	264	240	188	29.2
Fluoride	10	16	27	50	44	33	50	44	33	—
Chloride	332	523	948	2372	2181	1756	2361	2171	1748	—
Sulfate	30	51	110	1302	1281	1222	1296	1275	1216	—
Sulfide	0.3	0.4	0.4	0.2	0.1	0.1	0.2	0.1	0.1	—

[a] 1 lb/day = 0.454 kg
[b] lbs./1000 lbs. = kg/kkg

TABLE 8. CALCULATED CONTAMINANT DISCHARGE LOADING REDUCTIONS, PERCENT (SINGLE PASS)

Contaminant	Water Recovery Level		
	70%	80%	90%
Calcium as $CaCO_3$	2.3	3.8	8.2
Magnesium	2.3	3.8	8.2
Zinc	2.3	3.8	8.2
Total cyanide	70	80	90
Free cyanide	70	80	90
Thiocyanate	69	79	90
Phenol	74	84	95
Ammonia as nitrogen	14	22	39
Fluoride	17	27	45
Chloride	12	19	35
Sulfate	2.3	3.8	8.2
Sulfide	60	80	80

account.

6. Concentration polarization and membrane fouling did not appear to be significant. However, calcium-sulfate scaling could be a major operational problem. Appropriate pre-treatment procedures, such as dispersant and anti-precipitant addition, may be required to prevent fouling of the RO membrane.
7. Studies to determine membrane permeate flux and rejection decline were not conducted because of sample limitations and the validity of performing these studies in a batch mode. These studies would have to be made in order to determine the economic feasibility of RO in this application.
8. Because of differing physical and operational characteristics of blast-furnace gas-scrubber recycle systems, pilot studies would be required to establish the viability of RO in this application. Although the results of these batch tests appear encouraging recycle-water chemistry is not fully understood nor are the operational parameters which affect it. Variabilities of contaminant concentrations would have to be determined to properly size an RO unit and to provide protection against membrane fouling.

Additional data for this study may be found in the work of Terril [9]*.

* It is understood that the information in this paper is intended for general information only and should not be used in relation to any specific application without independent examination and verification of its applicability and suitability by professionally qualified personnel. Those making use thereof assume all risk and liability arising from such use or reliance.

LITERATURE CITED

1. Osantowski, R. and A. Geinopolos, "Physical-Chemical Treatment of Steel Plant Wastewaters Using Mobile Pilot Units," Proceedings: First Symposium on Iron and Steel Pollution Abatement Technology, Chicago, October 30-November 1, 1979, Environmental Protection Agency, Research Triangle Park, EPA-600/9-80-12, 325-340 (February, 1980).
2. Chian, E. S. K. and H. H. P. Fang, "RO Treatment of Power Plant Cooling Tower Blowdown for Reuse," *AIChE Symposium Series-Water*, **71**, No. 151, 82-86 (1975).
3. Kosarek, L. J., "Significantly Increased Water Recovery From Cooling Tower Blowdown Using Reverse Osmosis," *AIChE Symposium Series-Water*, **75**, No. 190, 148-155 (1979).
4. Costle, D. M. *et al.* "Development Document for Effluent Limitations Guidelines and Standards for the Iron and Steel Manufacturing Point Source Category, Vol. 11" (proposed), U.S. Environmental Protection Agency, EPA 440/1-80-024b (December, 1980).
5. Merten, U., ed., "Desalination by Reverse Osmosis," M.I.T. Press, Cambridge (1966), pp. 93-160.
6. Weber, Jr., W. J., "Physicochemical Processes For Water Quality Control," Wiley-Interscience, New York (1972), pp. 307-329.
7. Spatz, D., "Industrial Waste Processing With Reverse Osmosis," Osmonics, Inc. Hopkins, Minn., (1971), unpublished.
8. Lonsdale, H. K., U. Merten, and M. Tagami, "Phenol Transport in Cellulose Acetate Membranes," *Journal of Applied Polymer Science*, **11**, No. 9, 1807-1820 (September, 1967).
9. Terril, M. E. "The Applicability of Reverse Osmosis to the Treatment of Blast Furnace Gas Cleaning Water Recycle System Blowdown," M.S. Thesis, University of Pittsburgh, Pittsburgh, Pa. (December, 1980).

Mark E. Terril is a Research Engineer for the Environmental Research Division of United States Steel Corp.'s Research Laboratory in Monroeville, PA. Earning his B.S. in Biology and B.S.E. in Environmental Engineering from Purdue University in 1974 and 1975, he later attended the University of Pittsburgh, receiving his M.S. in Civil (Environmental) Engineering in 1980. His current assignment is to review proposed wastewater-treatment technology required to meet Best Available Technology Econmically Achievable guidelines.

Ronald D. Neufeld is a Professor of Civil Engineering, and Coordinator of Environmental Engineering at the University of Pittsburgh. He received a BE (ChE) from Cooper Union, MS (ChE) and Ph.D. (Civil/Environmental Health Engineering) from Northwestern University. His research is in process environmental engineering, and he directs sponsored projects in the areas of wastewater treatment and reuse technologies for industrial and synthetic fuels applications. He is a Diplomate of the American Academy of Environmental Engineers, and Member of AIChE.

Microcomputers for Control of Industrial Waste Treatment

Presently available microcomputers offer an inexpensive and powerful tool to operators of wastewater-treatment plants.

Thomas T. Jones and David L. Sullivan, ES Environmental Services, Berkeley, Calif. 94710

The use of computers is not new to the field of wastewater-treatment-plant operations. Several large municipal treatment facilities in the United States have incorporated the computer into their operations both for data logging and process control.

Computer control of industrial-waste plants is now becoming increasingly popular as the benefits and cost savings have become apparent. In some instances, the devices actually control the starting and stopping of certain unit-process components. Unfortunately, the relative complexity of such installations has kept capital and operating costs quite high and, until recently, these high costs have prevented the smaller plants from receiving the benefits that can be derived from computerization.

The advent of the microcomputer and its relatively small price tag have brought a new measure of operational control within reach of the smaller municipal and industrial waste-treatment plants. Already there is sufficient experience with microcomputer installations to establish performance records approaching the fine process decisions and adjustments realized by more costly, large computer systems.

The present paper discusses the benefits of using a small microcomputer in industrial waste-treatment plants for process control as well as data logging, inventory control, and other functions. The advantages of this type of system *versus* a terminal connected to a large system is discussed.

GENERAL APPROACH

Microprocessor control at an industrial wastewater-treatment facility is performed on a desk-top self-contained computer. Typically, hardware consists of a microprocessor with keyboard, a video display screen, two floppy-disk drives, and a printer with some graphics capability. Data are entered manually at the keyboard by the operator. Data requirements are limited to information which would normally be required in any case for proper plant operation. There are several advantages of manual versus automated data input:

1. The cost of remote sensor and telemetry equipment, as well as proper interfacing and data-logging programs within the computer, is extremely high.
2. The accuracy and reliability of remote sensors is presently a problem. It usually takes more time and money to keep remote sensing elements operational than it does to manually run the required lab tests.
3. Manual data entry forces the operator to look at the data on a daily basis, which keeps him constantly "in-touch" with the plant operating parameters.

Data are recorded on a data-logging sheet after being received from lab or field worksheets, and key parameters are then entered into the computer. Interactive, conversational software is provided to facilitate data entry and storage. This type of software requires the operator to know little or nothing about computer programming.

Process-control programs are provided for each unit process in a plant. The programs are specifically tailored to the plant to account for the specific factors at the plant which affect process performance, such as basin geometry, actual equipment capacity, etc. The process-control programs are designed to be run as often as needed, typically one to three times a day. The programs use pertinent data from various sources such as the lab, field measurements, flow meters, etc. Each day's data are stored on the data disk, and are recalled by the programs as needed. In pertinent cases, programs use data from previous entries to perform statistical trend analysis, averaging, or other numerical manipulation. Typically, one year's data can be stored on a single floppy disk. After data entry, the programs are run and print out the day's operating parameters. Any potential operational problems or deficiencies are identified and flagged for operator attention.

Such information as whether more individual unit processes need to be brought on-line, whether bypassing is required, how much polymer or nutrient should be added, etc., are provided by the computer. The operator then utilizes this information to implement operational decisions. This procedure provides the operator with a sophisticated control strategy while still retaining the reliability of having the operator himself carry out the operation functions. The following example has been selected to illustrate this approach for an industrial wastewater plant which treats a plastics manufacturing waste.

TYPICAL APPLICATION

A schematic diagram for the plant is shown on Figure 1. The influent to the plant averages 600 gpm, and the plant can accept a peak flow of 800 gpm. The influent is often high in suspended solids which must be removed prior to the activated-sludge treatment. The solids consist mostly of plastic particles sloughed during production. In addition, unreacted monomer is dissolved in the waste, which must be removed prior to biological treatment.

The process stream is as follows: the flow first passes through bar screens and then enters a blend pit where acid is added during periods of high influent pH. This occurs when a caustic boil is performed in the production area, and the purpose is to accomplish coarse or roughing pH control. The flow next enters hydrosieve screens which remove a substantial portion of the suspended solids. A

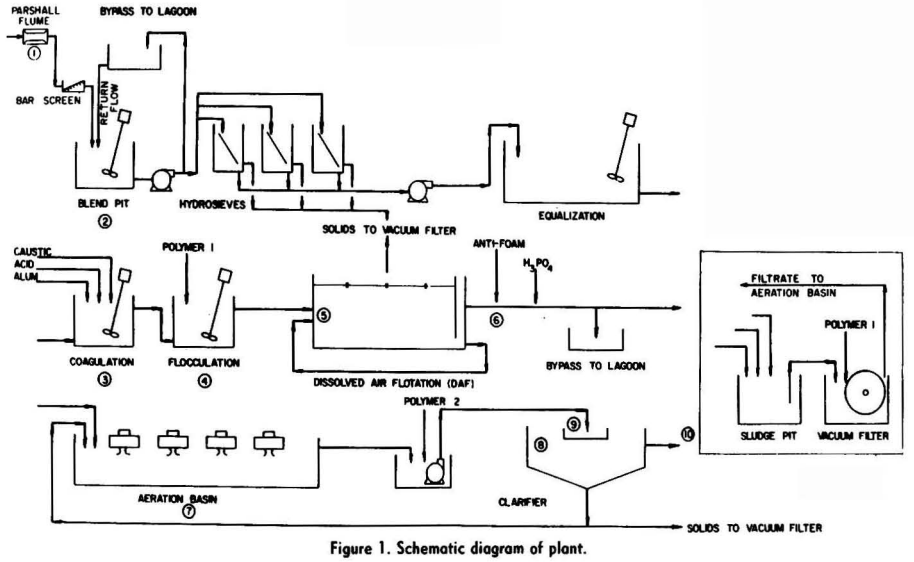

Figure 1. Schematic diagram of plant.

well-mixed equalization basin with a 10-hour detention time provides damping of the flow, solids load, and organic load to the rest of the plant. The equalization-tank effluent then enters a rapid-mix coagulation tank where alum is added to coagulate unreacted monomer. In addition, fine pH control is also accomplished by addition of acid or caustic as required. Polymer is then added to the flocculation tank before the flow enters a dissolved-air-flotation (DAF) unit. The subnatant then receives an antifoam agent if needed, as well as phosphoric-acid addition as a nutrient supplement before entering the aeration basin. The aeration-basin effluent then has more polymer addition, if necessary, to aid in final clarification before entering the final clarifier. Clarifier effluent is discharged to a river. Sludge from the hydrosieves, the DAF unit, and the final clarifier enter a sludge pit from which they are pumped to a vacuum filter for dewatering and subsequent disposal. Filtrate is returned to the aeration basin.

The plant is also provided with two bypass lagoons. The first is designed to hold influent whenever a high organic or hydraulic load is experienced. This lagoon is rarely used. The other lagoon holds DAF-unit effluent whenever an upset or DAF downtime causes a high solids content. Both lagoons return flow to blend pit at a low rate when normal plant flow is low.

The computerized process-control strategy for this plant involves individual programs for:

1. Organic overload control
2. Chemical coagulant feed control
3. MLSS control
4. SVI calculation
5. Zone settling-velocity computation
6. Final clarifier computations

To effectively provide process control, a sampling program for necessary parameters was established. The sampling points are shown by the circled numbers on Figure 1. The data collected at each location are entered into the computer for use by the programs. A brief description of each program follows.

Organic-Overload Control

This program is designed to compute the instantaneous *F/M* ratio as a means of determining if an organic overload condition exists. Several process decisions are based on the outcome of the calculated *F/M* ratio. If the calculated *F/M* ratio is greater than 0.30 lbs COD/lb MLVSS/day, the program indicates an existing organic overload condition. It then instructs the operator to divert sufficient plant influent to the lagoon or increase the diverted flow to the lagoon, causing a reduction in the *F/M* ratio to 0.28. If the calculated *F/M* ratio is between 0.25 and 0.30 and flow is being diverted, the computer instructs the operator to continue diverting at the same rate. However, if no flow is being diverted and the *F/M* ratio is less than 0.30, the computer instructs the operator to return wastewater from the lagoon back to the process, providing the lagoon is not empty. The return rate is fixed at 10 percent of the flow rate from the equalization tank or less if this would cause the *F/M* ratio to increase above 0.30. The following equations are used in the organic overload control program:

1) $K_T = K_{20}(1.03)^{(20-T)}$; T = °C (Temperature-adjusted COD load)
2) F/M, lb COD/lb MLVSS/day

$$= \frac{(\text{Flow, gpm})\,(\text{COD, mg/liter})\,(8.34)\,(100\%)\,(K_T)}{(694.44\ \text{gpm/mgd})\,(\text{MLSS, mg/liter})\,(\%\text{Volatile})\,(\text{Reactor volume, mg})\,(8.34)}$$

3) Return flow gpm = (Equalization effluent flow, gpm) (10%)

Data that must be known:
Flow from equalization tank, gpm
COD from DAF effluent, mg/liter (instantaneous)
Today's MLSS, mg/liter
% Volatile mixed-liquor, %
Reactor temperature, °C
Flow being diverted, gpm (if any)

Chemical Coagulant-Feed Control

This program is designed to compute the chemical feed rates for both alum and liquid polymer, given the process flow and the desired dosage. It is a general program and can be applied to any coagulant feed system in the plant. The following equations are programmed into the chemical coagulant feed control program:

1) Polymer feed, gallons/hr $= \dfrac{(\text{Process flow, gpm})\,(\text{Poly dose, mg/liter})\,(8.34)}{(\text{Polymer weight, lb/gal})\,(24\ \text{hrs/day})\,(694)}$

$$= \frac{(\text{Process flow, gpm})\,(\text{Poly dose, mg/liter})\,(8.34)}{(91\ \text{lb/gal})\,(24)\,(694)}$$

2) Alum feed, gallons/hr $= \dfrac{(\text{Process flow, gpm})\,(\text{Poly dose, mg/liter})\,(8.34)}{(\text{Alum wt., lb/gal})\,(24\ \text{hrs/day})\,(694)}$

$$= \frac{(\text{Process flow, gpm})\,(\text{Poly dose, mg/liter})\,(8.34)}{(5.4\ \text{lb/gal})\,(24\ \text{hrs/day})\,(694)}$$

Data that must be known:
Flow through process being considered, gpm
Alum or polymer dose from jar test, mg/liter.

MLSS Control

This program computes the desired mixed-liquor inventory and the projected waste rate which will achieve that desired inventory within the next 24-hour period. The computed mixed-liquor requirement is automatically corrected for temperature compensation. Sludge wastage is based on a materials balance approach, assuming a constant net cell yield from the previous day. The program uses a running average of the previous 7 days' influent COD values to smooth effects from transient high or low values. The following equations are used in the MLSS control program:

1) $K_T = K_{20}(1.03)^{(20-T)}$; T = °C

2) Required MLSS, mg/liter =
$$\frac{\text{(COD flux, lb/day) } (K_T)\ (100\%)}{\text{(MLVSS, \%) (Reactor volume, mg) (F/M) (8.34 lb/gal)}}$$

3) Waste Rate, gpm =
$$\frac{\text{(Yesterday's mass, lb/day)} + (\text{MLSS}_{\text{today}} - \text{MLSS}_{\text{req'd}})\ (8.34)\ \text{(Basin vol, MG)}}{\text{(Today's RAS, mg/liter) (8.34)}} \cdot \frac{1}{694\ \text{gpm/mgd}}$$

Yesterday's mass, lb/day =
$$\frac{\text{(Yesterday's waste, gpm) (Yesterday's RAS, mg/liter) (8.34)}}{\text{(694 gpm/mgd)}}$$

Data that must be known:
COD flux from influent COD data, lb/day
Today's MLSS, mg/liter
% volatile mixed-liquor, %
Today's RAS concentration, mg/liter
Yesterday's sludge-waste rate, gpm
Yesterday's RAS concentration, mg/liter
Reactor temperature, °C

SVI Calculation

This program calculates the sludge-volume index of a mixed-liquor (aeration-basin) sample. The following equation is programmed into the computer:

$$\text{SVI, ml/g sludge} = \frac{\text{(ml sludge) (1000 mg/g)}}{\text{(MLSS, mg/liter)}}$$

Data that must be known:
ml of sludge in graduate cylinder after 30-minutes settling MLSS, mg/liter, of that day's sampling of mixed-liquor effluent.

Zone Settling-Velocity Computation

This program computes the zone settling velocity (ZSV) of a mixed-liquor effluent sample. The following equation is programmed into the computer:

$$\text{ZSV, ft/hr} = \frac{\text{(1000 - ml settled sludge) (ft/100 ml) (60 min/hr)}}{\text{(settling time for free settling, min) (100 ml)}}$$

$$= \frac{\text{(1000 - ml settled sludge) (0.12) (60)}}{\text{(5 minutes) (100)}}$$

In the above equation, it is assumed that all free settling will occur in the first five minutes, which for most cases is a fairly close approximation.

Data that must be known:
Settled sludge volume after 5-minutes settling, ml.

Final Clarifier Computations

This program computes the proper sludge-return rate, the theoretical blanket thickness, clarifier solids loading, and the maximum allowable flow to the clarifier. Additionally, there are three process decisions made. These three determinations are made on the basis of excessive solids loading. Excessive flow is characterized by an existing flow greater than the maximum allowable flow computed on the basis of the zone settling velocity. In the event that an excessive flow is noted, the program instructs the operator to decrease the plant flow, possibly through diversion. A high blanket thickness is characterized as anything greater than 84 inches. If a high blanket is noted, the computer instructs the operator to add polyelectrolytes as an aid to secondary cell separation. Finally, excessive solids loading is characterized by anything greater than 1.5 lb/ft²/hr. If excessive solids loadings are noted, the computer instructs the operator to reduce the process flow and/or add polyelectrolytes to further enhance settling. The following equations are programmed into the final clarifier computations program:

1) Return rate, gpm =
$$\frac{\text{(Plant flow, mgd) (694 gpm/mgd)}}{\dfrac{\text{RAS, conc, mg/liter}}{\text{MLSS, mg/liter}} - 1}$$

2) RAS con, mg/liter =
$$\frac{1{,}000{,}000}{\text{SVI}}$$

3) Sludge blanket (thickness), inches

$$= \frac{\text{MLSS, mg/liter}}{\text{RAS, mg/liter}} \times \text{clarifier depth, ft} \times 12\ \text{in./ft}$$

$$= \frac{\text{MLSS, mg/liter}}{\text{RAS, mg/liter}} \times 156$$

4) Solids loading, lb/ft²/hr
$$= \frac{\text{(Plant flow + recycle flow, mgd) (MLSS, mg/liter) (8.34)}}{\text{(Clarifier surface area, ft²) (24 hr/day)}}$$

$$= \frac{\text{(Plant flow + recycle flow, mgd) (MLSS, mg/liter)}}{\text{(1,964) (24)}}\ 8.34$$

5) Maximum flow to clarifiers, gpm
$$= (\text{ZSV, ft/hr}) \times \frac{\text{(7.48 gal/ft}^3\text{) (24 hr/day) (Surface area of clarifier, ft}^2\text{)}}{1{,}000{,}000\ \text{gal/mg}}$$

$$= (\text{ZSV} \times \frac{(7.48)\ (24)\ (1964)\ (694)}{1{,}000{,}000}$$

Data that must be known:
Previous day's flow to aeration system, gpm
Mixed liquor as of that day, mg/liter
SVI of the MLSS effluent at the time of program operation, ml/m.
ZSV of the MLSS effluent at the time of program operation, ft/hr.

The above process-control programs have been in use for several years at the plant, and have had a demonstrable positive impact on plant operations. For instance, after the plant had been on-line for a short while, the hydraulics load to the plant began to increase. By using the computer, the secondary clarifier was quickly identified by the plant operators as the limiting unit process at higher flows. This eventually led to the addition of another secondary clarifier before the situation became critical and led to permit violations and possible fines.

OTHER APPLICATIONS

In addition to process control, the computer can also be used for a number of other time, labor, and money-saving functions at an industrial waste plant. Chief among these are the following:

1. Mathematical modeling of the plant. A theoretical mathematical model of the treatment system can be provided, which allows the operators to simulate plant performance under a wide variety of flows, loadings, and alternative plant configurations. This feature is particularly valuable in an industrial-waste

plant as rapid predications of the effects of production process changes on the treatment plant may be made. In addition, operators can model plant performance with the addition or deletion of various unit processes to help plan for future needs or to plan the best time to shut units down for maintenance.

2. Maintenance program. Maintenance records and a "tickler file" of weekly maintenance activities can be computerized. At the beginning of each week, the computer prints out the required routine maintenance duties for that week. At the end of the week, the operator enters into the computer those items which were performed. Those items not performed are carried over into the following week and can be "flagged" if allowed to lag for too long. In addition, the computer can identify those pieces of equipment which appear to have higher than usual maintenance requirements and flag these for possible overhaul or replacement.
3. Inventory. Each major piece of equipment can be entered into an inventory file on the computer. Each piece of equipment is assigned a coded serial number which identifies the type of equipment (e.g., a gate valve, an a.c. motor, a pump, etc.), its size, capacity, and any other pertinent characteristics. In addition, the file indicates where the equipment is located or stored, when it was purchased and installed, and its status or condition. Thus, if an operator quickly needed, say, a 6-inch plug valve, the computer could rapidly search the file for all 6-inch plug valves in the plant and the operator could then determine which, if any, are available for other use.
4. Operator training. A number of operator training programs are now being developed for use on desk-top microcomputers. Additionally, individual programs tailored to the needs of a particular plant can be provided and used to train the plant operators in various aspects of plant operation. These programs are particularly valuable for training new operators. A tremendous advantage of computerized training is that the operators can proceed at their own pace, learn at a time convenient to them, and not take away valuable time from those who would otherwise need to train them. Of course, computerized training will never totally replace conventional instruction, but is used as a valuable adjunct.
5. Statistical trend analysis. The computer can provide statistical trend analysis of plant data to detect trends or make predictions of future values.

Other possible applications include printing monthly NPDES reports, hazardous-waste management records, and other RCRA data management. Additional applications tailored to each plant's needs are limited only by the imagination and creativity of the user.

USE OF MICROCOMPUTER VERSUS MAINFRAME TERMINAL

As an alternate to using a dedicated microcomputer at the treatment plant for process control and other functions, a terminal connected to a company's central mainframe computer could be used. There are several drawbacks to this, chiefly:

1. Cost. The initial cost of a terminal and the associated interfacing and communications equipment is often substantially higher for a terminal than for a complete desk-top microcomputer system. In addition, continuing costs for use of the mainframe computer may be quite high because each user is paying for some portion of the entire system, not just those items he uses.
2. Software availability. Usually a microcomputer system with all associated process-control and other software can be bought from one consultant who specializes in wastewater engineering and can apply his own existing programs. However, few consultants would be willing to adapt programs available on the microcomputer system with which they are familiar to another computer system with which they are totally unfamiliar. Even if this could be done, the time and expense required would be considerable.
3. Computer availability. Mainframe computers, by the nature of their size and complexity, are usually "down" for one reason or another more often than a microcomputer system. Also, if a large number of users are on a mainframe system, turnaround time may be long.
4. Capability. Mainframe computers often have very complex operating systems, and even if relatively easy to use programs are provided, just signing on and calling the programs to be run may be troublesome for treatment-plant operators.

In contrast to the above, a desk-top microcomputer is dedicated to the treatment plant, is easy to use, always available, highly reliable, and inexpensive. Usually, a maintenance contract with a local computer store or dealer can be negotiated which allows a lender unit to be provided in the event the microprocessor does require maintenance. The cost of the hardware is quite low in any case, and is a one-time cost with no recurring user charges. Finally, the operators' pride is enhanced by having a system dedicated to their needs and installed solely for their convenience and use.

The major advantages of a mainframe computer over a microprocessor are faster computation and data-retrieval time and larger capacity. However, these attributes are not necessary for the application being discussed, as none of the programs described takes more than 15 minutes to run and print out, and most require far less time.

SUMMARY

The microcomputer system described in this paper provides an inexpensive and powerful tool to operators of wastewater-treatment plants. It allows complex process calculations and decisions to be made quickly and accurately by plant operators who usually are not highly technical people. The system is flexible enough to allow updating as needed and is highly reliable. The rapidly increasing use of these types of systems in wastewater-treatment plants as well as many other applications is testimony to their great benefits.

Thomas T. Jones is a Project Manager for ES Environmental Services, the plant operations subsidiary of Engineering-Science, Inc. He has experience in both design and operations of wastewater treatment plants, and has authored several papers on the subject. He has B.S. in chemical engineering from the University of Florida and a master's degree in chemical oceanography from the University of Miami. He is a Registered Professional Engineer in Calif.

David L. Sullivan is Vice President of ES Environmental Services, the plant operations subsidiary of Engineering-Science, Inc. He is an expert on wastewater treatment plant operations and troubleshooting and has over 25 years' experience in the field. He has lectured widely on wastewater treatment and has conducted numerous training seminars for EPA and other agencies. He is a Registered Professional Engineer in Calif.

Pervaporation Membranes—A Novel Separation Technique for Trace Organics

A viable separation of chlorinated hydrocarbons from dilute aqueous solutions has been demonstrated experimentally.

C. L. Zhu, C.-W. Yuang, J. R. Fried, and D. B. Greenberg, University of Cincinnati, Cincinnati, Ohio 45221

In recent years membrane separation processes have been viewed with considerable interest as a means of collecting valuable solutes or reducing solvent contamination in fluids. In particular, much work has focused on the problem of removing chlorinated organics, pesticides, herbicides, etc., long known for their toxicity [*1, 2, 3*] from industrial and municipal water supplies. Successful studies utilizing techniques such as ultrafiltration to separate chlorobenzene, hexachlorobenzene, etc., and reverse osmosis for the removal of phenol and other homologues from aqueous solutions have been reported in the recent past [*1*]. This research is concerned with the separation through polymer membranes of trace hydrocarbons in aqueous solutions by means of a liquid-vapor mass-transfer process known as pervaporation [*4, 5*]. A comparison among the various commercially significant membrane processes is presented in Table 1.

Essentially, the method involves the selective sorption of a liquid mixture, followed by diffusion and then desorption into a vapor phase on the downstream side of the membrane. The separation process at given operating conditions of temperature, pressure, etc., is therefore a function of the permselectivity and permeability of the membrane itself. Utilizing the range of solubilities and diffusivities among the toxic contaminants examined in aqueous solutions, as well as their chemical and physical properties, the present researchers have achieved some useful results with preferential membranes in the separation of water pollutants.

Pervaporation differs from reverse osmosis in that the latter requires a hydrostatic-pressure driving force across the membrane, whereas the former process involves a reduced-pressure system, in which the vaporized permeant is swept away by a carrier gas or a vacuum system (or a combination of both) that induces the selective permeation. Thus, pervaporation entails simultaneous solute permeation through, and evaporation from, the membrane. In reverse osmosis the role of the applied (upstream) pressure is to induce a concentration driving force across the membrane which results in a maximum flux when the solute concentration is reduced to zero at the downstream surface. Paul *et al.* [*6, 7*] have shown that the proposed maximum flux in reverse osmosis is equal to the pervaporation flux. This fact suggests that the process of pervaporation is an attractive alternate as a membrane separation technique.

Normally, in membrane processes such as reverse osmosis, the objective penetrant is the solvent rather than the solute [*6, 8*]. However, more recent studies [*9, 10, 11*] have shown that some organic compounds in dilute aqueous solutions become the primary penetrant in a process which may be similar to, but not necessarily identical with, dialysis. This situation, when achievable, is ideal, since the solute flux across the membrane for a given separation need be much less than that for the solvent. For pervaporation the physicochemical relationship between solution species and the membrane (molecular size, weight, shape, charge distribution, etc.) determines the preferential sorption and mobility of the solute/solvent through the medium. In this work the investigators indicate that membranes selected for solubility parameters compatible with preferential solutes exhibit separation factors that increase dramatically with increasing solute-membrane affinity.

To inhibit the obvious problem of dissolving the membrane in the diffusing solute some composite membranes can be prepared consisting of a thin layer of polymer with high preferential sorption qualities, coated upon an inactive porous support. In the present study a medium molecular weight poly(vinyl acetate) (PVAc) was cast onto a polysulfone (PSF) support matrix. It has been noted that, because of its superior mechanical qualities and chemical stability, polysulfone is most useful as the porous component of a composite membrane on which a variety of polymers can be deposited [*12*]. Furthermore, it has been found here that polysulfone itself offers some preferential separation qualities and, thus, becomes an ideal support matrix for PVAc, which is highly permaselective, but quite vulnerable in solution. The successful choice of inactive

TABLE 1. MEMBRANE INDUCED SEPARATION PROCESSES

Process	Driving Force	Transport Mechanism
1. Reverse osmosis	Pressure differential	Diffusive solvent transport
2. Ultrafiltration	Pressure differential	Molecular character (size, shape, etc.)
3. Dialysis	Concentration gradient	Diffusive solute transport
4. Electrodialysis	Electrochemical potential	Selective ion transport
5. Gel permeation	Concentration gradient	Diffusive solute transport
6. Pervaporation	Concentration	Selective physicochemical transport of solvent/solute

support combined with a selective coating will provide for a long-lived, stable membrane composite with a high separation factor. In this report the experimental results of such a marriage are presented and discussed.

THEORY

Pervaporation, as well as reverse osmosis and ultrafiltration, are generally considered to be non-mediated transport processes. For this type of permeation there are several theoretical treatments, among which the Pore Model, the Solution-Diffusion Model, and the Kedem and Katchalsky Relationships have received the most attention [*4, 13, 14*].

The Pore Model, perhaps the earliest treatment of a pressure-driven permeation process, is based upon the concept of flow through a porous medium. It is assumed here that all flow occurs through a complex interconnected capillary system occupying a given fraction of the membrane surface and having a characteristic pore-size distribution. Flow rates and permselectivity for this process are, therefore, governed by porosity, pore distribution, and physicochemical interactions within the pore fluid.

Kedem and Katchalsky relationships, most popular among biologists, are predicated upon the linear theory of irreversible thermodynamics [*15, 16*]. For describing membrane transport processes there are three defined phenomenological coefficients, derived reflection coefficients, and characteristic permeabilities which are obtainable from experimental measurements. Under certain conditions this model yields results that are comparable to those obtained utilizing the Solution-Diffusion [*4, 13, 17*] approach.

In the latter case the membrane is viewed as a stationary non-porous diffusion barrier with a finite thickness. All molecular species dissolve in the membrane according to prevailing phase-equilibrium considerations and diffuse through the membrane. Generally, this model, also relying upon irreversible thermodynamics and Fick's Law, indicates that the permeation rate of a liquid depends not only on its diffusivity, but also upon its solubility in the membrane itself. Thus, the Solution-Diffusion Model is most useful for describing processes where essentially homogeneous, highly permselective membranes are employed, such as in reverse osmosis and pervaporation [*4, 17*].

In the present work the Solution-Diffusion Model has been used to relate the solute-solvent pressure/concentration gradients with mass flux through the membrane. It has been assumed that the mechanism of pervaporation, as shown in Figure 1, can be most simply described by the following sequence of steps:

i) Absorption of the permeating molecules at the liquid-membrane interface;
ii) Diffusion of these molecules through the membrane;
iii) Removal of these molecules from the downstream surface of the membrane by evaporation into a vacuum or carrier-gas system.

The effective rates of diffusion for the components of the solution absorbed (dissolved) in the "homogeneous" medium are characterized by the local gradient of the average chemical potential in the medium; that is, the driving force is the chemical-potential gradient. In the pervaporation process this is achieved by removing the permeant product from the membrane by evaporation. Separation of diffusing species occurs when there is interaction which enhances the transport of some component solutes over the aqueous solvent. The chemical potential $\mu_i(x)$ for solute i can be written as:

$$\mu_i(x) = \int_{P_{ref}}^{P(x)} \bar{V} dp - \int_{T_{ref}}^{T(x)} S_i dT + RT \ln a_i(x) + \mu_{i0} \quad (1)$$

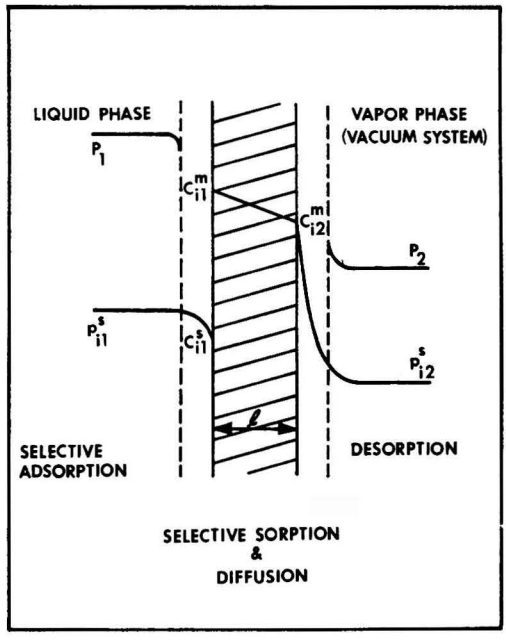

Figure 1. Pervaporation membrane transfer process.

And, the one-dimensional flux of specie, i, at uniform temperature T, with respect to the stationary medium becomes:

$$J_i(x) = -\frac{D_i(x)C_i(x)}{RT} \nabla\mu_i(x) \quad (2)$$

For the case of a flat membrane, the flux under steady isothermal conditions reduces to

$$J_i(x) = -\frac{D_i(x)C_i(x)}{RT}\left[RT\frac{\partial}{\partial x}\ln a_i(x) + \bar{V}_i\frac{\partial P(x)}{\partial x}\right] \quad (3)$$

Thus, for each component there are two contributions to the driving force, a concentration gradient and a pressure gradient. Moreover, the concentration profile becomes linear when it is assumed that the membrane properties are not a function of pressure and that the diffusion coefficient is independent of concentration.

Following the derivation of Lee *et al.* [*17*], the general equation for permeation is obtained as

$$J_i = D_i\{K_{i1}C^s_{i1} - K_{i2}C^s_{i2}\exp[-\bar{V}_i(P^s_1 - P^s_2)/RT]\}/\ell \quad (4)$$

Introducing $\alpha_i = K_{i2}/K_{i1}$, and noting that component i is partitioned between the membrane and solution by the relationship $C^m_{i1} = K_{i1}C^s_{i1}$, where the subscript 1 refers to the upstream side of the membrane, leads to

$$J_i = D_iK_{i1}\{C^s_{i1} - \alpha_iC^s_{i2}\exp[-\bar{V}_i(P^s_1 - P^s_2)/RT]\}/\ell \quad (5)$$

And, defining the permeability constant, Q_i, for component i, a phenomenological parameter dependent upon solubility and diffusivity, as

$$Q_i = D_iK_{i1} \quad (6)$$

leads to the expression below for the flux of specie, i:

$$J_i = Q_i\{C^s_{i1} - \alpha_iC^s_{i2}\exp[-\bar{V}_i(P^s_1 - P^s_2)/RT]\}/\ell \quad (7)$$

In the pervaporation process Equation (7) can be written

$$J_i = Q_iC^s_{i1}\left\{1 - \frac{p^s_{i2}}{p^s_{i1}}\exp[-\bar{V}_i(P^s_1 - P^s_2)/RT]\right\}/\ell \quad (8)$$

where $p_i^s = K_i C_i^s$ has been substituted in Equation (7). For most common cases it may be assumed that the exponential term

$$\exp\left[-\bar{V}_i(P_1^s - P_2^s)/RT\right] \approx 1.0$$

With this assumption, Expression (8) reduces to

$$J_i = Q_i C_{i1}^s \left(1 - \frac{p_{i2}^s}{p_{i1}^s}\right)/\ell \qquad (9)$$

Moreover, when $p_{i2}^s << p_{i1}^s$, Equation (9) is simplified to

$$J_i = Q_i C_{i1}^s/\ell \qquad (10)$$

Comparing with the development of Hwang *et al.* [4], for the case of gas-phase permeability where

$$Q_i' = \frac{J_i \ell}{P_i^0(x_i - P_{ri} y_i)} \qquad (11)$$

and, as before, when

$$P_{ri} = P_2^s f_i / P_i^0 \gamma i$$

The analogous expression obtains, namely

$$Q_i' = \frac{J_i \ell}{P_i^0 x_i} \qquad (12)$$

Contrasting Equations [10] and [12], it is obvious that they are identical except that the former uses liquid-phase concentration terms and the latter expresses the concentration of i in terms of partial pressures.

In order to express the separation efficiency between two permeants, "i" (solute) and "j" (solvent), a separation factor is defined

$$SF_{ij} = [y_i/(1 - y_i)]\,[(1 - x_i)/x_i] = \left(\frac{J_i}{J_j}\right)\left(\frac{C_j}{C_i}\right) \qquad (13)$$

which can be written

$$SF_{ij} = Q_i\left[1 - \left(\frac{p_{i2}^s}{p_{i1}^s}\right)\right]/Q_j\left[1 - \left(\frac{p_{j2}^s}{p_{j1}^s}\right)\right] \qquad (14)$$

And, when both p_{i2}^s, p_{j2}^s approach zero, then Equation (14) reduces to

$$SF_{ij} = Q_i/Q_j \qquad (15)$$

From Equation (15) it is clear that the separation factor for any two penetrants in the pervaporation process is simply the ratio of their respective permeability constants when the downstream pressure is close to zero (i.e., in a downstream vacuum). Thus, the separation factor and permeability are the key parameters in terms of which the separation process may be described. Each is a function of the system equilibrium characteristics, that is, of the mutual solubility of solute and solvent and of the molecular mobility within the medium (membrane).

From a theoretical point-of-view, the relationship between the separation factor and the permeability can be explained from a consideration of the extent of preferential sorption and the relative mobilities of the polymeric membrane-sorbed species. These are, of course, totally dependent upon the membrane characteristics. It is generally established that substances with similar solubility parameters have good mutual affinity, with the closer the similarity the higher the mutual solubility. This has been experimentally verified independently by both Barton [18] and Schneier [19], who found that liquids with solubility parameters, δ, numerically close to that of the polymer tend to sorb to a greater extent and permeate more rapidly than attendant solvents whose δ's are far removed from the polymer value.

The basic concept of a solubility parameter in any system is predicated on the assumption that there is a correlation between the cohesive energy density and the mutual solubility. The definition of the solubility parameter has been initially expressed in terms of the molecular cohesive energy $(-E)$ per unit volume, i.e., $\delta = (-E/V)^{1/2}$

In condensed phases (solids, liquid solutions) strong attractive forces exist between molecules, and, as a result, each molecule possesses considerable potential energy, that is, a molar cohesive energy, $(-E)$. Thus, this energy, which is the energy of a liquid relative to its ideal vapor at thermodynamic equilibrium conditions, can be assumed to be composed of two parts, as given by the relationship

$$-E = \Delta^v u + \int_{V=V_{vap}}^{V=\infty} \left(\frac{\partial u}{\partial V}\right)_T dV \qquad (16a)$$

Here $\Delta^v u$ is the vaporization energy and the second term in (16a) is the energy required to isothermally expand the saturated vapor *ad infinitum* (in vacuum). This latter term is usually negligible below the normal boiling point. The solubility parameter, δ, also called the cohesive energy density, can be evaluated from the relation

$$\delta = [\rho(\Delta H_V - RT)/M]^{1/2} \qquad (16b)$$

where $(\Delta H_v - RT) = \Delta^v u$ for an ideal vapor.

From the Hildebrand-Scatcherd Equation [18, 20] for the internal energy of mixing,

$$\Delta H_0 = (x_A V_A^* + x_B V_B^*)\,(\delta_A - \delta_B)^2 \phi_A \phi_B \qquad (17)$$

Thus, for compatible systems, as $(\delta_A - \delta_B)^2$ becomes small the heat of mixing is reduced, as predicted from a consideration of the Gibbs free energy of mixing.

Flory and Huggins [18] estimated the energy of mixing of a polymer-solvent system. In their work they proposed a polymer-solvent interaction parameter. This parameter, χ, is a dimensionless quantity which characterizes the difference in the energy of interaction between a substance dissolved in a polymer at the limit of solubility and one at infinite dilution. Clearly, to be a good solvent for pervaporation requires that a substance have a low polymer-interaction parameter. Equation (18) can be assumed to represent the potential energy of the system available for absorption and diffusion.

$$\Delta G_m = RT\left[x_A \ln\phi_A + x_B \ln\phi_B + \chi\phi_A\phi_B\left(x_A + \frac{x_B V_B}{V_A}\right)\right] \qquad (18)$$

(B denotes polymer)

It is reasonable, therefore, to correlate the energy assigned to absorption with the interaction parameter between the polymer film and the permeating liquid as expressed by Equations (19) below.

$$\chi = \chi_s + \chi_H \qquad (19a)$$

$$\chi_H = (V_A/RT)\,(\delta_A - \delta_B)^2 \qquad (19b)$$

Again, as $(\delta_A - \delta_B)^2$ becomes small, so does χ_H and the better is the interaction between polymer and liquid.

From the foregoing, one concludes that the solubility parameter is a key parameter influencing the separation factor for a particular system. This conclusion, and the fact that the membrane structural characteristics (crystallinity, morphology, etc.) are also of importance in defining the efficiency of a particular separation system, to be described later in the experimental results section, have been verified in the current work.

The role of hydrogen bonding in the separation process for organics in dilute aqueous solutions is quantitatively predictable. The observation that polar solutes permeate polar membranes more effectively than do non-polar solutes (and vice-versa) suggests that the solubility mecha-

nism can be described by three effects, namely, contributions from hydrogen bonding, polar interactions, and non-polar or dispersive interactions. This leads to the assumption that the cohesive energy ($-E$) is composed of contributions from those three effects.

EXPERIMENTAL

Apparatus

The equipment and instrumentation arrangement for the laboratory pervaporation process is shown in Figure 2. The system is composed of four parts: a feed section, the permeation cell, the product-collection section, and a vacuum system. The permeant-solution feed tank is a standard glass pipe of 3-in. diameter by 3-ft tall (approximately 4-liter capacity). It is flanged with appropriate piping and valving to the permeation cell (through a VMI laboratory metering pump).

The permeation cell consists of two 4-in. Pyrex-glass pipe end-caps flanged together. A stainless-steel ring holds the membrane sandwiched between two expanded-metal screen supports. O-rings and Teflon gaskets are used to insure tight seals throughout. An exploded view of the test section assembly is provided in Figure 3. The capacity of the upstream test section is 1.23 liters and the effective membrane-permeation cross-sectional area is 1.013×10^{-4} m^2. Temperature control to ± 0.1°C is achieved in the cell and is recorded manually with a heating tape, a potentiometer, and an appropriately positioned IC thermocouple.

In the product-collection system, a cold finger immersed in liquid nitrogen and housed in a Dewar flask is used to condense and trap the permeating vapor product. Vacuum in excess of 0.1 mm Hg is obtained with a 30 liter/min pump as measured by a Zimmerli gage. The condensed vapor product is weighed to the nearest 1/10 mg and analyzed by gas chromatography, as are also the feed solution and the liquid product streams. Analysis is performed with a Varian 1400 Series Chromatograph using an FI detector and a 6-ft column packed with 0.2% Carbowax 1500 on 80/100 Carbopack.

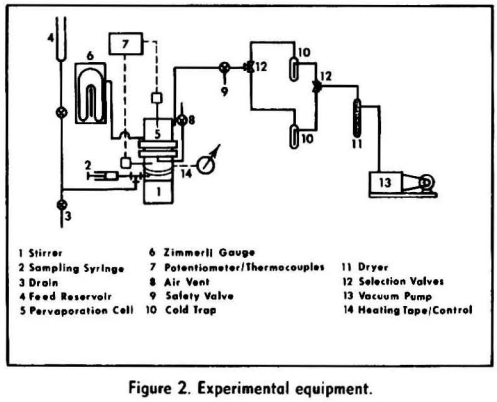

Figure 2. Experimental equipment.

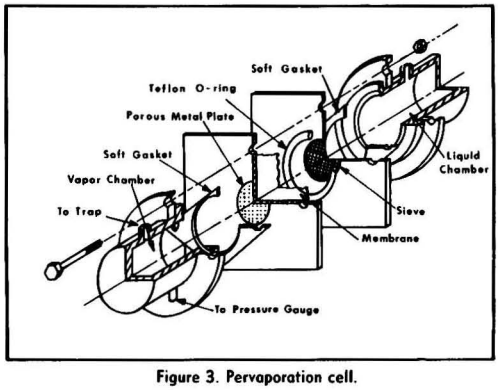

Figure 3. Pervaporation cell.

Procedure

The selected membrane, mounted in the permeation cell, is connected to the product-collection system and vacuum pump. Adequate sealing of the system is assumed when the vacuum system can be maintained at 0.1 mm Hg or less. Approximately 200 ml of the previously prepared feed solution is then charged into the feed compartment. Temperatures are monitored by the thermocouples which are placed in the upstream (liquid) and downstream (vapor) sides of the cell. To eliminate both thermal and concentration gradients in the feed-chamber, the liquid is mechanically agitated and the vacuum system maintains the permeating vacuum between 0.1 and 0.01 mm Hg for the entire period of the run. Roughly 30 minutes into the run, when the membrane becomes saturated (swollen) by the new feed solution, product sample collection is initiated and periodic GC analyses are performed. Upon reaching a steady-state operation, the cold finger is changed and the vapor product collected for a measured time period. The run terminates when sufficient product for analysis has been collected. At this point the product sample is removed, isolated from the vacuum system, warmed to room temperature, and then weighed. Both the vapor product sample as well as the liquid product are subjected to GC analysis.

Test Solutes

According to recent reports [21] a list of over 100 water-pollutant compounds have been identified by the U.S.E.P.A. as potential or incipient carcinogens. Many of such cited compounds are halogenated. Chloroform, 1,2-dichloroethane, and chlorobenzene, typical of these materials, have been selected as representative compounds for the current study. In Table 2 are presented the key parameters of significance to the pervaporation process for these particular substances.

Synthetic Polymeric "Simple" Membranes

The initial experimental work was concerned with the evaluation and characterization of single-component membranes, the so-called "simple" membranes. These included commercially available materials such as cellulose acetate, polystyrene, and untreated hydrophobic polytetrafluoroethylene (PTFE). Other materials tested such as polysulfone and poly(vinyl acetate) were prepared in-house, the details of which are included in the following section. Table 3 provides literature data available on solubility parameters for these materials.

Composite Membranes

Three types of membrane composites have been prepared and experimentally tested. They are:

1) PVAc/PSF(THF)—medium molecular weight poly(vinyl acetate) on polysulfone (with tetrahydrofuran, THF, as the solvent).
2) PVAc/PSF(THF)/PSF(DMF)—medium molecular weight poly(vinyl acetate) on polysulfone (using the solvent THF); the second layer of polysulfone was prepared with the solvent dimethyl formamide, DMF.

TABLE 2. PHYSICAL PROPERTIES OF PERMEANT LIQUIDS

Properties	Chloroform	1,2 Dichloroethane	Chlorobenzene	Water
Water solubility, 20°C (cc/liter H_2O) [*34, 35*]	5.606	6.963	0.4521	—
Solubility parameter*, δ [*18*]	9.3	9.8	9.5	23.4
3-D Structural $\delta(d)$	8.7	9.3	9.3	7.6
Solubility-parameter $\delta(h)$	2.8	2.0	1.0	20.7
Components* $\delta(p)$	1.5	3.6	2.1	7.8
Density, 20°C (g/cc)	1.472	1.246	1.101	1.00
Molecular volume (cc/mole) [22]	80.488	80.12	101.79	20.00
Molar size (10^{23} cc) [22]	13.36	13.30	16.90	3.32
Molecular weight (g/mol)	119.5	99.0	112.5	18.0
Vapor pressure, 22°C (mm Hg) [*11*]	170	70	10	19.8

* The 3-D structural solubility-parameter components (Ref. [18]) are defined as:
$\delta(d)$: dispersion component
$\delta(h)$: hydrogen-bonding component
$\delta(p)$: polar component
$\delta = [\delta(d)^2 + \delta(h)^2 + \delta(p)^2]^{1/2}$

TABLE 3. SOLUBILITY PARAMETERS FOR POLYMER MEMBRANE MATERIALS AS A FUNCTION OF SOLVENT HYDROGEN-BONDING STRENGTH

	Solubility Parameter [*18*]*			Structural Components Homomorphic [23]			Three Dimensional [23]		
Polymer	δ_p	δ_M	δ_S	$\delta(d)$	$\delta(p)$	$\delta(h)$	$\delta(d)$	$\delta(p)$	$\delta(h)$
Polyvinyl acetate (PVAc)	8.5-9.5	—	—	9.8	3.7	4.1	9.3	5.0	4.0
PTFE	5.8-6.4	—	—	—	—	—	—	—	—
Cellulose acetate (CA)	11.1-12.5	10.0-14.5	—	—	—	—	—	—	—
Polysulfone (PSF)	10.0-10.5	—	—	—	—	—	—	—	—
Polystyrene (PS)	8.5-10.6	9.1-9.4	—	10.0	1.4	0	8.6	3.0	2.0

*δ_p: Solubility parameter in a poorly hydrogen-bonded solvent
δ_M: Solubility parameter in a moderately hydrogen-bonded solvent
δ_S: Solubility parameter in a strongly hydrogen-bonded solvent

3) PTFE/PVAc/PTFE—commercial, untreated, hydrophobic PTFE sandwiched around medium molecular weight poly(vinyl acetate).

The membranes were prepared in the following manner:

Membranes A: PVAc/PSF(THF). Solutions were made by dissolving 7.6%-15% (wt.) poly(vinyl acetate) in solvent acetone. The mixture was stirred for 24 hours, then spread uniformly using an adjustable casting knife on a glass plate and allowed to partially dry (cure) under ambient conditions. A similar procedure was followed to obtain the porous polysulfone film from a 15% (wt.) solution of the polymer in THF. Before the films were completely dry they were carefully assembled to form a composite which was immersed in water for several hours and again air-dried.

Membranes B1-B5: PVAc/PSF(THF). Films B1-B5 were produced in a manner slightly different from the previous membrane. These specimens all had a very thin (0.2 mil) dense layer of poly(vinyl acetate) and a relatively thick (3.0 mil) porous support of polysulfone. In this method of preparation, after casting the acetate film and partially air-drying it as before, the polysulfone support-layer mixture was spread over this film to a controlled thickness using a casting knife, then immersed in water and air-dried afterwards. Thus, the support layer became an integrally bound part of the active PVAc film, both together forming the composite membrane.

Membranes B6-B7: PVAc/PSF(THF)/PSF(DMF). These samples were prepared in an essentially similar fashion to the previous B-type membranes except that a second layer of polysulfone support material was added. The PSF(DMF) generated a higher porosity layer than did the PSF cast from the solvent THF. Together these two elements provided reasonably good support along with a better pervaporation flux than was obtained with the previous B-type membrane samples.

Membrane C: PTFE/PVAc/PTFE. This composite was prepared by casting the poly(vinyl acetate) film dissolved in an acetone solvent over a film of commercial PTFE and then carefully covering the partially dried casting with a second sample of PTFE. The composite was then immersed and thoroughly air-dried before testing.

EXPERIMENTAL RESULTS AND DISCUSSION

The first of two series of studies was performed with the "simple" (single-component) membranes in order to identify the individual characteristics of these materials. The experimental data and associated calculations are summarized in Table 4. With these initial results as a guide, and from appropriate physical property information, membrane composites were prepared and evaluated in a more comprehensive experimental program. These runs are reported in Table 5 and Table 6.

Separation Factor

An examination of the data in Figure 4 confirms the fact that, for a particular membrane—solute system, high separation factors are achieved when the corresponding solubility parameters are numerically close, the membrane-solute interaction parameter psi (Equation 18) is small, and the heat of mixing, ΔH_n (Equations 16, 17), is low. Such compatibility leads to good interaction between membrane and solute, better preferential sorption, and, finally, to the high separation factors observed. This information is summarized in Figure 4 for the materials examined in the present work. For example, note that for chloroform (δ = 9.3) the highest separation factor was observed with poly-

TABLE 4. EXPERIMENTAL RESULTS: PERVAPORATION THROUGH "SIMPLE" MEMBRANES

Organic Solute [i]	Solute Concentration in: Feed C_i (ppm)	Vapor Y_i (10^{-3}mol%)	Liquid x_i (10^{-4}mol%)	Separation Factor, SF_{ij}	Solute Flux, J_i (10^{-8}kmol/m-s)	Permeability (10)* Q_i (10^{-8}kmol/m-s)
	Membrane: PTFE (untreated, ℓ = 1.5 mil, 22°C, p = 2.0 mm Hg)					
Chloroform	5.6	1.96	1.20	16.5	0.110	3.49
	10	2.44	2.13	11.5	0.189	3.39
	21	3.26	4.83	6.76	0.309	2.24
	51	41.8	11.0	3.80	—	—
	63	47.3	13.5	3.50	—	—
1,2-Dichloroethane	5.6	1.09	1.30	8.4	0.210	6.16
	7.5	1.47	1.84	8.0	0.309	6.42
	7.9	1.46	1.95	7.5	0.310	6.06
	30.2	4.22	6.75	6.2	0.700	3.95
	Membrane: PTFE (untreated, ℓ = 1.5 mil, 22°C, p = 0.1 mm Hg)					
Chlorobenzene	11.4	3.52	2.10	16	0.220	3.99
	12.2	3.37	2.23	15	0.230	3.89
	15	3.42	2.65	14	0.239	3.43
	27.5	5.05	5.32	9.5	0.295	2.11
	32	5.17	5.90	8.9	0.246	1.59
	30	5.52	5.80	9.0	0.312	2.05
	Membrane: PSF (Solvent: THF) (ℓ = 10 mil, 22°C, p = 1.0 mm Hg)					
Chloroform	5	0.84	1.10	7.63	0.112	25.8
	59	3.4	12.0	2.83	0.585	12.4
	150	8.5	31.0	2.74	48.5	13.3
	200	10.4	39.9	2.59	69.5	14.4
1,2 Dichloroethane	25	2.8	6.15	4.68	4.35	17.9
	50	3.9	11.2	3.24	6.08	13.7
	75	4.2	16.2	2.64	7.50	11.7
	(Membrane: PSF (Solvent THF) (ℓ = 10 mil, 22°C, p = 0.1 mm Hg)					
Chlorobenzene	2	0.360	0.36	10	0.0074	5.2
	8	0.710	1.42	5	0.014	2.5
	25	0.929	4.65	2	0.141	7.7

*Equation 10

(vinyl acetate) (δ = 9.3). Both chlorobenzene (δ = 9.5) and dichloroethane (δ = 9.8) show similar results with PVAc. However, for other membranes whose solubility parameters diverge from this range, such as CA (δ = 11.5), PSF (δ = 10.2), and PTFE (δ = 6.2), the separation factors decrease accordingly, as Figure 4 indicates. It appears, however, that a high separation factor which arises from the compatibility between membrane and solute will eventually lead to vulnerability and rapid deterioration of the membrane material itself. Therefore, membrane composites whose components are chosen to provide both structural strength as well as good separation properties are the logical solution to the observed dichotomy. Thus, in the definitive phase of this project, predicated upon these early results, composites were prepared with PVAc upon PTFE and PSF, respectively, as the supporting members. These materials were selected primarily because of their superior mechanical qualities and relative chemical stability. Moreover, since the supporting porous membranes provide the primary contact with the feed liquid, they screen and enhance the PVAc membrane's resistance to attack by the solution.

The effect of solute feed concentration upon the separation factor is clearly evident for the "simple" membranes as demonstrated in Figure 5 and more dramatically for the composites in Figures 6 and 7, respectively. These results indicate that the separation factor decreases with increasing solute feed concentration until an apparent limiting concentration is reached, each membrane exhibiting its own limiting value. A review of the Solution-Diffusion mechanism for permeation indicates that, due to the strong membrane-solute interaction, a point of saturation within the matrix is achieved, thus reinforcing this experimental observation. Moreover, Paul *et al.* [26] also observed that there was a liquid-membrane equilibrium which, when reached, appeared to be independent of the imposed driving force. In all cases here, the limiting value of the separation factor for the composites appeared to be considerably higher than for those obtained with the single-membrane materials alone.

In addition to the strong dependence on solute concentration, the B-type composite membrane (PVAc/PSF) separation factors also show a marked dependence upon the solutes themselves. For the three organics studied, the separation factors at any given solute concentration varied from extraordinarily high values with chloroform (Figure 6) to more moderate values with dichlorothane, and still lower values with chlorobenzene (Figure 7). As predicted by Solution-Diffusion theory, separation factors are influenced strongly by vapor pressures, chloroform and chloroethane both are more volatile than water while chlorobenzene is not, and by chemical reactivity, wherein the two former compounds are considered to be proton donors and, hence, interact more strongly with the PVAc membrane. On the other hand, thermal variations, as shown in Figure 6, of the separation factor, are relatively

TABLE 5. EXPERIMENTAL RESULTS: PERVAPORATION THROUGH COMPOSITE MEMBRANES

Organic Solute [i]	Organic Solute Concentration: Feed C_i (ppm)	Vapor Y_i (10^{-3}mol%)	Liquid x_i (10^{-4}mol%)	Separation Factor, SF_{ij}	Solute Flux, J_i (10^{-8}kmol/m-s)	Permeability (9)* Q_i (10^{-8}kmol/m-s)
Membrane: Composite membrane B-1 (PVAc/PSF(THF) total ℓ = 3 mil, PVAc dense membrane $\ell \leq$ 0.2 mil, 22°C, p = 0.1 mm Hg)						
Chloroform	5.5	120.4	1.21	995	2.010	21.62
	7.1	148.0	1.56	948	2.352	20.61
	9.6	147.7	2.11	700	2.450	15.02
	20.0	150.9	4.40	343	2.713	5.90
1,2 Dichloroethane	1.5	4.662	0.3070	152	0.1889	6.113
	4.5	14.52	1.023	142	0.4046	3.886
	7.0	5.51	1.574	35		
	7.5	11.81	1.689	70	0.4079	2.048
	7.7	11.69	1.720	68	0.510	2.521
Membrane: Composite membrane B-2 (PVAc/PSF(THF) total ℓ = 3 mil, PVAc dense membrane $\ell \leq$ 0.2 mil, 22°C, p = 0.1 mm Hg)						
Chloroform	12.2	117.2	3.03	585	4.61	17.69
	13.4	191.4	3.30	580	4.75	16.68
	4.0	96.0	0.99	910	2.89	47.93
	7.0	139	1.54	908	4.49	47.63
	50	157	11.0	143	4.68	3.53
	60	163	13.2	124	4.78	2.97
Membrane: Composite membrane B-4 (PVAc/PSF(THF) total ℓ = 3 mil, PVAc dense membrane $\ell \leq$ 0.2 mil, 22°C, p = 0.1 mm Hg)						
Chlorobenzene	14.78	4.190	2.62	16	0.1203	0.4165
	15.82	3.956	2.82	14.1	0.1224	0.3846
	20.75	2.607	3.65	7.14	0.1368	0.3063
Membrane: Composite membrane B-5 (PVAc/PSF(THF) total ℓ = 3 mil, PVAc dense membrane $\ell \leq$ 0.2 mil, 22°C, p = 0.1 mm Hg)						
Chlorobenzene	2.88	8.13	0.51	160	0.0927	1.653
Membrane: Composite membrane C(PTFE/PVAc/PTFE) (total ℓ = 3 mil, PVAc dense membrane $\ell \leq$ 0.2 mil, 22°C, p = 0.1 mm Hg)						
Chlorobenzene	4.11	3.355	0.72	46.6	11.99	254
	6.58	2.799	1.16	24.1	6.659	61.15
	18.69	5.285	3.30	16.0	22.56	66.07
	41.09	13.48	7.20	18.7	67.62	93.33
Chloroform	6.8	8.60	1.50	57.5	53.25	69.7
	14.6	18.06	3.20	56.2	56.07	137.5

*Equation 9

small [18], since temperature has a similar effect on both the solubility parameters and permeabilities of solute and solvent alike.

Permeation Flux, Permeability and Diffusivity

The permeation flux for pervaporation, as well as for the other similar membrane transport processes, is a function of solute concentrations as well as of the equilibrium and transport characteristics (i.e., solubility and mobility) obtaining within the membrane. These results are presented by the curves of Figure 8 for single membranes and by Figures 9 and 10 for the composites used in this investigation. The simplified mathematical model given by Equations 9-12 seems to fit the data reasonably well over this range of study. However, for chlorobenzene, with its lower vapor pressure, the term p^s_{i2}/p^s_{i1} can become sufficiently large to influence the result. Physically this suggests that, under such circumstances, desorption (evaporation) of solute from the downstream membrane surface becomes the controlling mechanism for the pervaporation process as pressure increases. Obviously, a low downstream pressure will always enhance the permeation flux, especially for a relatively low-vapor-pressure solute, as is chlorobenzene.

The permeability constant which defines the phenomenological coefficient across the membrane is, for given operating conditions of temperature and pressure, strongly dependent on the solute concentrations in both the bulk liquid and in the membrane phase. It is also a function of the molecular properties of the membrane and permeant substances (e.g., it is dependent on the diffusivity and solubility of the solute in the membrane phase). Solute saturation in the membrane imposes an upper limit on the solubility constant which, along with the permeability is, therefore, usually proportional to the concentration as indicated in Figure 11 for the solute, chloroform, and the type- B composite membrane.

Diffusion of organic molecules which interact with the polymeric membrane is enhanced and, hence, controlled by the micro-Brownian motion (mobility) of the unit polymer segments. As the temperature is increased, the system tends to expand and absorb more solute (swells), inducing greater polymer-segment micromovement and, thus, promotes greater mobility of the diffusing solute molecules. Therefore, as observed here (see Figure 13) and reported elsewhere [27], the diffusion coefficients of polymer-organic molecule systems generally increase with both concentration and temperature.

Experimentally, it can be seen from Figures 11-13 and Figure 14 that both chloroform and chlorobenzene behave similarly in composite membrane type B. As expected, Arrhenius-type equations best express these relationships

TABLE 6. EXPERIMENTAL RESULTS: PERVAPORATION THROUGH COMPOSITE MEMBRANES

Organic Solute [1]	Organic Solute Concentration: Feed C_i (ppm)	Vapor Y_i (10^{-3}mol%)	Liquid x_i (10^{-4}mol%)	Separation Factor, SF_{ij}	Solute Flux, J_i (10^{-9}kmol/m-s)	Permeability (9)* Q_i (10^{-8}kmol/m-s)	Diffusivity D_i (10^{-11}m²/s)
Membrane: Composite membrane B-1 (PVAc/PSE(THF) total ℓ = 3 mil, PVAc dense membrane $\ell \leq$ 0.2 mil, 22℃, p = 0.1 mm Hg)							
Chloroform	6.7	86.8	1.47	592	1.858	14.80	2.02
	8.5	68.4	1.90	360	1.938	9.861	2.22
	10	50.5	2.20	230	1.993	7.778	2.74
	13.7	57.2	3.01	190	2.12	6.047	2.58
Membrane: Composite membrane B-3 (PVAc/PSE(THF) total ℓ = 3 mil, PVAc dense membrane $\ell <$ 0.2 mil, 31.9℃, p = 0.1 mm Hg)							
Chloroform	8.0	84.96	1.80	472	4.296	22.39	3.85
	8.6	61.01	1.90	320	2.989	13.64	3.46
	11.3	47.37	2.50	190	3.075	10.17	4.34
	13.7	56.77	3.02	188	3.620	9.87	4.26
	15.0	61.05	3.30	185	3.963	9.88	4.33
Membrane: Composite membrane 3 (PVAc/PSF(THF) total ℓ = 3 mil, PVAc dense membrane $\ell <$ 0.2 mil, 22℃, p = 0.1 mm Hg)							
Chloroform	9.5	67.76	2.05	330	5.018	18.84	4.63
	10.5	60.75	2.25	270	5.065	17.29	5.19
	11.0	48.34	2.34	206	4.993	16.39	6.45
Membrane: Composite membrane B-6 (PVAc/PSF(THF)/PSF(DMF) total ℓ = 3 mil, PVAc dense membrane < 0.2 mil, 22℃, p = 0.1 mg)							
Chlorobenzene	4.0	3.712	0.71	52.2	0.1033	1.169	5.44
	3.0	3.708	0.67	59.6	0.1022	1.343	4.77
Membrane: Composite membrane B-7 (PVAc/PSF(THF)/PSF(DMF) total ℓ = 3 mil, PVAc dense membrane $\ell <$ 0.2 mil, p = 0.01 mm Hg)							
Chlorobenzene	2.5	1.10	0.44	25	0.049	0.926	3.78(49.4℃)
	2.5	1.40	0.44	32	0.044	0.899	2.87(37.8℃)
	2.5	1.48	0.44	34	0.039	0.846	2.54(33.8℃)
	1.3	0.62	0.22	28	0.013	0.789	2.87(30.0℃)

Note:
Diffusivity: $D_i = Q_i/K_i$
Solubility: $K_{ii} = C_i''/C_{ii}$
Where C_i'' is the equilibrium concentration of solute in the membrane boundary. Assume permeant concentration in the vapor product to be the concentration in the membrane, at steady-state and under conditions where accumulation in the membrane and boundary layers can be considered negligible.
* Equation 9

for diffusivity and permeability:

$$D = D_o e^{-(E_D/RT)} \quad (20)$$

$$Q = Q_o e^{-(E_Q/RT)} \quad (21)$$

where E_D and E_Q are the apparent activation energies for diffusion and permeation, respectively. From the slopes of the respective curves in Figures 11-14, average activation energy values are obtained for each system as:

Membrane: PVAc/PSF(THF)
Solute: Chloroform
$(E_Q)_{avg} = 5.37 \times 10^3$ kcal/kg-mol
$(E_D)_{avg} = 4.47 \times 10^3$ kcal/kg-mol
Membrane: PVAc/PSF(THF)/PSF(DMF)
Solute: Chlorobenzene
$(E_Q)_{avg} = 1.59 \times 10^3$ kcal/kg-mol
$(E_D)_{avg} = 2.73 \times 10^3$ kcal/kg-mol

Unfortunately, the solute diffusivity is not readily determined, since it is a function of conditions obtaining within the membrane that are not directly measurable. Furthermore, membrane imperfections which allow bulk flow of both solute and solvent complicate the situation even more. The measured permeation flux in such a case normally includes both diffusion and viscous pore flow. Moreover, according to Frijta [27], organic solutes in polymers exhibit different behavior above and below the glass-transition temperature, T_g, which for PVAc is 31℃.

Generally, above T_g the character of the substrate matrix is relatively stable and diffusion proceeds normally and predictably. However, below T_g the system becomes irregular and the diffusivity tends to be a rather complex function of concentration and temperature.

The relatively small water molecule is strongly associated in the liquid as well as in the solid state by hydrogen bonding. This feature distinguishes it from the vast majority of organic solvents. Thus, the diffusion coefficient for water increases with concentration in polar polymers, is relatively constant in hydrophobic polymers, and decreases with concentration in hydrophilic polymers. Therefore, in PVAc the diffusion coefficient is roughly constant, as the present investigation confirms. Consequently, the effects of temperature, pressure, concentration, diffusivity, and permeability on the separation factor and permeation flux as experimentally measured in this study agree well with the theory proposed.

CONCLUSIONS AND RECOMMENDATIONS

The experimental results indicate that a viable separation of chlorinated hydrocarbons from dilute aqueous solutions can be achieved by the process known as pervaporation. Results obtained on preferential sorption and mobility of solutes through suitable membranes under given operating conditions suggest that the solubility parameter is the most important factor for determining

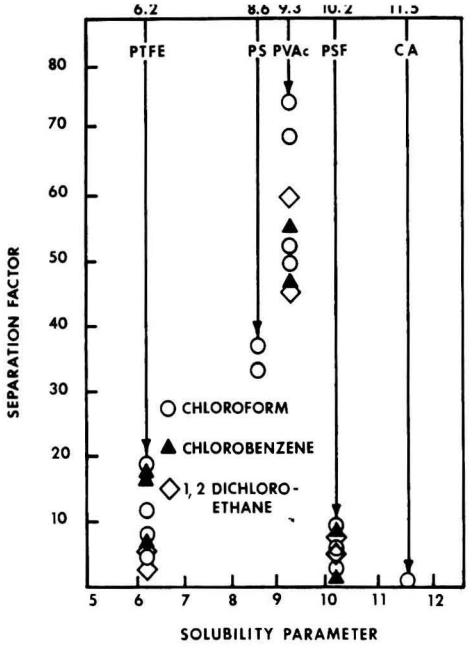

Figure 4. Relationship between separation factor and solubility parameter for various membrane-solute systems.

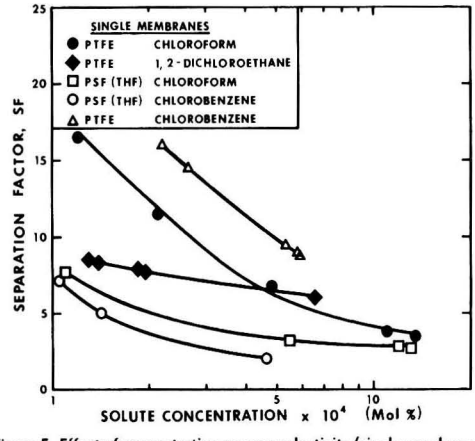

Figure 5. Effect of concentration on permselectivity (single membranes).

permselectivity. Therefore, polymeric membranes with solubility parameter values in a range which overlap those of the contaminants will preferentially absorb such materials and thereby provide a high degree of separation.

Although excellent separations were achieved with organic-polymeric materials related through the solubility parameter, such chemical compatible systems generally lead to rapid membrane failure, since permeant and matrix are mutually soluble. This led to the development of new composite membranes consisting of a thin dense highly sorptive layer cast upon a porous stable supporting member, which still offered good selectivity along with a larger operating period at a relatively high permeation rate. For the separations of volatile organics such as chloroform and dichloroethane, as well as for chlorobenzene (less volatile than water), a membrane system consisting of polyvinyl acetate as the active member on a polysulfone support (type-B membrane) has been successfully prepared and investigated.

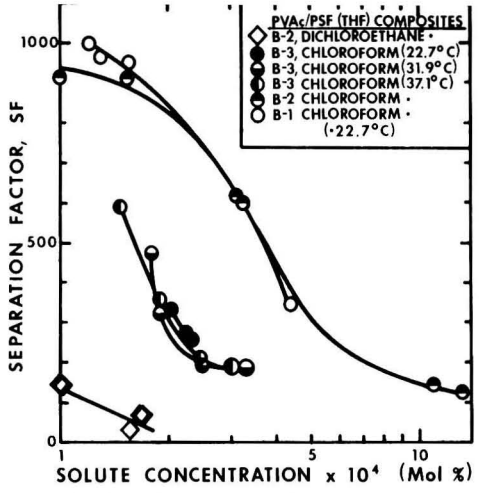

Figure 6. Effect of concentration on permselectivity (composite membranes).

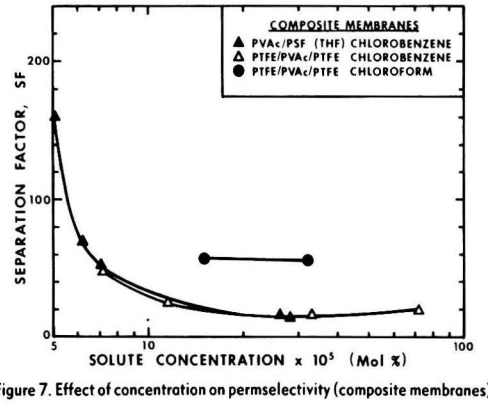

Figure 7. Effect of concentration on permselectivity (composite membranes).

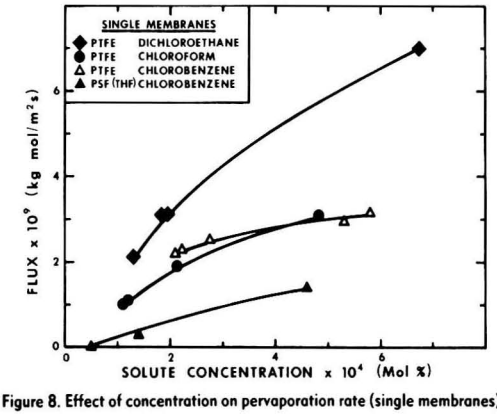

Figure 8. Effect of concentration on pervaporation rate (single membranes).

This system has proven to yield a significantly high selectivity along with stable performance for the solutes studied. The experimental results, although based upon a limited number of data points, appear to follow the Solution-Diffusion theory as adapted to the pervaporation process.

Another composite system consisting of polyvinyl acetate sandwiched between layers of PTFE (type-C membrane) was also prepared and studied experimentally under the same operational conditions. This composite had a

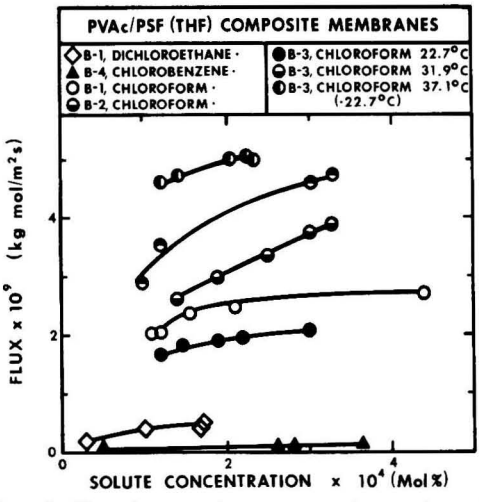

Figure 9. Effect of concentration on pervaporation rate (composite membranes).

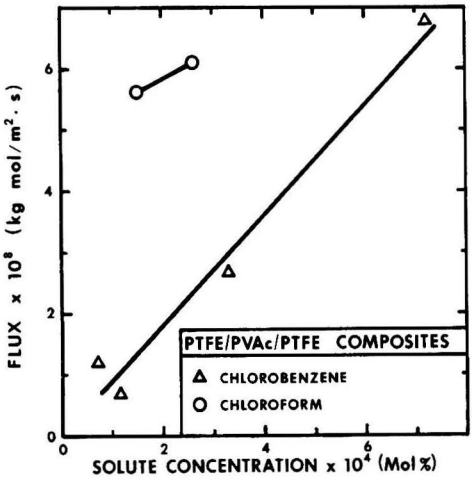

Figure 10. Effect of concentration on pervaporation rate (composite membranes).

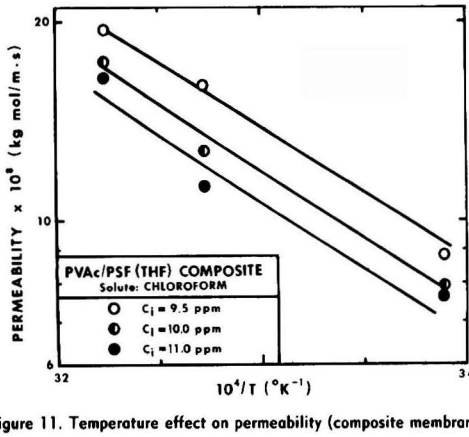

Figure 11. Temperature effect on permeability (composite membranes).

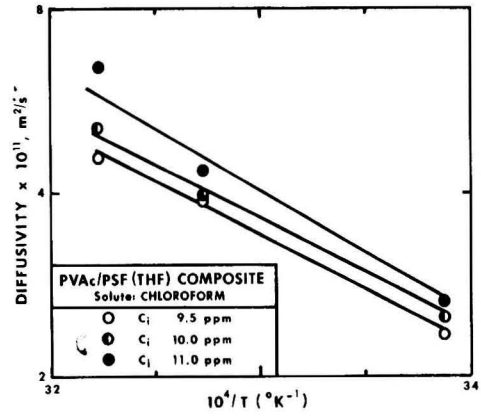

Figure 12. Temperature effect on diffusivity (composite membranes).

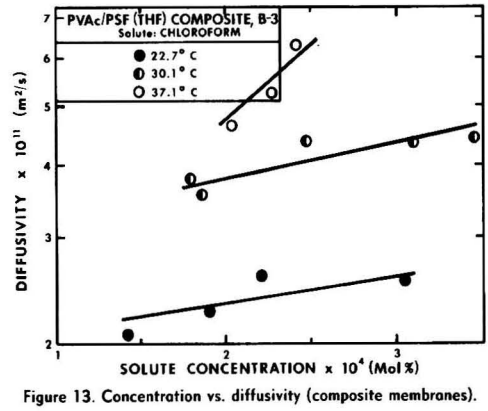

Figure 13. Concentration vs. diffusivity (composite membranes).

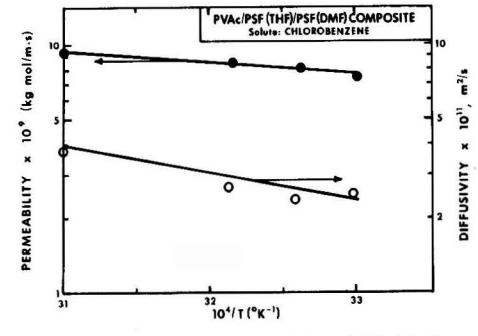

Figure 14. Temperature effect on permeability and diffusivity (composite membranes).

higher porosity, which promoted a better permeability flux than was obtained with the type-B membranes; however, its permselectivity was measurably less than with the former membrane composite. It appears that, due to the larger pore dimension in the PTFE supporting matrix, a greater percentage of the overall permeation flux is due to viscous flow, which reduces the separation factor accordingly.

Generally, target penetrants in pervaporation processes should have reasonably high volatilities; otherwise, the operational system requires a very high downstream vacuum. Therefore, desorption from the membrane downstream surface is the critical step in the pervaporation process—often it becomes rate controlling for the separation. Thus, for low-volatility substances, despite poten-

tially high solubility in the preferential membrane, good separation factors mandate high downstream vacuums, and the lower the volatility the higher is the requisite vacuum required.

Future studies in this area should be expanded to seek a wider range of suitable membrane materials. The casting and coating procedures for preparing composites must also be improved in order to generate better uniformity and better stability in membranes. This suggests that gamma-ray irradiation might be used to induce more crosslinking within the support matrix for selectivity and strength. And, finally, hollow fibers [*29, 30*] and continuous-membrane column techniques [*31, 32*] employing these membrane composites are natural systems for future studies, especially when potentially commercial applications are to be considered.

NOMENCLATURE

$a_i(x)$ = activity of component i at position x in membrane
$C_i(x)$ = concentration of component i at position x in membrane
$C^s_{i1}(C^s_{i2})$ = concentration of component i in solution upstream (downstream) of membrane
$C^m_{i1}(C^m_{i2})$ = concentration of component i in membrane upstream (downstream) of membrane
$D_i(x)$ = self-diffusion coefficient of component i at position x in membrane
D_i = diffusion coefficient of component i
D_0 = diffusion coefficient at reference state
E = molar cohesive energy
E_D = apparent activation energy
E_Q = activation energy for permeation
E_d = dispersion component of cohesive energy
E_p = polar component of cohesive energy
E_h = hydrogen component of cohesive energy
f_i = fugacity coefficient of component i in vapor phase
ΔH_0 = heat of mixing
ΔH_v = energy of vaporization
ℓ = thickness of membrane
M = molecular weight
$J_i(x)$ = permeation rate of component i at position x in membrane
J_i = permeation rate at steady state
$K_{i1}(K_{i2})$ = solubility constant of component i at upstream side (downstream side)
P^0_i = vapor pressure of pure component i
$P(x)$ = pressure at position x in membrane
P_{ref} = reference pressure
$P^s_1(P^s_2)$ = pressure upstream (downstream) of membrane
$p^s_{i1}(p^s_{i2})$ = partial pressure of component i upstream (downstream) of membrane
Q_i = permeability constant of component i (driving force of concentration gradient)
Q'_i = permeability constant of component i (driving force of partial pressure gradient)
SF_{ij} = separation factor of component i and j
$T(x)$ = temperature at position x in membrane
T_{ref} = reference temperature
$\bar{V}_i(x)$ = partial molar volume of component i at position x in membrane
V_i = molar volume of component i
$V^*_A(V^*_B)$ = molar quantity of pure component A, (B)
$v_a(v_B)$ = molar volume of pure component A, (B)
x = distance in membrane in flux direction
x_i = molar concentration of component i in liquid product
y_i = mole concentration of component i in vapor product
$\mu_i(x)$ = chemical potential of component i at position x in membrane
$\mu_{io}(0)$ = chemical potential of component i at reference-state
ρ = density
δ_i = solubility parameter of component i
δ_p = solubility parameter in poorly hydrogen-bonded solvent
δ_M = solubility parameter in moderately hydrogen-bonded solvent
δ_s = solubility parameter in strongly hydrogen-bonded solvent
$\delta_{(d)}$ = dispersion component of solubility parameter
$\delta_{(p)}$ = polar component of solubility parameter
$\delta_{(h)}$ = hydrogen bonding component of solubility parameter
δ_r = volume-dependent solubility parameter
δ_r = residual solubility parameter
γ_i = activity coefficient of component i in liquid phase
ϕ_i = volume fraction of component i
χ = polymer-solvent interaction parameter
χ_H = polymer-solvent interaction parameter for enthalpy
χ_s = polymer-solvent interaction parameter for entropy

LITERATURE CITED

1. Berkau, E. E., C. E. Frank, and I. A. Jefcoat, "A Scientific Approach to the Identification and Control of Toxic Chemicals in Industrial Waste Water," Industrial Pollution Control Division, Industrial Environmental Research Laboratory, Cincinnati, Ohio (1980).
2. Hersheft, A. and I. A. Jercoat, "Emission and Control of Volatile Organic Compounds," The Mitre Corporation Metrek Division, McLean (1979).
3. "Research and Assessment of Water Problems Relating to the Mount St. Helen's Eruption (RMSH)," Office of Water Research and Technology (OMRT), Washington, D.C. (1980).
4. Hwang, Sun-Tak and Karl Kammermeyer, "Membranes in Separation," Wiley-Interscience, New York (1975).
5. Michails, A. S., "Progress in Separation and Purification" (E. S. Perry, Editor), Wiley-Interscience, New York (1968).
6. Paul, D. R. and O. M. Ebra-Lima, *J. Appl. Polym. Sci.* **14,** 2201 (1970).
7. Paul, D. R. and O. M. Ebra-Lima, *J. Appl. Polym. Sci.* **15,** 2199 (1971).
8. Huang, R. Y. M. and N. R. Jarvis, *J. Appl. Polym. Sci.* **14,** 2341 (1970).
9. Dickson, J. M., T. Matsuura, and S. Sourirajan, *I.E.C. Process Des. Dev.* **18,** 641 (1979).
10. Dickson, J. M., T. Matsuura, and S. Sourirajan, *I.E.C. Process Des. Dev.* **15,** 529 (1976).
11. Kerr, R. S., "Dialysis For Concentration and Removal of Industrial Wastes," Environmental Protection Technology Series (1976).
12. Cabasso, I. and A. P. Tamvakis, *J. Appl. Polym. Sci.* **23,** 1509 (1979).
13. Lacey, R. E. and S. Loeb, "Industrial Processing with Membranes," Wiley-Interscience, New York (1972).
14. Lightfoot, E. N., "Transport Phenomena and Living Systems," Wiley-Interscience, New York (1974).
15. Tombalakian, A. S., *Can. J. Chem. Eng.* **50,** 131 (1972).
16. Long, R. B., *A.I.Ch.E.J.* **15,** 73 (1969).
17. Lee, C. H., *J. Appl. Polym. Sci.* **19,** 83 (1975).
18. Barton, A. F. M., *Chem. Rev.* **75,** 731 (1975).
19. Schneier, B., *J. Appl. Polym. Sci.* **16,** 2343 (1972).
20. Hildebrand, J. H., "Solubility of Nonelectrolytes" (3rd ed.), Reinhold, New York (1950).
21. "Recommended List of Priority Pollutants," E.P.A., Cincinnati, Ohio, (1978).
22. Weast, R. C., "Handbook of Chemistry and Physics" (59th ed.), CRC Press, Florida (1979).
23. Huggins, M. L., *Polym. J.* **4,** 502 (1973).
24. Cabasso, I., E. Klein, and J. K. Smith, *J. Appl. Polym. Sci.* **20,** 2377 (1976).

25. Dack, M. R. J., "Solutions and Solubilities, Part I, Techniques of Chemistry, Vol. VIII," Wiley-Interscience, New York (1976).
26. Paul, D. R. and J. D. Paciotti, *J. Appl. Polym. Sci.* **13,** 1201 (1975).
27. Crank, J. and G. S. Park, "Diffusion in Polymers," Academic Press, London (1968).
28. Sinkar, J. K., *Chem. Eng. Sci.* **32,** 1137 (1977).
29. Cabasso, I., Klein, and K. Smith, *J. Appl. Polym. Sci.* **21,** 165 (1977).
30. Cabasso, I., E. Klein, and J. K. Smith, *J. Appl. Polym. Sci.* **20,** 2377 (1976).
31. Hwang, Sun-Tak and J. M. Thorman, *A.I.Ch.E.J.* **26,** 558 (1980).
32. Hwang, Sun-Tak and K. H. Yuen, *Separation Science and Technology* **15,** 1069 (1980).
33. Rodriguez, F., "Principles of Polymer Systems," McGraw-Hill, New York (1978).
34. Washburn, E. W., "International Critical Tables," McGraw-Hill, New York (1930).
35. Stephen, H. and T. Stephen, "Solubilities of Inorganic and Organic Compounds," Pergamon Press, New York (1964).

Chang-Loh Zhu, a native of Shanghai, China, is a 1958 graduate of Zhejiang University, Hangzhou, China. She is currently a lecturer in Chemical Engineering at that institution and a specialist in thermodynamics and mass transfer research. She spent the 1980-82 academic years with the Department of Chemical and Nuclear Engineering, University of Cincinnati as a visiting scientist where this research was performed.

Ching-Whua Yuang received his BS in chemical engineering from National Taiwan University in 1973. In 1982, he received his MS in chemical engineering from the University of Cincinnati and is presently a graduate student in the Department of Computer Science at the University of Houston.

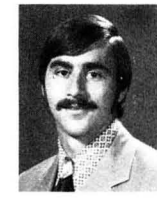

J. R. Fried is Assistant Professor of Chemical Engineering in the Department of Chemical and Nuclear Engineering and an advisory board member of the Polymer Research Center. Prior to joining the University of Cincinnati, in 1978, he was a Senior Research Engineer involved in membrane development for Monsanto's Prism Separators. He holds degrees in biology (B.S.) and chemical engineering (B.S., M.E.) from RPI and in polymer science and engineering (M.S., Ph.D.) from the University of Massachusetts and has authored over 30 publications in the polymer field.

David B. Greenberg, Professor of Chemical Engineering has been on the faculty in Chemical Engineering at the University of Cincinnati since 1974. His educational background in chemical engineering includes a BS from Carnegie-Tech and graduate degrees from the Johns Hopkins University and L.S.U. (PhD). His current research interests are primarily in the environmental and life sciences.

AIChE ENVIRONMENTAL DIVISION NEWSLETTER

Environmental Division (1970)

It shall (a) further the application of chemical engineering in the environmental field; (b) provide, in cooperation with the national Program Commitee, suitable programs on environmental topics of current interest; (c) provide a communication medium for chemical engineers and other individuals to exchange nonconfidential information concerning all facets of environmental activity; (d) promote publication of papers of interest to chemical engineers in environmental activities; (e) coordinate the Institute's activities with other societies active in the environmental field; (f) act as a source of information for chemical engineers who are not actively engaged in the environmental field to bring to their attention the importance of concern for the environment, the need for its consideration in the design and operation of process plants, and opportunities in research and design of equipment and processes to solve environmental problems; (g) encourage chemical engineering educators to place suitable emphasis on protecting our environment and encourage excellence in courses in environmental engineering.

ENVIRONMENTAL DIVISION

EXECUTIVE COMMITTEE — 1983

CHAIRMAN.....David L. Becker
NUS Corporation, 1300 N. 17th Street
Rosslyn, VA 22209.....703 / 522-8802

FIRST VICE CHAIRMAN.....Theodore M. Fosberg
Resources Conservation Co., P.O. Box 3766
Seattle, WA 98124.....206 / 828-2416

SECOND VICE CHAIRMAN.....Alexander H. Danzberger
Consultant 13245 Willow Lane
Golden, Colorado 80401.....303 / 238-4750

SECRETARY.....Richard Prober
Havens and Emerson, Inc., 700 Bond Court Bldg.
Cleveland, OH 44114.....216 / 621-2407

TREASURER.....Louis J. Thibodeaux
University of Arkansas, 227 Engineering Building
Fayetteville, AR 72701 501 / 575-4951

PAST CHAIRMAN.....Herman L. Davis
ARCO Chemical Co., P.O. Box 777
Channelview, TX 77530.....713 / 457-4430

COUNCIL LIAISON.....David B. Nelson
Monsanto Research Corporation, Sta. B, Box 8
Dayton, OH 45407.....513 / 268-3411

DIRECTORS

DIRECTOR (1981-1983).....Stacy L. Daniels
Dow Chemical Co., 1702 Building
Midland, MI 48640.....517 / 636-4991

DIRECTOR (1981-1983).....John F. Erdmann
Union Carbide Corporation, P.O. Box 471
Texas City, TX 77590.....713 / 948-5126

DIRECTOR (1982-1984).....B. Bhattacharyya
Dept. of Chemical Engr., University of Kentucky
Lexington, KY 40506.....606 / 258-4958

DIRECTOR (1982-1984).....Gary L. Leach
2210 South Memorial
Pasadena, TX 77502.....713 / 946-9340

DIRECTOR (1983-1985).....Michael R. Overcash
North Carolina State University, P.O. Box 5035
Raleigh, NC 27650.....919 / 737-2325

DIRECTOR (1983-1985).....Leo Weltzman
Acurex Waste Technology, Inc., 8074 Beechmont Ave.
Cincinnati, OH 45230.....513 / 474-4420

TECHNICAL SECTION CHAIRMEN

AIR SECTION.....Richard D. Siegel
Stone & Webster Engineering Corp., P.O. Box 2325
Boston, MA 02107 617 / 589-7620

WATER SECTION.....Robert L. Irvine
Department of Civil Engineering, University of Notre Dame
Notre Dame, IN 46556 219 / 239-6306

SOLIDS SECTION.....B. Tod Delaney
Ground/Water Technology, Inc. 100 Ford Road
Denville, NJ 07834.....201 / 625-5558

COMMITTEE CHAIRMEN

PROGRAMMING BOARD.....D. Bhattacharyya
Dept. of Chemical Eng., University of Kentucky
Lexington, KY 40508.....606 / 258-4958

NEWSLETTER EDITOR.....Marx Isaacs
1513 Barbee Ave.
Houston, TX 77004.....713 / 523-6049

AID/LIFE.....Michael R. Overcash
Chemical Engineering Department, No. Carolina State Univ.
P.O. Box 5035, Raleigh, NC 27650 919 / 737-2325

AMERICAN ACADEMY OF ENVR. ENGRS.....Robert T. Jaske
7980 Chelton, Bethesda, MD 20014 202 / 287-0204

AWARDS.....Les Lash
2877 Kentucky Avenue (H)801 / 277-9319
Salt Lake City, UT 84117 (O)801 / 272-4415

CONTINUING EDUCATION.....Michael R. Overcash
Chemical Engineering Department, North Carolina State Univ.
P.O. Box 5035, Raleigh, NC 27650 919 / 737-2325

PUBLIC RELATIONS & MEMBERSHIP.....Marx Isaacs
1513 Barbee, Houston, TX 77004 713 / 523-6049

NOMINATING.....Herman L. Davis
Arco Chemical Co., P.O. Box 777
Channelview, TX 77530 713 / 457-4430

WATER TASK FORCE.....David B. Nelson
Monsanto Research Corporation, Station B, Box 8
Dayton, OH 45407 513 / 268-3411

SOLIDS & HAZARDOUS WASTE TASK FORCE.....David P. Schoen
Coulton Chemical Corporation, 6600 Sylvania Avenue
Sylvania, OH 43560 419 / 885-4661

AIR TASK FORCE.....John (Jack) F. Erdmann
Union Carbide Corporation, P.O. Box 471
Texas City, TX 77590 713 / 948-5126

INTERSOCIETY LIAISON.....Robert A. Baker
U.S. Geological Survey, Gulf Coast Hydroscience Center
NSTL Station, MS 39529 601 / 688-3130

EDITOR - ENVIRONMENTAL PROGRESS.....Gary F. Bennett
Department of Chemical Engineering, University of Toledo
Toledo, OH 43606 419 / 537-2520

AIChE Environmental Division Officers and Directors, 1983

The Environmental Division of the American Institute of Chemical Engineers (AIChE), a national professional society with a total membership of over 52,000, installed officers and directors for 1983 at its annual meeting in Los Angeles. AIChE is celebrating its Diamond Jubilee in 1983, the 75th Anniversary of its founding, with national meetings in Houston March 27-31, along with PetroExpo '83; in Denver August 28-31; and (the principal celebration) in Washington, DC October 30-December 4.

David L. Becker, Chairman, has over eighteen years experience involving chemical and environmental engineering and management. He has managed and has been a participant in numerous major projects having national significance. Mr. Becker's work has resulted in over fifty publications, presentations, patents and awards. He is currently Manager of Chemical Engineering in the Superfund Zone 1 Project Management Office of NUS Corporation. The officer is responsible for the planning and implementation for the cleanup of uncontrolled hazardous waste sites in the eastern United States. Mr. Becker was previously Assistant General Manager of the Environmental Services Division at NUS Corporation where he directed and coordinated marketing activities, developed strategic plans, bid strategies, financial management system, and marketing plans for the Technical Departments and Regional Environmental Centers of the Division. Prior to that he started up and was Operations Manager for the Washington Office of Acurex Corporation for three years. At EPA, Mr. Becker was Chief of the Environmental Protection Agency's Organic Chemicals and Products Branch in Cincinnati and was responsible for EPA's research, development, and demonstration program for air, water, solid and hazardous waste pollution control technologies for the organic chemicals and related industries. Prior to that he was project officer for EPA's Effluent Guidelines Division where he was responsible for drafting regulations and guidelines for industrial wastewater discharges from many industries. Prior to joining EPA, Mr. Becker obtained experience in pilot plant management, plant startup, production troubleshooting and waste utilization while working for the Silicone Products Division of General Electric, the Davison Chemical Division of W. R. Grace, and the Dairy Products Laboratory of the U.S. Department of Agriculture.

Theodore M. Fosberg, First Vice Chairman, is currently Manager, Process Equipment Engineering, for Resources Conservation Company (RCC) responsible for process design of wastewater treatment equipment involving advanced softening, reverse osmosis, evaporation, drying, dewatering and sludge handling technologies. He has been actively involved in environmental engineering for over 18 years. Previous responsibilities include Research and Development Manager for RCC and biotechnology research involving atmospheric contaminant management, environmental control and waste treatment for aircraft and spacecraft projects of The Boeing Company. He is a past chairman of the Puget Sound Section of AIChE (1974-75) and both organized and chaired that Section's Pollution Solution Group. He has been active in the Environmental Division as Director (1979-81) and through participation in environmental sessions at National AIChE meetings. Ted received his B.S. degree in Chemical Engineering from the University of Washington in 1959 and Ph.D. in 1964. He is author of publications in the wastewater treatment, atmospheric contaminant management and environmental control fields; holder of a related patent and is a registered chemical engineer in the State of Washington.

(Continued on following page)

Alexander H. Danzberger, Second Vice Chairman, is Manager of the Pollution Control Group of Dames & Moore, Denver, Colorado, where his practice includes chemical process engineering and waste management. Most recently, he was Vice President of Hydrotechnic Corporation of New York City and was previously associated with Union Carbide Corporation, Arthur D. Little, Inc., and a unit of Booz, Allen, Hamilton. Alex has a B.S. in Chemical Engineering from MIT where he was an active study member of AIChE and later an Icthyologist upon graduation in 1953. He handled the water programming at the Boston National AIChE Meeting and was Secretary of the Environmental Division for two years and served as a Director of the Environmental Division, 1979-1982. Alex also is an active member of the Water Quality Force of GPSC. He is a P.E. and a Fellow of AIChE, a Diplomate of AAEE and a member of NSPE, WPCF, AWWA, ASME, API and AIME. He is listed in Who's Who in Engineering. Alex has prepared and presented numerous technical papers for AIChE. Recently, Alex was recipient of the Kenneth B. Allen Award from the New York Water Pollution Control Association as co-author of a paper titled "Synfuels Wastewater Treatment."

Richard Prober, Secretary, has chemical engineering credentials including a B.S. from the Illinois Institute of Technology in 1957; M.S. in 1958 and Ph.D. in 1962 from the University of Wisconsin-Madison; industrial experience with Shell Development Company and academic experience at Case Western Reserve University. His activities in the environmental area began with industrial experience at the Permutit Company. At Case Western Reserve Dick developed chemical engineering-oriented environmental programs and courses for both graduate and undergraduate students. He is now a consultant with the Cleveland-based environmental engineering firm of Havens and Emerson and specializes in process engineering for industrial and municipal waste water treatment, hazardous waste assessment and water supply systems. Dick is a registered Professional Engineer and author of over 50 published papers and presentations. His recent professional activities include the Intersociety Standard Methods Committee, peer review panel for EPA's Industrial Environmental Research Laboratory, editor of the CRC Press Handbook of Environmental Control and water pollution control technology book series, and organizer-chairman for national meeting technical sessions of WWEMA. His services to the Environmental Division have also included reviews for the Water Annual and Environmental Progress and arrangements chairman for the Divisional dinner at the Cleveland National AIChE meeting.

Uncertainty Analysis for Engineers, AIChE Symposium Series 220, Vol. 78 (1982) 62 pp. Order from Publications Sales Dept., American Institute of Chemical Engineers, 345 E. 47th St., New York, N.Y. 10017. members; $10, others: $20.

Louis J. Thibodeaux, Secretary, received his B.S. (1962) from the Department of Petroleum Engineering, Louisiana State University, Baton Rouge. Upon graduation, he joined E. I. du Pont de Nemours in the Works Technical Department, where his duties included activities in storage and disposal of radioactive wastes. Entering graduate school, he received a M.S. (1966) and Ph.D. (1968) from LSU, majoring in chemical engineering and specializing in diffusion and mass-transfer. As a graduate student, he was a Fellow of the National Council for Air and Stream Improvement. He is currently a Professor of Chemical Engineering at the University of Arkansas, Fayetteville, and has taught environmental engineering courses in the Civil Engineering Department. In 1974, he was a visiting Professor of Chemical Engineering at Oregon State University. His fields of specializations are chemical separation, diffusion and mass transfer, environmental chemistry, and engineering. Professor Thibodeaux is a Registered Professional Engineer in the states of Arkansas and Louisiana. He served as University of Arkansas' Chapter President of Sigma Xi for the papers of 1977-78. In 1979, he was appointed to the State of Arkansas Hazardous Waste Technical Advisory Committee.

Michael R. Overcash, Director (1983-1985), is currently a Professor in the Departments of Biological and Agricultural Engineering and Chemical Engineering at North Carolina State University. He has conducted research in such areas as technology development for land-based treatment systems of industrial wastes; fundamental investigations, modeling and control methods for nonpoint source pollution; chemical engineering input in agricultural systems; process development and selection for utilization recycling of wastes and implementation of wastewater management alternatives in developing and developed countries. Overcash has been responsible for ten research grants and has authored over 120 technical papers and seven books.

Leo Weitzman, Director (1983-1985) is currently the Research Manager for Acurex Waste Technologies, a high technology firm specializing in the chemical destruction of PCB's and other difficult-to-handle wastes. In this capacity he has developed a commercial mobile PCB destruction system. Prior to this position, Leo was with the U.S. EPA in the Industrial Environmental Research Laboratory where he managed research programs into the measurement and control of the pollution problems of the

(Continued on following page)

chemical and related industries. Previous experience also include two years with the Air Permits Section of the Illinois Environmental Protection Agency where he developed evaluation procedures for air pollution control equipment. Leo received his Bachelor of Chemical Engineering from the Cooper Union in 1966 and his M.S. and Ph.D., also in Chemical Engineering, from Purdue University in 1967 and 1972, respectively. He has been a member of AIChE throughout his career. Leo is also a member of the Air Pollution Control Association and is currently working on developing closer cooperation between the Environmental Division's and the APCA's programming.

Incumbent Directors are (1981-1983) **Stacey L. Daniels**, Research Specialist in the Environmental Sciences Research Laboratory of Dow Chemical Company, Midland, Michigan; **John F. Erdmann**, Environmental Protection Coordinator for Union Carbide's Texas City Plant; (1982-84) **Dibakar Bhattacharyya**, Associate Professor of Chemical Engineering at the University of Kentucky and **Gary L. Leach**, Manager of Corporate Engineering, Merichem Company.

Air Task Force Activities

The Air Task Force, under the direction of Jack Erdmann and Richard Siegel, is preparing four position statements related to Congressional reauthorization of the Clean Air Act. These papers have been authorized by AIChE's Government Programs Steering Committee (GPSC) and will represent Institute advocacy positions. Topics of the statements are:

- Prevention of Significant Deterioration
- The Bubble Program
- Section 112 of the Clean Air Act (Hazardous Air Pollutants)
- The Use of Atmospheric Dispersion Models in a Regulatory Setting

These papers are targeted for completion by early midsummer. If you are interested in helping us develop these documents, or wish to obtain copies of the finished statements, please contact Jack Erdmann or myself.

Richard D. Siegel, PhD
Chairman, Air Technical Section

PRELIMINARY ENVIRONMENTAL DIVISION PROGRAM PHILADELPHIA, PA. NATIONAL MEETING AUGUST, 1984

	Involved Sections (Designated Contact)	Session Title
1)	A(Siegel)	Process Modification in the Biotechnology and Pharmaceutical Industries
2)	A(Siegel)	Reuse, Recovery, Recycling in the Biotechnology and Pharmaceutical Industries
3)	A(Siegel)	Environmental Impact in the Biotechnology and Pharmaceutical Industries
4)	W(Irvine)	Tutorial on Genetic Engineering
5)	W(Irvine)	Genetic Engineering and Pollution Control
6)	A(Siegel)	Process Modification in the Synthetic Chemicals and Plastics Industries
7)	A(Siegel)	Reuse, Recovery, Recycling in the Synthetic Chemicals and Plastics Industries
8)	A(Siegel)	Environmental Impact on the Synthetic Chemicals and Plastics Industries
9)	A,W,S(Siegel)	Synfuels Update
10)	S,A(Delaney)	Hazardous Waste Incineration
11)	S,W(Delaney)	Advanced Technology in Waste Treatment Fundamentals
12)	S,W(Delaney)	Advanced Technology in Waste Treatment Design Considerations
13)	W,S,A(Irvine)	Environmental Policy—Multimedia
14)	W,S(Delaney)	Liability Questions/Hazardous Waste
15)	A,S(Siegel)	Monitoring at Hazardous Waste Sites—I
16)	W,S(Irvine)	Monitoring at Hazardous Waste Sites—II
17)	A,S(Siegel)	Modeling at Hazardous Waste Sites—I
18)	W,S(Irvine)	Modeling at Hazardous Waste Sites—II
19)	S,W(Delaney)	Uncontrolled Hazardous Waste Sites—Case Studies
20)	S,W(Delaney)	Remedial Action at Hazardous Waste Sites—Case Studies
21)	S(Delaney)	Reuse, Recovery, Recycling of Bioproducts of Manufacturing
22)	W,S(Irvine)	Use of Biological Treatment Processes for Treatment of Hazardous Wastes
23)	W,S(Irvine)	Use of Physical-Chemical Processes for Treatment of Hazardous Wastes
24)	W,S(Irvine)	Innovative Processes for *In-Situ* Treatment of Hazardous Wastes
25)	S(Delaney)	Considerations in Disposal of Solids/Hazardous Materials

A = Air Section
W = Water Section
S = Solids Section

CALL FOR PAPERS

The Fifth International Conference on Finite Elements in Water Resources will be held at the University of Vermont, Burlington, VT June 18-22, 1984. The object of the meeting is to bring together researchers in chemical and civil engineering and hydrology who have an interest in numerical modeling of water resource problems, to help clarify directions of future research. Conference topics include:

- Groundwater and Seepage
- Tital Processes
- Ocean Dynamics
- River Flow Problems
- Wave Modeling
- Fluid-Forces on Structures
- Viscous Flow
- Turbulence Modeling
- Transport Phenomena
- Heat Waste Problems
- Seawater Intrusion
- Water Quality
- Acid Rain Transport
- Environmental Protection
- Meteorological Dynamics
- Sedimentation Processes
- Parameter Identification
- Calibration Techniques
- Flow Control
- Finite Element Techniques
- Boundary Element Techniques
- Numerical Mathematics
- Software Systems
- Pre- and Post-Data-Processing
- Hard- and Software Developments

Submit abstracts of papers by September 1, 1983 to: Dr. William G. Gray, Associate Professor of Civil Engineering, Princeton University, Princeton, NJ 08544, (609) 452-4600. Notices of acceptance will be given by December 1, 1983; final papers are due before February 1, 1984. All papers will be published in the Conference Proceedings.

Dr. Robert L. Irvine, Jr.
Chairman, Water Technical Section
AIChE Environmental Division

Are We Civil Engineers or Chemical Engineers?

For years the Environmental Division of the AIChE has operated under an Air, Solids and Water Sections structure which, by its nature, has more of a traditional Civil Engineering than a Chemical Engineering programming orientation. During the New Orleans meeting in November, 1981, the Executive Committee of the Environmental Division decided to explore a restructuring of the Division which emphasizes the strengths of the Chemical Engineer and, as a result, serves better both the AIChE and the environmental community as a whole.

The restructuring proposal took the form of four sections to replace the current three. They are: (*a*) Process Modification, (*b*) Reuse, Recycle and Recovery, (*c*) Treatment and (*d*) Fundamental and Effects. The first two sections are concepts that are best handled by Chemical Engineers to the possible exclusion of almost all other disciplines. These areas were tested at the August, 1982 Cleveland meeting and at the March, 1983 Houston meeting. In addition, five of the twelve Air/Solids/Water sessions at the Diamond Jubilee meeting in Washington, D.C. will emphasize these two sections. We have learned from these initial efforts that the restructuring program will require intimate cooperation with all Chemical Engineers. By this, we mean the other divisions of the AIChE, the Industries that have supported the AIChE for the past 75 years and, of course, the AIChE membership as a whole. As a result, we ask all interested parties to contact any member of the Environmental Divisions Executive Committee with suggestions, comments and assistance. We will need new members of the AIChE to "man" the new sections should restructuring be adopted through a change in the Division's Bylaws. Without your help, the AIChE may have to maintain its Civil Engineering programming posture in the environmental community.

The program listed below for the August, 1984 Philadelphia meeting is a result of meetings between the Air/Solids/Water Section Chairmen. We have fully integrated these three sections in the Philadelphia program. The proposed new sections naturally involve these three sections without specifically identifying them.

Approval, modification or rejection of the proposed restructuring must come soon. As a result, we ask each of you who would like us to achieve a leadership role for Chemical Engineering in environmental matters to attend the Environmental Division's Programming Committee meeting in Washington, D.C. Contact any of the below for time and location of this and other future meetings.

David L. Becker, Division Chairman
NUS Corporation
1300 North 17th St.
Arlington, VA 22209
(703) 522-8802

Dibakar Bhattacharyya,
Programming Committee Chairman
University of Kentucky
Dept. of Chemical Engineering
Lexington, KY 40506
(606) 257-2794

Richard D. Siegel, Air Section Chairman
Stone & Webster Engineering Corporation
245 Summer Street
Boston, MA 02107
(617) 589-7620

B. Tod Delaney, Solids Section Chairman
Ground/Water Technology, Inc.
100 Ford Road
P.O. Box 99
Denville, NJ 07834
(201) 625-5558

(Continued on following page)

Robert L. Irvine, Water Section Chairman
University of Notre Dame
Dept. of Civil Engineering
Notre Dame, IN 46545
(219) 239-6306

Your input in this matter will help us to succeed.

R. D. Siegel
B. T. Delaney
R. L. Irvine

AIChE'S 1983 CONTINUING EDUCATION COURSES RELATED TO THE ENVIRONMENT

	Denver	Washington, D.C.
Advanced Waste Water Treatment	Aug. 27-28	Oct. 29-30
Air Pollution Control	—	Oct. 28-30
Fundamentals of Corrosion	—	Nov. 2-3
Hazard Control in the Chemical and Allied Industries	Aug. 29-30	Oct. 31-Nov. 1
Hazard Waste Incineration	—	Nov. 2-3
Hazardous Waste Management	Aug. 31-Sept. 1	Nov. 2-3
Industrial Water Conditioning	Aug. 29-30	Oct. 31-Nov. 1
Land Treatment of Hazardous and Non-Hazardous Industrial Wastes	—	Nov. 4-5
Industrial Toxicology	Aug. 27-28	Oct. 31-Nov. 1
Transport and Fate of Chemicals in the Environment-Chemodynamics	Aug. 29-30	Oct. 31-Nov. 1
Water Quality Engineering	Aug. 25-26	Oct. 27-28

ENVIRONMENTAL DIVISION AWARD NOMINATIONS

Les Lash, Chairman of the Awards Committee of the Environmental Division, needs nominations for the 1984 Environmental Division Award. (The 1983 awardee has been chosen but announcement will not be made for a few months.) Send your suggestions to:

Leslie D. Lash
2877 Kentucky Ave.
Salt Lake City, UT 84117

Past nominees for the award are *not* automatically renominated in the following years, so if you have a worthy candidate, nominate him whether or not he has been nominated before.

THE ENVIRONMENTAL DIVISION NEEDS MEMBERS!!

Membership in the Environmental Division has dropped to about 2050, which is an alarming decrease of about 400 members compared to the same time last year. This has been attributed to the general economic situation as well as to the fact that many of the dropouts may not have been aware of the reason for the increase in dues.

The increase, as shown without explanation on the dues notice from National AIChE, was from $3.00 to $13.00 per year. The additional $10.00 is a bargain price to cover the high printing, publication and mailing costs of the excellent new quarterly journal ENVIRONMENTAL PROGRESS, which has met with wide acclaim although only released since February 1982. Ask any member receiving the Journal to let you see a copy; you should not be without it if you want to keep up with the latest developments in the environmental control field. Then JOIN or REJOIN the Division.

Marx Isaacs, Membership Chairman
AIChE Environmental Division

IMPORTANT NOTICE

If your address has changed, please fill out this form and mail to *Environmental Progress*, AIChE, 345 East 47th Street, New York, N. Y. 10017. Allow up to six weeks for changes to become effective.

ATTACH MAILING LABEL HERE

OR

print old address below

Old Address

Name _____

Address _____

City _____ State _____

New Address

Name _____

Address _____

City _____ State _____ Zip # _____

Member Ref. # _____ Eff. date of change _____

AIChE 1983 Publications Catalog

For a complete listing of all process control titles available from AIChE, consult our 1983 Publications Catalog. If you have not received your copy, send your request to: AIChE Marketing Dept., 345 East 47 St., New York, N.Y. 10017.

ENVIRONMENTAL®
PROGRESS

May 1983
Vol. 2, No. 2

PB 84-[illegible]